

AD _____

Award Number: DAMD17-97-1-7059

TITLE: Isolation of Genes Required for the Regulated Separation
of Sister Chromatids

PRINCIPAL INVESTIGATOR: Duncan Clarke, Ph.D.

CONTRACTING ORGANIZATION: The Scripps Research Institute
La Jolla, California 92037

REPORT DATE: June 2000

TYPE OF REPORT: Final

PREPARED FOR: U.S. Army Medical Research and Materiel Command
Fort Detrick, Maryland 21702-5012

DISTRIBUTION STATEMENT: Approved for Public Release;
Distribution Unlimited

The views, opinions and/or findings contained in this report are those of the author(s) and should not be construed as an official Department of the Army position, policy or decision unless so designated by other documentation.

20010323 026

REPORT DOCUMENTATION PAGEForm Approved
OMB No. 074-0188

Public reporting burden for this collection of information is estimated to average 1 hour per response, including the time for reviewing instructions, searching existing data sources, gathering and maintaining the data needed, and completing and reviewing this collection of information. Send comments regarding this burden estimate or any other aspect of this collection of information, including suggestions for reducing this burden to Washington Headquarters Services, Directorate for Information Operations and Reports, 1215 Jefferson Davis Highway, Suite 1204, Arlington, VA 22202-4302, and to the Office of Management and Budget, Paperwork Reduction Project (0704-0188), Washington, DC 20503

1. AGENCY USE ONLY (Leave blank)		2. REPORT DATE June 2000	3. REPORT TYPE AND DATES COVERED Final (1 Jun 97 - 31 May 00)	
4. TITLE AND SUBTITLE Isolation of Genes Required for the Regulated Separation of Sister Chromatids			5. FUNDING NUMBERS DAMD17-97-1-7059	
6. AUTHOR(S) Duncan Clarke, Ph.D.				
7. PERFORMING ORGANIZATION NAME(S) AND ADDRESS(ES) The Scripps Research Institute La Jolla, California 92037 E-MAIL: duncs@scripps.edu			8. PERFORMING ORGANIZATION REPORT NUMBER	
9. SPONSORING / MONITORING AGENCY NAME(S) AND ADDRESS(ES) U.S. Army Medical Research and Materiel Command Fort Detrick, Maryland 21702-5012			10. SPONSORING / MONITORING AGENCY REPORT NUMBER	
11. SUPPLEMENTARY NOTES This report contains colored photographs				
12a. DISTRIBUTION / AVAILABILITY STATEMENT Approved for public release; distribution unlimited				12b. DISTRIBUTION CODE
13. ABSTRACT (Maximum 200 Words) Failure in cell cycle checkpoint controls causes aneuploidy which is a significant factor in the tumorigenic progression of breast cancer cells. We identified and characterised a novel Pds1-dependent checkpoint pathway that prevents aneuploidy by coordinating DNA replication with mitotic anaphase. The yeast anaphase inhibitor Pds1 is critically involved in this regulation. It is a distinct checkpoint control system from the previously described S-phase checkpoint pathway. Two more genes required for regulated chromosome segregation were identified, Rad23 and Ddi1. When overproduced, these proteins suppress the S-phase checkpoint defect of a <i>pds1</i> mutant strain. Structure/function studies revealed a likely mechanism through which Rad23 and Ddi1 may regulate Pds1 (by binding to ubiquitinated Pds1). Rad23 and Ddi1 contain a novel protein interaction domain (UBA) that binds to ubiquitin and ubiquitinated proteins. Rad23 and Ddi1 UBAs are essential for suppression of the <i>pds1</i> mutant. These genes have closely related human homologues that are likely to be required for human checkpoint controls. Failure in such checkpoint mechanisms are a potential cause of aneuploidy that contributes to the etiology of breast cancer.				
14. SUBJECT TERMS Breast Cancer, Aneuploidy, Nondisjunction, Chromosome segregation, Cohesion				15. NUMBER OF PAGES 146
				16. PRICE CODE
17. SECURITY CLASSIFICATION OF REPORT Unclassified	18. SECURITY CLASSIFICATION OF THIS PAGE Unclassified	19. SECURITY CLASSIFICATION OF ABSTRACT Unclassified	20. LIMITATION OF ABSTRACT Unlimited	

NSN 7540-01-280-5500

Standard Form 298 (Rev. 2-89)
Prescribed by ANSI Std. Z39-18
298-102

FOREWORD

Opinions, interpretations, conclusions and recommendations are those of the author and are not necessarily endorsed by the U.S. Army.

___ Where copyrighted material is quoted, permission has been obtained to use such material.

___ Where material from documents designated for limited distribution is quoted, permission has been obtained to use the material.

___ Citations of commercial organizations and trade names in this report do not constitute an official Department of Army endorsement or approval of the products or services of these organizations.

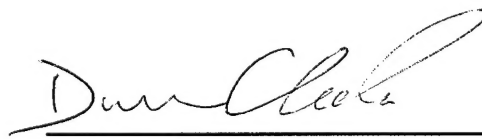
___ In conducting research using animals, the investigator(s) adhered to the "Guide for the Care and Use of Laboratory Animals," prepared by the Committee on Care and use of Laboratory Animals of the Institute of Laboratory Resources, national Research Council (NIH Publication No. 86-23, Revised 1985).

X For the protection of human subjects, the investigator(s) adhered to policies of applicable Federal Law 45 CFR 46.

X In conducting research utilizing recombinant DNA technology, the investigator(s) adhered to current guidelines promulgated by the National Institutes of Health.

X In the conduct of research utilizing recombinant DNA, the investigator(s) adhered to the NIH Guidelines for Research Involving Recombinant DNA Molecules.

___ In the conduct of research involving hazardous organisms, the investigator(s) adhered to the CDC-NIH Guide for Biosafety in Microbiological and Biomedical Laboratories.

 6/23/00

PI - Signature Date

Table of Contents

Cover.....	1
SF 298.....	2
Foreword.....	3
Table of Contents.....	4
Introduction.....	5
Body.....	6-20
Key Research Accomplishments.....	21
Reportable Outcomes.....	22
Conclusions.....	23
References.....	24-26
Appendix.....	27
Bibliography.....	28
Figures.....	29-34

Introduction

Subject, purpose and scope of research

Aneuploidy, the loss or gain of genetic information, is a significant factor contributing to malignancies including those of the breast. Since aneuploidy can result from mitotic non-disjunction, understanding the process of chromosome segregation is important. The fidelity of chromosome segregation relies on elaborate mechanics that are themselves precisely regulated by cell cycle checkpoint controls. The purpose of this research has been to identify new proteins that are required for this regulation. In budding yeast, chromosome segregation is controlled by ubiquitin-dependent degradation of the anaphase inhibitor Pds1⁽¹⁻⁶⁾. Pds1 becomes poly-ubiquitinated at the metaphase to anaphase transition by multi-enzyme APC/cyclosome complexes; the modified forms are then recognized and degraded by 26S proteasome particles. Pds1 degradation releases separin Esp1, and it is the activity of Esp1 that initiates displacement of chromatid cohesion proteins, thus allowing sister separation and the onset of anaphase^(7, 8). Our goal has been to characterize new proteins that function to maintain the fidelity of chromosome segregation. Pds1 is critically involved in this regulation. Therefore we aimed to identify new proteins that interact with Pds1p. We describe the identification of two genes which are required for regulated chromosome segregation: these genes have very closely related human homologues. In addition we have identified a novel Pds1-dependent checkpoint pathway that is crucially required to prevent aneuploidy. A detailed characterisation of this checkpoint pathway has been achieved.

Body of 2000 final report

1. Results Summary

The yeast anaphase inhibitor Pds1 is stabilized in response to DNA damage and spindle assembly checkpoint controls ^(5, 9). In the 1998 and 1999 annual reports we described the novel finding that the yeast anaphase inhibitor Pds1 is required for S-phase checkpoint control ⁽¹⁰⁾. *pds1* mutants lose sister chromatid cohesion and initiate spindle elongation during S-phase. Here we summarize this data and report all further discoveries made to date. Our study of the Pds1-dependent checkpoint, that coordinates DNA replication with mitotic anaphase, has revealed a complex organization of the pathways involved. Here we show that Pds1 protein levels are maintained in response to S-phase checkpoint activation, and that this depends on Mec1 kinase (the yeast homologue of human ATM/ATR kinases) ⁽¹¹⁾. In contrast, Rad53 and Chk1 kinases are dispensable for Pds1 persistence, demonstrating that S-phase checkpoint control operates by two distinct sequential branches downstream of Mec1. We further demonstrate that Pds1 cannot regulate spindle elongation in early S-phase, and that the inhibitory target of Pds1, separin Esp1, is dispensable for spindle elongation in early S-phase. Thus, there are 2 separate pathways involved in coordinating replication with anaphase. Loss of either of these checkpoint controls causes aneuploidy.

We also identified 2 novel high copy suppressors of a *pds1* mutant (*pds1-128*) by genetic screening. Currently, we have been working towards understanding the functions of Rad23 and Ddi1 which are likely to be important regulators of chromosome segregation. Dissection of their functions has been a complex task. Rad23 is a multi-domain protein thought to function solely in nucleotide excision repair (NER) ⁽¹²⁻¹⁷⁾. Our results suggests that Rad23 has a second function responsible for the suppression of the *pds1* S-phase checkpoint defect. Ddi1 has a very similar structure to Rad23, and thus may perform a similar function. The presumed multi-functionality of Rad23 has made analysis of the phenotypes of *rad23* and *ddi1* mutants inherently complicated. For this reason we decided to employ a structure/function study of Rad23 and Ddi1.

This lead to a very exciting observation - that the UBA domains of Rad23 and Ddi1 are essential for the suppression of *pds1-128*. The function of UBA domains is not known⁽¹⁸⁾, though they are present in enzyme involved in ubiquitin-dependent proteolysis; an intriguing coincidence given the dependence of Pds1 proteolysis on the ubiquitin system. Analysis of the UBAs revealed that they are novel protein interaction domains. Rad23 and Ddi1 form hetero- and homo-dimers and in addition can interact with ubiquitin. The interaction of ubiquitin with Rad23 and Ddi1 is UBA-dependent. The UBA-dependent suppression of the *pds1* S-phase checkpoint defect suggests that the UBAs mediate checkpoint activation by binding to a ubiquitinated target protein.

TECHNICAL OBJECTIVE 1

Screens for new proteins involved in chromatid segregation

TASK 1

1.1

Detailed analysis of the Pds1-dependent checkpoint that couples DNA replication with mitosis.

1.1a

Premature spindle elongation and loss of sister chromatid cohesion during S-phase in pds1 mutants

For a detailed study of the role of Pds1 in S phase checkpoint control, we monitored the onset of anaphase in kinetic cell cycle analysis experiments. In budding yeast, mitotic spindles assemble during S-phase. Replication is normally completed before short G2 spindles form, but in the presence of 100 mM hydroxyurea (HU), replication proceeds at a reduced rate and the S-phase checkpoint must delay anaphase to allow the completion of replication⁽¹⁹⁾. Under these conditions, loss of S phase checkpoint control can be demonstrated by measuring the relative timing of DNA replication and the onset of anaphase. Using this analysis, we found that *pds1-128* cells initiate anaphase onset (the mitotic spindles elongate and the sub-centromere regions of sister chromatids separate) when the genome is partially replicated (1999 Report Fig.1-4). Thus, *pds1-128* cells are unable to correctly couple S phase with mitosis⁽¹⁰⁾.

1.1b

The Pds1-dependent late S-phase checkpoint control becomes essential once the genome has been partially replicated

The initial experiments did not address what factor determines the timing of establishment of the Pds1-dependent S-phase checkpoint. *pds1-128* mutants consistently initiated anaphase 3 1/2 hours after release from G1 in the presence of 100 mM HU, when approximately 1/2-2/3 of genome replication was complete. However, the timing of anaphase onset could be due to the length of time spent in S-phase, or more interestingly, it could be dependent on the actual extent of DNA replication. To distinguish between these possibilities, *pds1-128* cells released from G1 arrest, were grown with various HU concentrations (50 mM, 100 mM or 150 mM), and the timing of loss of cohesion monitored using a GFP-tagged sub-centromere-linked probe (Fig.1a). In these experiments, cells progressed from G1 (budded) at a similar rate, regardless of the HU concentration. In contrast, loss of cohesion occurred at different times following entry into S-phase, dependent on the concentration of HU. The higher the HU dose, the longer the delay before cohesion was lost. Thus, the timing of loss of cohesion correlated with the extent of DNA replication accomplished. In similar experiments we determined that the timing of spindle elongation in *pds1* mutants was also dependent on HU concentration (Fig.1b). These data provided good evidence that *pds1-128* cells are unable to perceive that DNA replication has not been completed during the latter part of S-phase. Since the requirement for Pds1 correlated with the extent of ongoing replication, we speculate that the Pds1-dependent checkpoint becomes critical once sister chromatid cohesion has been established ⁽¹¹⁾.

1.1c

The Pds1-dependent checkpoint is a novel S-phase checkpoint pathway

To gain more information about the Pds1-dependent S-phase checkpoint, we compared the checkpoint defect of *pds1-128* with that of other S-phase checkpoint mutants, *mec1*, *rad53*, *rad9* and *chk1*. Unlike *pds1-128*, *mec1* and *rad53* mutants were defective in early S-phase checkpoint control. These cells initiated anaphase as soon as spindle assembly occurred (1999 report Fig.5-6) ⁽¹⁰⁾. Therefore, Pds1, as well as Mec1 and

Rad53, is essential to coordinate ongoing DNA replication with mitosis. But, these components must act at different times in S-phase and in distinct pathways. Mec1/Rad53 are needed early in S-phase, Pds1 is needed late in S-phase. Based on these data, we proposed that an event intrinsic to the progression of DNA replication elicits a switch in the mode of checkpoint regulation from an “early S-phase” to a “late S-phase” mode (see model, Fig.8) ⁽¹⁰⁾. Since Pds1 is required for maintaining sister cohesion, the Pds1-dependent pathway may operate only once cohesion has been established.

1.1d

Pds1 protein levels are maintained during a prolonged S-phase

We determined whether Pds1-dependent delay in loss of cohesion and spindle elongation, in the presence of 100 mM HU, relied on persistent Pds1 levels ⁽¹¹⁾. The kinetics of anaphase onset in wild type and *pds1-128* cells expressing HA epitope tagged versions of Pds1 or mutant Pds1-128, respectively, were compared (Fig.2). Both strains were synchronized in G1 with mating pheromone, then released into rich medium containing 100 mM HU. Cell cycle progression was monitored by scoring budding index, mitotic spindle formation and elongation (using the GFP-TUB1 construct) and by FACScan analysis. Wild type cells began anaphase 5 h following release from G1, when the genome had been fully replicated. Under these conditions of slow DNA replication, Pds1⁽²⁰⁾ persisted for about 3 hours longer than in cells released from G1 into rich medium without HU (data not shown), and its degradation occurred coincidentally with the onset of anaphase. Thus, Pds1 levels are maintained while DNA replication is ongoing in yeast. *pds1-128* mutant cells began anaphase 3 h after release from G1, when approximately 2/3 of bulk DNA replication was complete. Epitope tagged Pds1-128⁽²⁰⁾ was undetectable after 2.5 h suggesting that the mutant protein could not be stabilized in response to S-phase checkpoint activation. This was consistent with the checkpoint defect observed in *pds1-128* cells.

TASK 2

1.2

The Pds1-dependent S-phase checkpoint prevents aneuploidy

1.2a

The pds1 mutant S-phase checkpoint defect results in aneuploidy

Uncoupling S phase from mitosis in *pds1-128* cells resulted in aberrant anaphase that caused aneuploidy (1999 report, Fig.3-4) ⁽¹⁰⁾. By FACScan analysis and by using centromere probes, we demonstrated that *pds1-128* cells suffered gain and loss of chromosome regions following HU treatment ⁽¹⁰⁾. We conclude that *pds1* mutants are defective in S-phase checkpoint control and that this defect results in the generation of aneuploid progeny.

TASK 3

1.3

Comparison of the Pds1-dependent S-phase checkpoint pathway with the established checkpoint pathways that couple DNA replication with mitosis

1.3a

Mec1 kinase maintains Pds1 levels under S-phase checkpoint conditions

Taken together our results indicated that maintenance of functional Pds1 is critical for coupling mitotic progression with the completion of DNA replication under conditions where replication is impaired. An outstanding question is whether the early S-phase, Mec1/Rad53-dependent, pathway is biochemically linked to the Pds1-dependent late S-phase pathway. To address this, we compared the kinetics of anaphase initiation and Pds1 destruction in *mec1*, *rad53*, and *chk1* mutant cells, released from G1 arrest, in the presence of 100 mM HU (Fig.3). The mutants budded and formed short G2 spindles with similar timing. In *mec1* mutant cells, Pds1⁽²⁰⁾ was degraded during S-phase, indicating that Mec1 is required to prevent Pds1⁽²⁰⁾ proteolysis when replication is perturbed. This result placed Mec1 upstream of Pds1 in the late S-phase checkpoint (see model; Fig.8). In contrast, Pds1⁽²⁰⁾ levels were maintained in *rad53* cells and *rad53 chk1* cells. Therefore, Rad53 and Chk1 are not required to inhibit Pds1⁽²⁰⁾ proteolysis in S-phase. These data revealed that Rad53 does not perform all of the Mec1-dependent S-

phase checkpoint functions, and demonstrated that separate S-phase checkpoint pathways can be distinguished biochemically. In agreement with this proposal, the phenotype of *mec1* and *rad53* mutants differed with regard to cell cycle progression once spindle elongation had taken place in the presence of HU. Indeed, *mec1* mutants exited mitosis and eventually re-budded, whereas *rad53* cells became arrested with elongated mitotic spindles (Fig.4). (Under the same conditions, *pds1-128* cells also exited mitosis and rebudded; see Fig.4.) Still, the kinetic analyses also showed that both *mec1* and *rad53* mutants initiated spindle elongation with similar timing in early S-phase (1.5 - 2 h following release from G1), when very little DNA had been replicated. Thus, *rad53* and *mec1* mutants similarly failed to prevent spindle elongation in response to S-phase checkpoint activation. This is consistent with biochemical analyses suggesting that Rad53 and Mec1 function in the same pathway ^(21, 22). Thus, we propose that Rad53 and Pds1 define distinct branches of the S-phase checkpoint, both acting downstream of Mec1 (see model; Fig.8).

1.3b

Pds1 is not required for spindle elongation in early S-phase

The above data suggested that Mec1 controls the S-phase checkpoint by dual mechanisms, targeting Rad53 in early S-phase, and Pds1 in late S-phase. It follows that, in early S-phase, the Mec1/Rad53-dependent checkpoint pathway inhibits spindle elongation without targeting Pds1. This is consistent with the fact that, unlike *mec1* and *rad53* mutants, *pds1* mutant cells do not attempt anaphase when replication is blocked early in S-phase ^(10, 23, 24). However, an alternative explanation could be that *pds1* mutants are not capable of initiating spindle elongation early in S-phase, reflecting an underlying requirement for Pds1 for normal spindle function. Pds1 and Esp1, as well as the fission yeast homologues Cut2 and Cut1, localize to mitotic spindles, and Pds1 is required for the association of Esp1 with the spindle ⁽²⁵⁻²⁷⁾. In fact, *pds1* mutants are unable to initiate spindle elongation during mitosis, if shifted to the non-permissive temperature in G1 of the cell cycle ^(23, 24). We therefore compared the kinetics of cell cycle progression and spindle elongation in *rad53* and *pds1-128 rad53* mutant cells in the presence of 100 mM HU (Fig.5). After release from G1 arrest, both mutants budded

and formed short G2 spindles with similar timing. Onset of anaphase also occurred with comparable kinetics in both mutants. Clearly, cells that lack Pds1 are competent to initiate spindle elongation in early S-phase. Thus, deregulated spindle elongation in *rad53* cells is indeed independent of a Pds1 requirement for spindle function. Given this result, we can safely conclude that Pds1 is only required for the S-phase checkpoint part way through S-phase. Moreover, these data demonstrate unequivocally that the S-phase checkpoint is composed of dual mechanisms that are employed sequentially (see Fig.8).

1.3c

Esp1 is needed for spindle elongation in mitosis but not in Early S-phase

As described in section 1.3b, Pds1 is not required for spindle elongation in early S-phase. Perhaps more surprisingly, the presence of Pds1 is not sufficient to inhibit spindle elongation in early S-phase (see section 1.3a). Both *mec1* and *rad53* cells began anaphase well before Pds1 was degraded in the presence of HU. Thus, although Pds1 must be stabilized to prevent premature initiation of anaphase during late S-phase, the presence of Pds1 in early S is not sufficient to inhibit spindle elongation in HU-treated *mec1* or *rad53* cells. This could be explained by any of several mechanisms. First, Pds1 might be unable to bind and/or inhibit Esp1 in early S-phase upon checkpoint activation in *rad53* cells. To test this, we immunoprecipitated Pds1-Esp1 complexes from wild type and *rad53* cells treated with HU (Fig.6a). We analyzed samples of budded wild type and *rad53* cells that had short G2 spindles, and samples of budded *rad53* cells with anaphase spindles. In each sample, similar amounts of Pds1-Esp1 complexes were isolated. Therefore, the ability of *rad53* cells to initiate spindle elongation in the presence of Pds1 cannot be explained by a lack of Pds1 binding to Esp1.

This result suggested that Pds1 is incapable of inhibiting Esp1 in early S-phase, and that Rad53 might inhibit Esp1 directly. An alternative possibility is that Esp1 activity is not required for spindle elongation in early S-phase. This would seem to be an unlikely scenario, however, since Esp1 activity is absolutely required for spindle elongation in mitosis ⁽²⁶⁾. Still, we tested this hypothesis by generating a novel *esp1* mutant (*esp1-B3*), temperature sensitive at a relatively low temperature (30°C), making it suitable for

analysis of the kinetics of spindle elongation in synchronous cell cycles. After release from G1 into rich medium at 31°C, *esp1-B3* and *esp1-B3 rad53* could not elongate spindles when these cells reached mitosis (Fig.6b). Therefore, the *rad53* mutation could not relieve the inability of *esp1-B3* cells to elongate spindles in mitosis. In the presence of HU, *esp1-B3* cells arrested with short G2 spindles while DNA replication was ongoing, confirming that *esp1-B3* cells are S-phase checkpoint proficient. However, *esp1-B3 rad53* cells and *rad53* cells initiated spindle elongation with similar timing when grown in the presence of HU. Thus, while Esp1 is needed for spindle elongation at mitosis, spindle elongation in early S-phase, upon checkpoint activation, occurs by a mechanism that involves neither Pds1 nor Esp1. This result mechanistically explains the need for distinct and sequential branches of the S-phase checkpoint system. While the late S-phase checkpoint targets Pds1/Esp1, the early S-phase checkpoint must have a novel target (see Fig.8).

1.3d

Cdc20p is needed for spindle elongation in rad53 cells in hydroxyurea

Cdc20 is needed for spindle elongation in mitosis since it activates Pds1 destruction ^(1, 4). Therefore, we asked if Cdc20 is needed for spindle elongation in early S-phase.

rad53, *cdc20* and *rad53 cdc20* strains were released from G1 into medium containing 200 mM hydroxyurea (HU) at 30°C (the restrictive temperature for *cdc20*) (Fig.7a). Each strain formed short G2 spindles (open symbols) with similar timing and replication was arrested in early S phase (not shown). *cdc20* cells arrested with G2 spindles even when the cultures were returned to the permissive temperature (20°C) after 3.5 hours, confirming that *cdc20* cells are S-phase checkpoint proficient. *rad53* cells initiated spindle elongation (solid symbols) after 1.5-2 hours due to the S-phase checkpoint defect of these cells. However, *rad53 cdc20* cells were unable to initiate spindle elongation until after the temperature shift to 20°C.

1.3e

Overproduction of CDC20 causes an S-phase checkpoint defective phenotype

Since Cdc20 is needed for spindle elongation in *rad53* cells, we asked if premature induction of *CDC20* induces spindle elongation in wild type cells during S-phase in HU (Fig.7b). Wild type, *pds1*, *rad53* and cells carrying a *GAL:CDC20* construct were released from G1 arrest into rich galactose medium containing 100 mM HU. Overproduction of *CDC20* (*GAL:CDC20*) produced an S-phase checkpoint defect similar to that of *rad53*. G2 spindles (open symbols), anaphase spindles (solid symbols).

1.3f

Cdc20 is deregulated in mec1 and rad53 mutants in hydroxyurea

Since these experiments implicate Cdc20 in early S-phase checkpoint control, we tested if Cdc20 is regulated in a checkpoint-dependent manner. Wild type, *rad53* and *mec1* cells carrying an epitope tagged *CDC20* were released from G1 into medium containing 100 mM HU (Fig.7c). Cdc20 levels were kept low in wild type cells until late S-phase, but Cdc20 accumulated prematurely in *rad53* and *mec1* cells. (Anaphase onset is indicated on the graph which is a quantification of the raw protein data). Together, these experiments indicate that Cdc20 is a target of the early S-phase checkpoint system.

TASK 4

Analysis of other factors that affect Pds1 function: Dosage suppressors of *pds1-128*.

1.4a

*Genetic Screen for dosage suppressors of mutant *pds1-128**

To identify genes that interact genetically with Pds1, we screened for genes whose increased dosage suppress the lethality of *pds1-128* grown at 37°C. From a genomic *Saccharomyces cerevisiae* library (maintained at high copy in a yeast episomal vector), 3 dosage suppressors of were identified: *ESP1*, *RAD23* and *DDI1* (see 1998 report, section 1.2a). We were most interested in the interactions between Pds1 and

Rad23/Ddi1, since a functional link of Pds1 with Esp1 had already been determined⁽⁸⁾. An important question was whether the Rad23 and Ddi1 suppressor effects are dependent on the presence of the mutant Pds1-128 protein. To address this we determined that overexpression of *RAD23* or *DDI1* could not rescue *pds1* null strains at the non-permissive temperature of 28°C. Thus, high dosage of *DDI1* and *RAD23* cannot bypass the *pds1*Δ temperature sensitivity; these proteins might therefore act in the same pathway as Pds1, possibly by directly increasing Pds1 stability (see 1998 report, section 1.2a).

1.4b

Overproduction of RAD23/DDI1 enhances esp1 mutants

Pds1 binds to Esp1 and thereby inhibits the anaphase-promoting activity of Esp1. If Rad23/Ddi1 are specific regulators of Pds1 stability, overproduction of Rad23/Ddi1 would be expected to enhance an *esp1* mutant temperature sensitivity. Indeed, we found that the lethality of strains with temperature sensitive *esp1* alleles (*esp1-N5* and *esp1-B7*) was greatly enhanced by over-expression of *RAD23* or *DDI1* (see 1998 report, section 1.2a).

1.4c

Overproduction of RAD23 stabilizes mutant pds1-128 protein

The data in sections 1.4a,b suggest that overproduction of *RAD23* might stabilize mutant *pds1-128* protein levels. We found that epitope tagged Pds1-128⁽²⁰⁾ levels were increased in asynchronous cells overexpressing *RAD23* (Fig.9). The increase in levels was enhanced in cells progressing through S-phase in the presence of 100 mM HU (Fig.9). These effects can therefore account for the ability of Rad23 overproduction to rescue both the temperature sensitivity and the HU sensitivity (see below) of *pds1-128* cells.

1.4d

Overproduction of RAD23/DDI1 rescues the S-phase checkpoint defect of pds1-128

As eluded to above, overproduction of *RAD23* and *DDI1* were shown suppress the

sensitivity of *pds1-128* to hydroxyurea (see 1998 report, section 1.2e). Overproduction of *RAD23* and *DDI1* did not rescue the HU sensitivity of *pds1* null strains, again revealing that rescue is dependent on the presence of Pds1 protein (see 1998 report, section 1.2e). Overproduction of *RAD23* or *DDI1* could not rescue the radiation sensitivity nor the nocodazole sensitivity of *pds1-128* cells, however, suggesting that Rad23 and Ddi1 function in a subset of Pds1-dependent checkpoint controls (namely the S-phase checkpoint).

1.4e

rad23 ddi1 mutants are sensitive to replication inhibition

The genetic and biochemical data suggested that Rad23 and Ddi1 have a function in the Pds1-dependent late S-phase checkpoint pathway. We found that *rad23 ddi1* mutants were sensitive to HU, and that these proteins probably share a redundant function in this pathway since deletion of both genes caused a far more severe phenotype than deletion of either one gene by itself. Like *pds1* mutants, *rad23 ddi1* cells initiated spindle elongation before replication was complete in the presence of HU, but in contrast with *pds1* cells, *rad23 ddi1* cells were unable to efficiently complete the spindle elongation process (see 1998 report, section 1.2d).

TASK 5

1.5 Functions of Rad23 and Ddi1: Structure/function analysis.

1.5a

Rad23 UBA domains are dispensable for nucleotide excision repair

Next we determined which domains of Rad23 are required for *pds1-128* suppression, and which domains are needed for the nucleotide excision repair (NER) function of Rad23. We tested whether the UBA domains of Rad23 are required for the NER function by replacing the endogenous *RAD23* gene with a *rad23 Δ UBA{MYC}6X* fusion (lacking the UBA domains) or a full length *RAD23{MYC}6X* fusion. Both fusion proteins were present in equal amounts in yeast cells. These strains were wild type with regard to UV sensitivity; clearly the Rad23 UBA domains are dispensable for

nucleotide excision repair (see 1999 report, 1.2a).

1.5b

*RAD23 and DDI1 UBA domains are required for suppression of *pds1-128**

In contrast to the above (1.5a), we found that the UBA domains of Rad23 and Ddi1 were needed for rescue of the temperature sensitivity and HU sensitivity of *pds1-128* (see 1999 report, Fig.7-8). The UBA domains were also required for the enhancement of the *esp1* mutant temperature sensitivity (see 1999 report, Fig.9). Together, the genetic data show that the UBA domains of Rad23 and Ddi1 mediate the function of these proteins that can suppress the defective phenotypes of *pds1-128*. In contrast, the UBA domains of Rad23 are not needed for nucleotide excision repair of damaged DNA.

1.5c

UBAs are novel domains that mediate protein-protein interactions

We used the yeast 2-hybrid system to ask if we could detect a physical interaction between Pds1 and Rad23/Ddi1. Such an interaction could not be detected in yeast cells, but surprisingly we could identify interactions between Rad23 and Ddi1. Rad23 and Ddi1 could form both hetero- and homo-dimers and these interactions were confirmed in vivo by co-immunoprecipitation. However, further genetic analysis revealed that the interaction between Rad23 and Ddi1 is not needed for suppression of *pds1-128*. Therefore we reasoned that both Ddi1 and Rad23 must target a third protein via their UBA domains. One possibility was ubiquitin since degradation of Pds1 depends upon it being ubiquitinated by the APC.

1.5d

Rad23 and Ddi1 UBA domains interact physically with ubiquitin

By 2-hybrid analysis, we could demonstrate that both Rad23 and Ddi1 interact with ubiquitin. These interactions were dependent on the UBA domains of each protein. Given that this work had identified a novel protein interaction, likely to be of importance to the functions of Rad23 and Ddi1, we decided to identify the UBA residues critical for ubiquitin binding. For this we employed a combination of random

mutagenesis and site directed mutagenesis of the Ddi1 UBA domain, and screened for mutants that disrupted binding with ubiquitin and Rad23. While in progress, an NMR structural analysis of the human Rad23 UBA domain was published ⁽²⁸⁾. This allowed us to map our mutants onto the UBA structure. A summary of this data is presented in Fig.10 and the accompanying table. This information allowed us to propose that one of the two hydrophobic residues (L426 and A407) within a putative hydrophobic face of the UBA domain are critical for ubiquitin binding. Conservative substitution of L426 to an alanine residue completely abolished the interaction of Ddi1 with ubiquitin and Rad23. Other mutations selectively affected binding to either Rad23 or ubiquitin. Although we are presently at an early stage, this analysis will ultimately help us to understand the cellular functions of Rad23 and Ddi1 that are relevant to chromosome stability.

1.5e

2-hybrid screening for Ddi1 UBA interactors

An extension of this work has been to begin screening for *DDI1* interactors, using a UBA deleted version as a negative control. Several interactors have been identified so far, some of which associate with Ddi1 dependent on its UBA. Co-immunoprecipitation experiments are underway to confirm that these 2-hybrid positives are indeed Ddi1 interactors. One interesting putative Ddi1-interactor is Bub2, a spindle assembly checkpoint component that regulates exit from mitosis ⁽¹⁹⁾.

2. Summary and Discussion

We identified a novel Mec1/Pds1-dependent checkpoint system in yeast that coordinates DNA replication with mitotic anaphase. The checkpoint is a distinct control system from the previously documented Mec1/Rad53 pathway. While the Mec1/Rad53 pathway operates in early S-phase, the Mec1/Pds1 system only becomes essential in late S-phase. Failure of the Mec1/Pds1-dependent checkpoint pathway results in aneuploidy. These experiments were made possible by our ability to accurately measure cell cycle kinetics using GFP-tagged mitotic spindles and a sub-

centromeric chromosome locus. The genetic and cell biology techniques developed during this work will be important for future analysis of checkpoint controls.

To identify novel components of Pds1-dependent checkpoint controls we screened for suppressors of mutant *pds1-128*. Rad23, a nucleotide excision repair protein, and a protein of unknown function, Ddi1, were isolated as high copy suppressors of the temperature sensitivity and HU sensitivity of *pds1-128*. These suppressors share a common domain (the UBA) of unknown biological function ⁽¹⁸⁾. A structure/function analysis of Rad23 and Ddi1 revealed that the UBA domains are required for suppression of *pds1-128*. Overproduction of Rad23 was found to increase the stability of mutant Pds1-128 protein. Rad23 was recently shown to interact physically with the complex responsible for Pds1 degradation: the M-phase specific 26S proteasome, but this complex apparently functions in DNA repair rather than in protein degradation ^(29, 30). It is therefore likely to be significant that we find interactions between Rad23/Ddi1 and ubiquitin and ubiquitinated proteins. Moreover, these interactions are dependent on the UBA domains, and as described above, these domains are required for suppression of *pds1-128*. More recently we have identified residues in the Ddi1 UBA that are required for ubiquitin binding. L426 is essential, and this residue is positioned within the putative hydrophobic protein binding site of the UBA. Substitution of L426 to an alanine obliterates binding to ubiquitin and renders Ddi1 unable to suppress *pds1-128*. This provides a mechanism through which Rad23 and Ddi1 might act: by binding to ubiquitinated Pds1, the suppressors may prevent Pds1 proteolysis. The human homologues of *RAD23* and *DDI1* are structurally conserved ⁽³¹⁾, suggesting that they have analogous functions in human cell cycle control. In terms of training, the structure/function studies have been a valuable learning experience. We are currently collaborating with several other PIs at The Scripps Research Institute to solve crystal structures and NMR structures of Rad23/Ddi1 with ubiquitin.

TECHNICAL OBJECTIVE 2

Characterization of CST1

(Discontinued - no longer relevant; see 1998 annual report)

TECHNICAL OBJECTIVE 3

Characterization of DAM1

(Discontinued - no longer relevant; see 1998 annual report)

Key Research Accomplishments

- Identification of a novel Pds1-dependent checkpoint control that couples DNA replication with mitosis
- Characterization of Pds1, Mec1 and Rad53 functions in S-phase checkpoint control
- Identification of high copy suppressors of a *pds1* mutant (Rad23 and Ddi1)
- Demonstration that Rad23 and Ddi1 UBAs are required for suppression of *pds1*
- Demonstration that Rad23 and Ddi1 UBAs are novel protein interaction domains
- Demonstration that Rad23 and Ddi1 bind to ubiquitin
- Identification of UBA residues critical for ubiquitin binding

Reportable Outcomes

Manuscripts

1. Clarke, D.J., Segal, M., Mondésert, G. and Reed, S.I. (1999). **The Pds1 anaphase inhibitor and Mec1 kinase define distinct checkpoints coupling S phase with mitosis in budding yeast.** *Current Biol.* 9:365-368.
2. Clarke, D.J., and Giménez-Abián, J.F. (2000). **Review Article: Checkpoints controlling entry into mitosis.** *Bioessays* 22:351-364.
3. Segal, M., Clarke, D.J., Maddox, P., Salmon, E.D., Bloom, K. and Reed, S.I. (2000). **Coordinated spindle assembly and orientation requires Clb5-dependent kinase in budding yeast.** *J. Cell Biol.* 148:441-451.
4. Clarke, D.J., Segal, M., Jensen, S. and Reed, S.I. **Mec1-dependent control of Pds1 levels in response to S-phase checkpoint activation.** Submitted to *Nature Cell Biology*.
5. Jensen, S., Segal, M., Clarke, D.J. and Reed, S.I. **Live cell imaging of the mitotic regulators Esp1 and Pds1 in budding yeast: evidence that localisation of Esp1 to the nucleus and mitotic spindle is regulated by Pds1.** Submitted to *J. Cell Biol.*
6. Bertolaet, B., Clarke, D.J., and Reed, S.I. **UBAs are novel protein-protein interaction domains.** In preparation.
7. Clarke, D.J., Mondésert, G., Segal, M., and Reed, S.I. **Dosage suppressors of *pds1* link UBA domains to cell cycle control in yeast.** In preparation.

Platform Presentations

1. **Upstream elements activating the Pds1-dependent anaphase-checkpoint in yeast.** Duncan J. Clarke, Marisa Segal, Guillaume Mondésert and Steven I. Reed. *EMBO Fellows Meeting, 12-14th July 1998, Heidelberg, Germany.*
2. **Distinct and sequential S-phase checkpoint controls in yeast.** Duncan J. Clarke, Marisa Segal, Sanne Jensen, Guillaume Mondésert and Steven I. Reed. *The Salk Institute Inaugural Cell Cycle Meeting, 18th-22nd June 1999, La Jolla, CA.*
3. **Cyclin-dependent kinase and Cks/Suc1 interact with the proteasome in yeast to control proteolysis of M-phase targets.** Mark H. Watson, Peter Kaiser, Vincent Moncollin, Duncan J. Clarke, Bonnie L. Bertolaet, Steven I. Reed and Eric Bailly. *The Salk Institute Inaugural Cell Cycle Meeting, 18th-22nd June 1999, La Jolla, CA.*

Poster Presentations

1. **Role Of Pds1 In S-Phase Checkpoint Control.** Duncan J. Clarke, Marisa Segal, Guillaume Mondésert and Steven I. Reed. *British Society for Cell Biology Spring Meeting 1999, Manchester, U.K.*
2. **Distinct and sequential S phase checkpoint controls in yeast.** Duncan J. Clarke, Marisa Segal, Sanne Jensen, Guillaume Mondésert and Steven I. Reed. *DOD Breast Cancer Research Program Meeting 2000, Atlanta, USA.*

Submitted Applications for Funding

1. NIH Grant (RO1).

Conclusions

Inaccurate chromosome segregation causes aneuploidy which is a key event in the etiology of breast cancer. Our goal is to understand checkpoint controls which regulate chromosome segregation and to identify new proteins involved in these control pathways. Using yeast as a model, we have identified a novel checkpoint control system, dependent on the anaphase inhibitor Pds1, which ensures that late S-phase is completed before mitosis is initiated. In addition, we have established a productive strategy for isolating novel components of this pathway. This revealed strong genetic interactions of *RAD23* and *DDI1* with *PDS1*. We determined that Rad23 and Ddi1 are likely to function in the Pds1-dependent checkpoint system that couples DNA replication with mitosis. We have therefore identified 2 proteins required for the regulation of chromosome segregation in yeast. Both *RAD23* and *DDI1* are highly conserved in human cells, though defects in these genes have not been previously implicated in the generation of aneuploid cells.

Recently, a wealth of information has appeared in the literature concerning the functions of human homologues of yeast cell cycle checkpoint proteins. These human checkpoint proteins include ATM/ATR (yeast Mec1), Chk1 (yeast Chk1), Chk2 (yeast Rad53), and a putative vertebrate Pds1 homologue, PTTG. Many of these genes are overproduced, modified or deleted in tumor cells. These data highlight the importance of our goal, to understand the organization of eukaryotic checkpoint pathways. Clearly, our central hypothesis has proven to be true; that proteins involved in regulating chromosome segregation will be defective in people more prone to develop breast cancer and other diseases in which aneuploidy is a key contributing factor.

Our genetic approaches in yeast have rapidly identified 2 proteins (Rad23 and Ddi1) that seem to be important for regulated chromosome segregation. These are likely to be highly relevant proteins since they have a high degree of evolutionary conservation. The 2 genes that we identified so far have very closely related human homologues. Future work must aim to determine whether modification of these particular proteins is an event associated with breast cancer. Defects in these proteins may cause reduced segregation efficiency in humans and therefore increase the frequency of aneuploidy in dividing cells of the breast epithelium. An ability to recognize such defects would have an impact on our capacity to identify individuals prone to acquiring aneuploid cells. Equally important is a detailed analysis of the function of Rad23 and Ddi1 at a molecular level. Knowledge such as this will eventually allow us to define genetic and environmental factors that cause aneuploidy.

References

1. Lim HH, Goh PY, Surana U. Cdc20 is essential for the cyclosome-mediated proteolysis of both Pds1 and Clb2 during M phase in budding yeast. *Curr Biol* 1998;8(4):231-4.
2. Nasmyth K. Separating sister chromatids. *Trends Biochem Sci* 1999;24(3):98-104.
3. Peters JM. Subunits and substrates of the anaphase-promoting complex. *Exp Cell Res* 1999;248(2):339-49.
4. Visintin R, Prinz S, Amon A. CDC20 and CDH1: a family of substrate-specific activators of APC- dependent proteolysis. *Science* 1997;278(5337):460-3.
5. Cohen-Fix O, Peters JM, Kirschner MW, Koshland D. Anaphase initiation in *Saccharomyces cerevisiae* is controlled by the APC-dependent degradation of the anaphase inhibitor Pds1p. *Genes Dev* 1996;10(24):3081-93.
6. Cohen-Fix O, Koshland D. The metaphase-to-anaphase transition: avoiding a mid-life crisis. *Curr Opin Cell Biol* 1997;9(6):800-6.
7. Uhlmann F, Lottspeich F, Nasmyth K. Sister-chromatid separation at anaphase onset is promoted by cleavage of the cohesin subunit Scc1. *Nature* 1999;400:37-42.
8. Ciosk R, Zachariae W, Michaelis C, Shevchenko A, Mann M, Nasmyth K. An ESP1/PDS1 complex regulates loss of sister chromatid cohesion at the metaphase to anaphase transition in yeast. *Cell* 1998;93(6):1067-76.
9. Cohen-Fix O, Koshland D. The anaphase inhibitor of *Saccharomyces cerevisiae* Pds1p is a target of the DNA damage checkpoint pathway. *Proc Natl Acad Sci U S A* 1997;94(26):14361-6.
10. Clarke DJ, Segal M, Mondesert G, Reed SI. The Pds1 anaphase inhibitor and Mec1 kinase define distinct checkpoints coupling S phase with mitosis in budding yeast. *Curr Biol* 1999;9(7):365-8.
11. Clarke DJ, Segal M, Jensen S, Reed SI. Mec1-dependent control of Pds1 levels in reponse to S-phase checkpoint activation. 2000.
12. Guzder SN, Habraken Y, Sung P, Prakash L, Prakash S. Reconstitution of yeast

- nucleotide excision repair with purified Rad proteins, replication protein A, and transcription factor TFIIH. *J Biol Chem* 1995;270(22):12973-6.
13. Guzder SN, Sung P, Prakash L, Prakash S. Affinity of Yeast Nucleotide Excision Repair Factor 2, Consisting of the Rad4 and Rad23 Proteins, for Ultraviolet Damaged DNA. *J Biol Chem* 1998;273(47):31541-31546.
 14. He Z, Wong J, Maniar HS, Brill SJ, Ingles CJ. Assessing the requirements for nucleotide excision repair proteins of *Saccharomyces cerevisiae* in an in vitro system. *J Biol Chem* 1996;271(45):28243-9.
 15. Li L, Lu X, Peterson C, Legerski R. XPC interacts with both HHR23B and HHR23A in vivo. *Mutat Res* 1997;383(3):197-203.
 16. Masutani C, Sugasawa K, Yanagisawa J, Sonoyama T, Ui M, Enomoto T, Takio K, Tanaka K, van, der, Spek, Pj, Bootsma D, et al. Purification and cloning of a nucleotide excision repair complex involving the xeroderma pigmentosum group C protein and a human homologue of yeast RAD23. *Embo J* 1994;13(8):1831-43.
 17. Prakash L, Prakash S. Excision repair genes of *Saccharomyces cerevisiae*. *Ann Ist Super Sanita* 1989;25(1):99-113.
 18. Hofmann K, Bucher P. The UBA domain: a sequence motif present in multiple enzyme classes of the ubiquitination pathway. *Trends Biochem Sci* 1996;21(5):172-3.
 19. Clarke DJ, Gimenez AJ. Checkpoints controlling mitosis. *Bioessays* 2000;22(4):351-363.
 20. Taylor SS, Ha E, McKeon F. The human homologue of Bub3 is required for kinetochore localization of Bub1 and a Mad3/Bub1-related protein kinase. *J Cell Biol* 1998;142(1):1-11.
 21. Sanchez Y, Bachant J, Wang H, Hu F, Liu D, Tetzlaff M, Elledge SJ. Control of the DNA damage checkpoint by chk1 and rad53 protein kinases through distinct mechanisms. *Science* 1999;286(5442):1166-71.
 22. Sanchez Y, Desany BA, Jones WJ, Liu Q, Wang B, Elledge SJ. Regulation of RAD53 by the ATM-like kinases MEC1 and TEL1 in yeast cell cycle checkpoint pathways. *Science* 1996;271(5247):357-60.

23. Yamamoto A, Guacci V, Koshland D. Pds1p, an inhibitor of anaphase in budding yeast, plays a critical role in the APC and checkpoint pathway(s). *J Cell Biol* 1996;133(1):99-110.
24. Yamamoto A, Guacci V, Koshland D. Pds1p is required for faithful execution of anaphase in the yeast, *Saccharomyces cerevisiae*. *J Cell Biol* 1996;133(1):85-97.
25. Funabiki H, Kumada K, Yanagida M. Fission yeast Cut1 and Cut2 are essential for sister chromatid separation, concentrate along the metaphase spindle and form large complexes. *Embo J* 1996;15(23):6617-28.
26. McGrew JT, Goetsch L, Byers B, Baum P. Requirement for ESP1 in the nuclear division of *Saccharomyces cerevisiae*. *Mol Biol Cell* 1992;3(12):1443-54.
27. Jensen S, Segal M, Clarke DJ, Reed SI. Live cell imaging of the mitotic regulators Esp1 and Pds1 in budding yeast: evidence that localization of Esp1 to the nucleus and mitotic spindle is regulated by Pds1. Submitted Manuscript 2000.
28. Dieckmann T, Withers WE, Jarosinski MA, Liu CF, Chen IS, Feigon J. Structure of a human DNA repair protein UBA domain that interacts with HIV-1 Vpr. *Nat Struct Biol* 1998;5(12):1042-7.
29. Schaubert C, Chen L, Tongaonkar P, Vega I, Lambertson D, Potts W, Madura K. Rad23 links DNA repair to the ubiquitin/proteasome pathway. *Nature* 1998;391(6668):715-8.
30. Russell SJ, Reed SH, Huang W, Friedberg EC, Johnston SA. The 19S regulatory complex of the proteasome functions independently of proteolysis in nucleotide excision repair. *Mol Cell* 1999;3(6):687-95.
31. Sugasawa K, Masutani C, Uchida A, Maekawa T, van der Spek, Pj, Bootsma D, Hoeijmakers JH, Hanaoka F. HHR23B, a human Rad23 homolog, stimulates XPC protein in nucleotide excision repair in vitro. *Mol Cell Biol* 1996;16(9):4852-61.

Appendix

List of Published Manuscripts (three reprints of each enclosed)

1. Clarke, D.J., Segal, M., Mondésert, G. and Reed, S.I. (1999). **The Pds1 anaphase inhibitor and Mec1 kinase define distinct checkpoints coupling S phase with mitosis in budding yeast.** *Current Biol.* 9:365-368.
2. Clarke, D.J., and Giménez-Abián, J.F. (2000). **Review Article: Checkpoints controlling entry into mitosis.** *Bioessays* 22:351-364.
3. Segal, M., Clarke, D.J., Maddox, P., Salmon, E.D., Bloom, K. and Reed, S.I. (2000). **Coordinated spindle assembly and orientation requires Clb5-dependent kinase in budding yeast.** *J. Cell Biol.* 148:441-451.

List of Submitted Manuscripts (three copies of each enclosed)

1. Clarke, D.J., Segal, M., Jensen, S. and Reed, S.I. **Mec1-dependent control of Pds1 levels in response to S-phase checkpoint activation.** Submitted to *Nature Cell Biology*.
2. Jensen, S., Segal, M., Clarke, D.J. and Reed, S.I. **Live cell imaging of the mitotic regulators Esp1 and Pds1 in budding yeast: evidence that localisation of Esp1 to the nucleus and mitotic spindle is regulated by Pds1.** Submitted to *J. Cell Biol.*

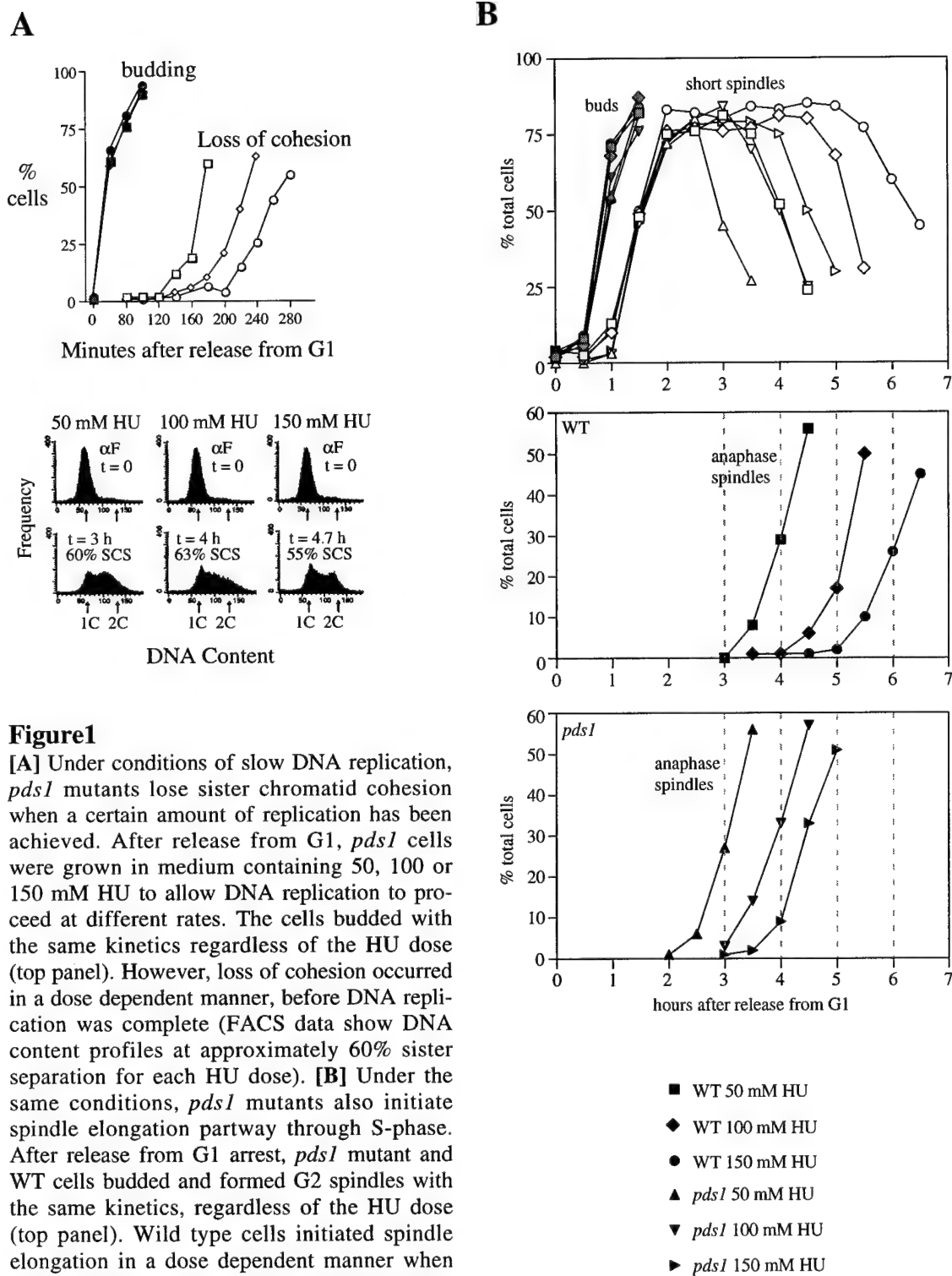
Bibliography

Manuscripts

1. Clarke, D.J., Segal, M., Mondésert, G. and Reed, S.I. (1999). **The Pds1 anaphase inhibitor and Mec1 kinase define distinct checkpoints coupling S phase with mitosis in budding yeast.** *Current Biol.* 9:365-368.
2. Clarke, D.J., and Giménez-Abián, J.F. (2000). **Review Article: Checkpoints controlling entry into mitosis.** *Bioessays* 22:351-364.
3. Segal, M., Clarke, D.J., Maddox, P., Salmon, E.D., Bloom, K. and Reed, S.I. (2000). **Coordinated spindle assembly and orientation requires Clb5-dependent kinase in budding yeast.** *J. Cell Biol.* 148:441-451.
4. Clarke, D.J., Segal, M., Jensen, S. and Reed, S.I. **Mec1-dependent control of Pds1 levels in response to S-phase checkpoint activation.** Submitted to *Nature Cell Biology*.
5. Jensen, S., Segal, M., Clarke, D.J. and Reed, S.I. **Live cell imaging of the mitotic regulators Esp1 and Pds1 in budding yeast: evidence that localisation of Esp1 to the nucleus and mitotic spindle is regulated by Pds1.** Submitted to *J. Cell Biol.*
6. Bertolaet, B., Clarke, D.J., and Reed, S.I. **UBAs are novel protein-protein interaction domains.** In preparation.
7. Clarke, D.J., Mondésert, G., Segal, M., and Reed, S.I. **Dosage suppressors of *pds1* link UBA domains to cell cycle control in yeast.** In preparation.

Abstracts

1. **Upstream elements activating the Pds1-dependent anaphase-checkpoint in yeast.** Duncan J. Clarke, Marisa Segal, Guillaume Mondésert and Steven I. Reed. *EMBO Fellows Meeting, 12-14th July 1998, Heidelberg, Germany.*
2. **Distinct and sequential S-phase checkpoint controls in yeast.** Duncan J. Clarke, Marisa Segal, Sanne Jensen, Guillaume Mondésert and Steven I. Reed. *The Salk Institute Inaugural Cell Cycle Meeting, 18th-22nd June 1999, La Jolla, CA.*
3. **Cyclin-dependent kinase and Cks/Suc1 interact with the proteasome in yeast to control proteolysis of M-phase targets.** Mark H. Watson, Peter Kaiser, Vincent Moncollin, Duncan J. Clarke, Bonnie L. Bertolaet, Steven I. Reed and Eric Bailly. *The Salk Institute Inaugural Cell Cycle Meeting, 18th-22nd June 1999, La Jolla, CA.*
4. **Role Of Pds1 In S-Phase Checkpoint Control.** Duncan J. Clarke, Marisa Segal, Guillaume Mondésert and Steven I. Reed. *British Society for Cell Biology Spring Meeting 1999, Manchester, U.K.*
5. **Distinct and sequential S phase checkpoint controls in yeast.** Duncan J. Clarke, Marisa Segal, Sanne Jensen, Guillaume Mondésert and Steven I. Reed. *DOD Breast Cancer Research Program Meeting 2000, Atlanta, USA.*



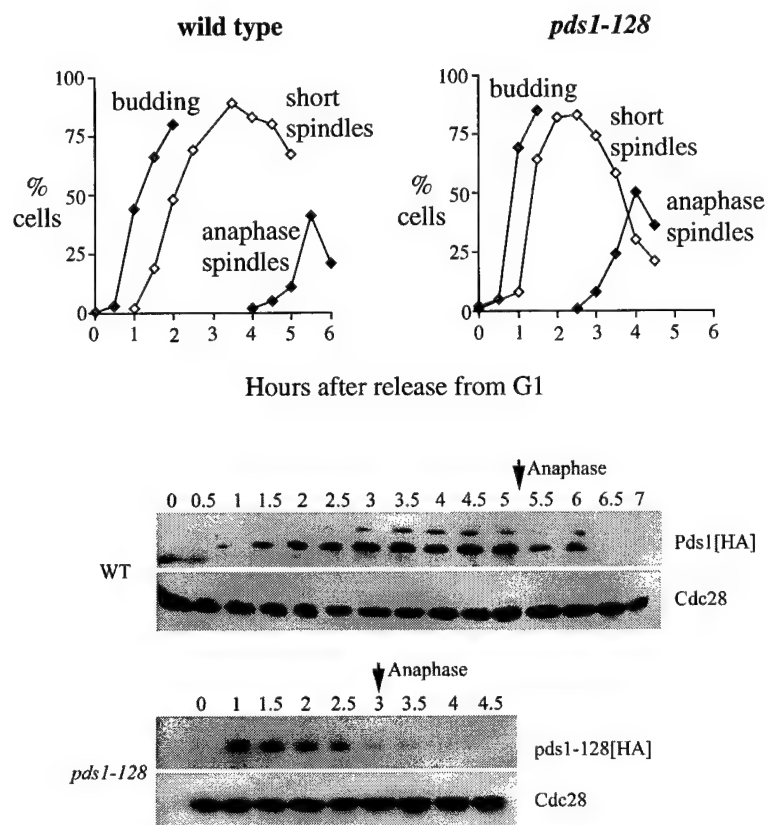


Figure 2

Pds1 levels are maintained under S-phase checkpoint conditions (in HU). We monitored the kinetics of Pds1 degradation and spindle elongation in wild type or *pds1-128*. Cells expressing epitope tagged Pds1 or Pds1-128 were released from G1 arrest into rich medium containing 100 mM HU. The protein data show that in wild type cells, Pds1 is maintained until S-phase is complete and anaphase is initiated. In contrast, Pds1-128 levels diminish during S-phase, roughly coincident with the onset of premature anaphase in the *pds1-128* mutant cells. Cdc28 levels were used as loading controls.

Figure 3

To examine what factors control Pds1 levels under S-phase checkpoint conditions (in HU), we monitored the kinetics of Pds1 degradation and spindle elongation in different checkpoint mutants. Cells expressing epitope tagged Pds1 were released from G1 arrest into rich medium containing 100 mM HU. *mec1*, *rad53* and *rad53chk1* mutants all initiate spindle elongation in early S-phase. The protein data show that Mec1 is required to maintain Pds1 levels in S-phase, while Rad53 and Chk1 are not. Thus Pds1 and Rad53 define two distinct S-phase checkpoint systems, both of which are controlled by Mec1.

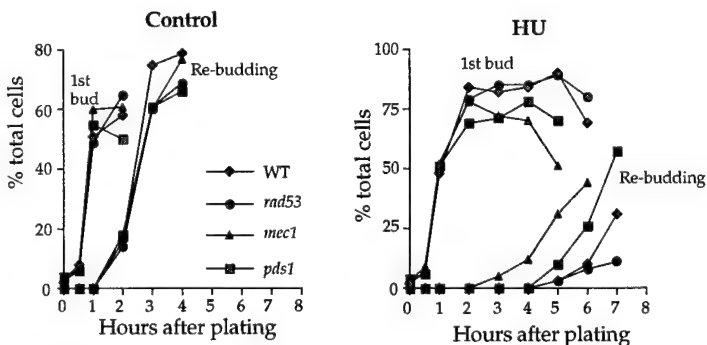
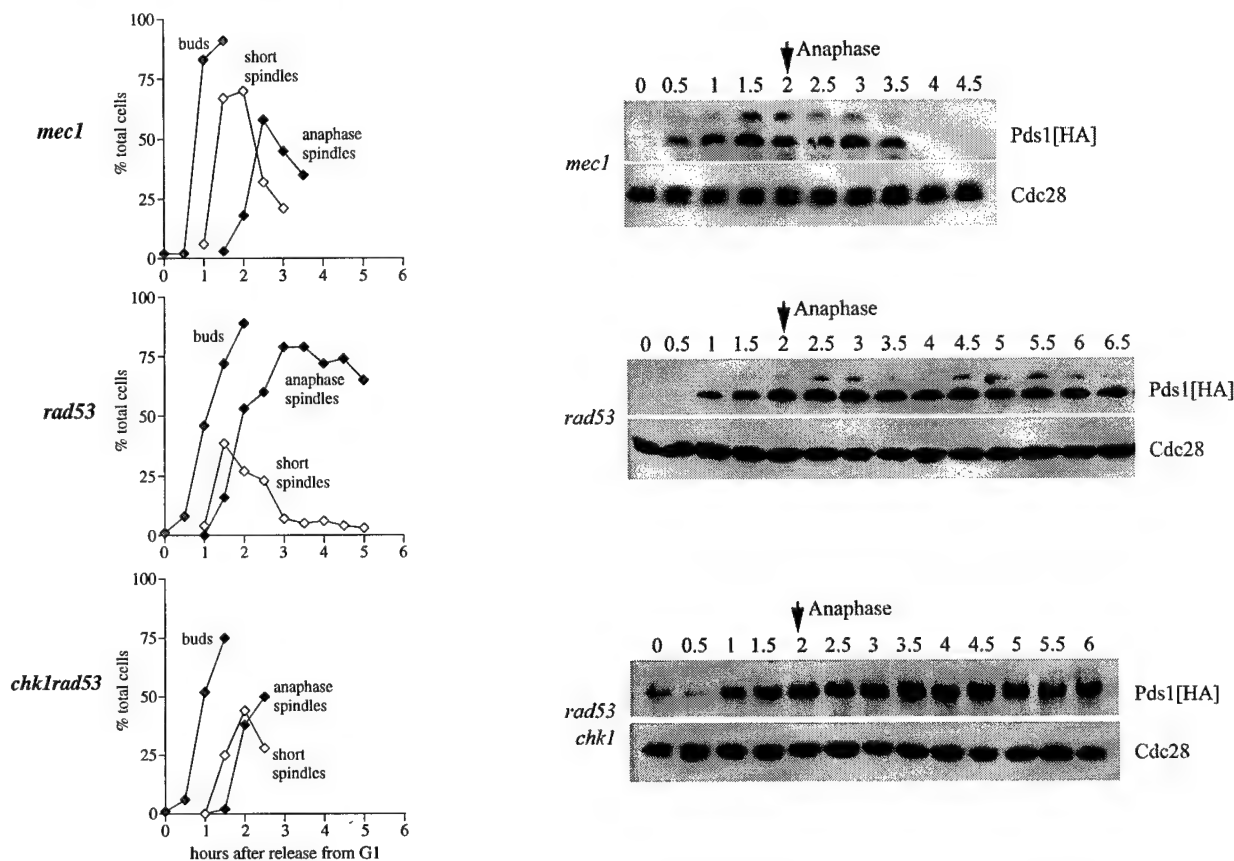


Figure 4

mec1 and *pds1* mutants re-bud following mitosis in the presence of HU. *rad53* mutants do not. Cells were released from G1 arrest and plated onto control solid medium or solid containing HU. Re-budding was scored at intervals.

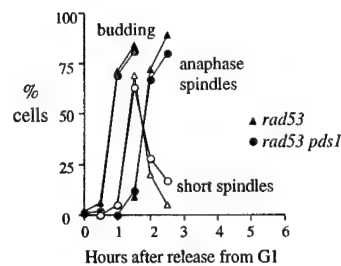


Figure 5

Pds1 is not needed for spindle elongation in early S phase. *rad53* and *pds1 rad53* mutant cells were released from G1 arrest and grown in medium containing 100 mM HU. Premature spindle elongation occurred with similar timing in each strain.

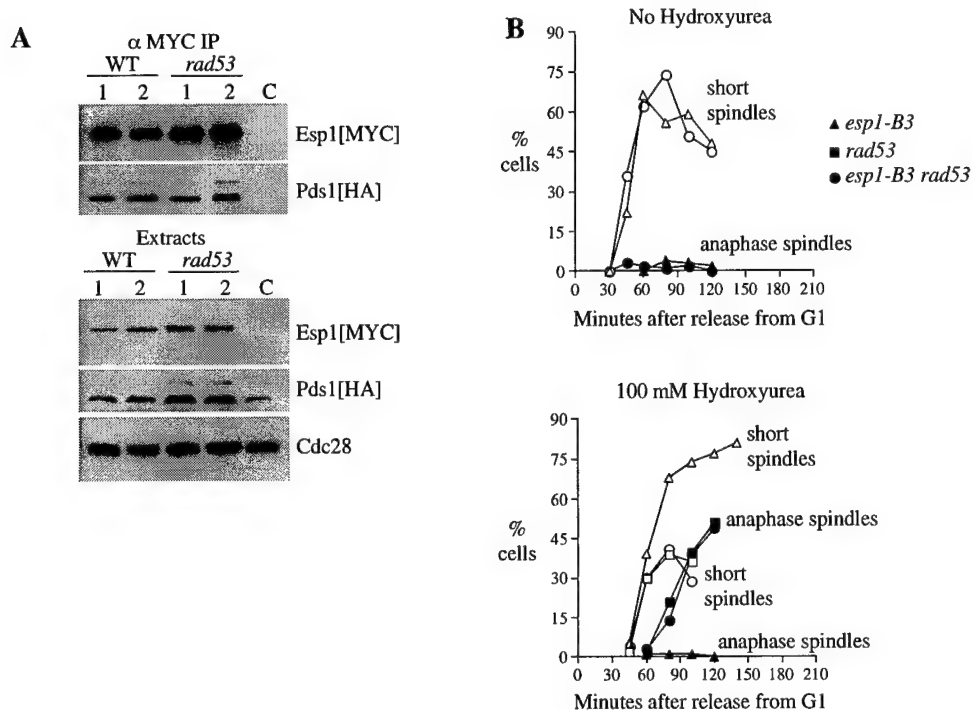
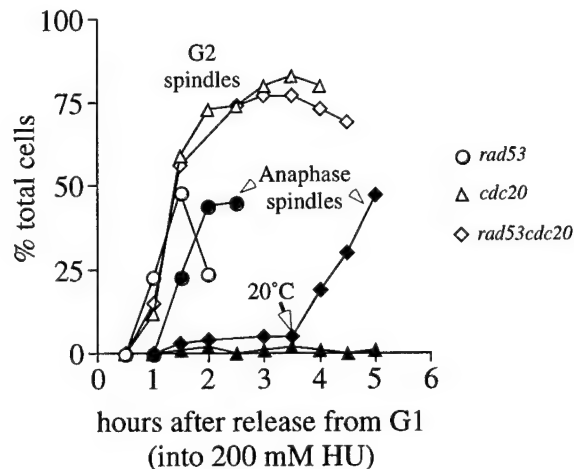


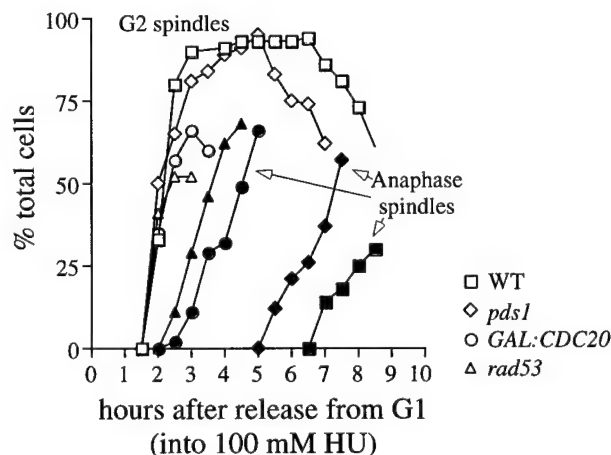
Figure 6

[A] Immuno-precipitation of Esp1-Pds1 complexes from *rad53* cells after HU treatment. For wild type, samples (1) and (2) contained cells arrested with short G2 spindles and partially replicated DNA. For *rad53*, samples contained cells arrested with short G2 spindles and partially replicated DNA (1), or anaphase cells with partially replicated DNA (2). These data show that Pds1-Esp1 complexes do exist in *rad53* mutants in HU. [B] Esp1 is not needed for spindle elongation in early S-phase. After release from G1 into rich medium at 31°C (the restrictive temperature for the *esp1-B3* mutant), *esp1-B3* and *esp1-B3 rad53* could not elongate spindles when these cells reached mitosis (top). Therefore, the *rad53* mutation could not relieve the inability of *esp1-B3* cells to elongate spindles in mitosis. In the presence of HU, *esp1-B3* cells arrested with short G2 spindles while DNA replication was ongoing, confirming that *esp1-B3* cells are S-phase checkpoint proficient. However, *esp1-B3 rad53* cells and *rad53* cells initiated spindle elongation with similar timing when grown in the presence of HU (bottom). Thus, while Esp1 is needed for spindle elongation at mitosis, spindle elongation in early S-phase, upon checkpoint activation, occurs by a mechanism that does not involve Esp1.

A Cdc20p is needed for spindle elongation in *rad53* cells



B GAL:CDC20 induces spindle elongation during S-phase



C Cdc20p accumulates prematurely in *rad53* and *mec1*

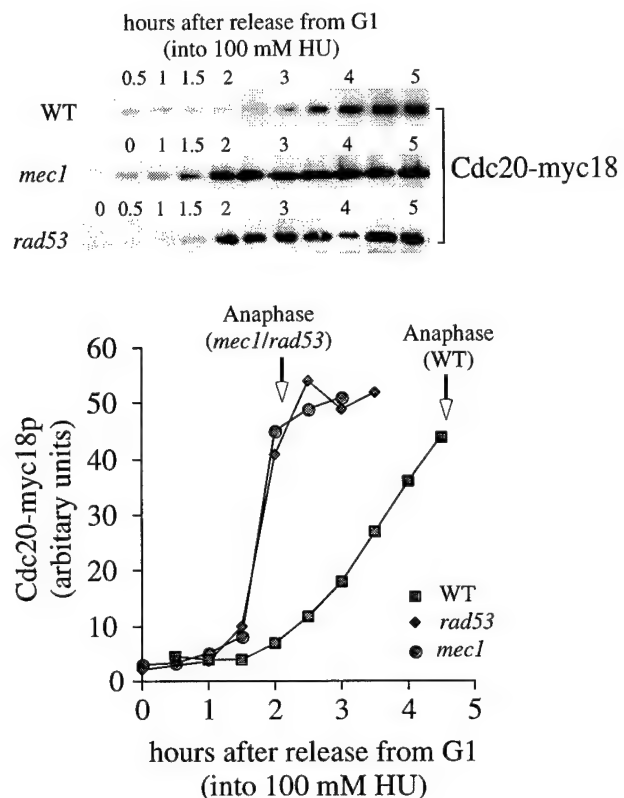


Figure 7

[A] Cdc20p is needed for spindle elongation in *rad53* cells. *rad53*, *cdc20* and *rad53 cdc20* strains were released from G1 arrest into rich medium containing 200 mM hydroxyurea (HU) at 30°C (the restrictive temperature for *cdc20* mutants). Each strain formed short G2 spindles (open symbols) with similar timing and replication was arrested in early S phase (not shown). *cdc20* cells arrested with short G2 spindles even when the cultures were returned to the permissive temperature (20°C) after 3.5 hours, confirming that *cdc20* cells are S-phase checkpoint proficient. *rad53* cells initiated spindle elongation (solid symbols) after 1.5-2 hours due to the S-phase checkpoint defect of these cells. However, *rad53 cdc20* cells were unable to initiate spindle elongation until after the temperature shift to 20°C. **[B] GAL:CDC20 induces spindle elongation during S-phase.** Wild type, *pds1*, *rad53* and cells carrying a *GAL:CDC20* construct were released from G1 arrest into rich galactose medium containing 100 mM hydroxyurea (HU) at 30°C. Each strain formed short G2 spindles (open symbols) with similar timing. Overproduction of *CDC20* produced an S-phase checkpoint defect similar to that of *rad53* cells. Both strains initiated spindle elongation (solid symbols) when little of the genome had been replicated. *pds1* cells, defective in a late S-phase checkpoint control system, initiated spindle elongation part way through S-phase. **[C] Cdc20p accumulates prematurely in *rad53* and *mec1* cells.** Wild type, *rad53* and *mec1* cells carrying an epitope tagged version of *CDC20* were released from G1 arrest into rich medium containing 100 mM hydroxyurea (HU) at 30°C. Cdc20p was analysed after Western blotting and cell cycle progression monitored by scoring budding and spindle morphologies (Anaphase onset is indicated on the graph which is a quantification of the raw protein data). Cdc20p accumulated at the time of anaphase onset in the *rad53* and *mec1* mutants.

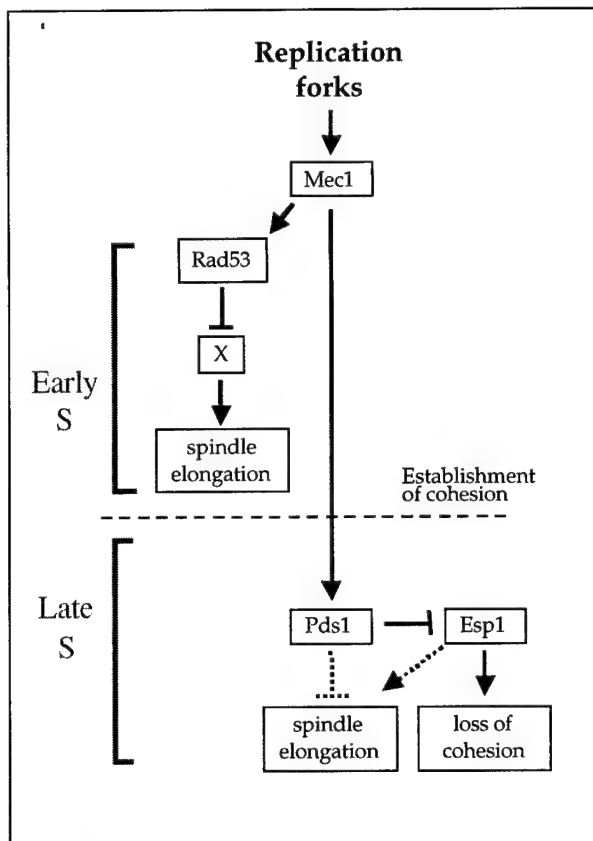


Figure 8

Model for S-phase checkpoint control.
See text for discussion

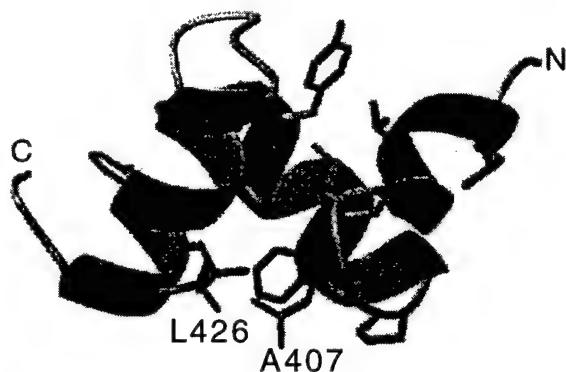


Figure 10

Putative structure of Ddi1 UBA domain (based on NMR structure of human Rad23 UBA). Hydrophobic residues L426 and A407 form a possible protein interaction face.

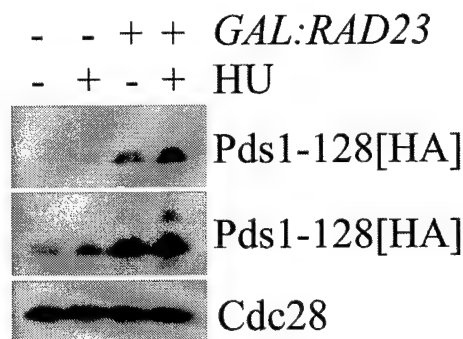


Figure 9

Pds1-128 protein levels are increased by overproduction of Rad23 in asynchronously growing cultures and in cells accumulated in S-phase with hydroxyurea (HU). (Two different exposures of the same Western blot are shown.) Cdc28 protein used as a loading control.

Ddi1 UBA domain mutants

Mutation	Interactions		
	Ddi1	Rad23	Ubiquitin
WT DDI1	+++++	+++++	+++++
V408L	nd	-	-
V408E	nd	-	-
L412P	nd	-	-
G417R	nd	-	+
G417V	+++++	-	++
L426H	nd	-	-
L426A	+++++	-	-
K413I	nd	-	++
E420V	nd	+++	+++++
A407L	nd	+++++	+++++
A407T	nd	nd	nd

Table 1

2-hybrid interactions of wild type (WT) Ddi1 and mutant versions of Ddi1 (left column) with Ddi1, Rad23, and ubiquitin. The relative strength of each interaction is indicated by the number of "+". Partners that did not interact are marked "-". nd=not determined. Of particular interest is L426A in which a leucine within the putative hydrophobic binding face of the Ddi1 UBA is changed to an alanine. This conservative substitution disrupts binding to Rad23 and ubiquitin but does not affect the ability of Ddi1 to homodimerise. When overproduced, this mutant was unable to rescue the temperature sensitivity of *pds1-128*.

The Pds1 anaphase inhibitor and Mec1 kinase define distinct checkpoints coupling S phase with mitosis in budding yeast

Duncan J. Clarke^{*†}, Marisa Segal^{*†}, Guillaume Mondésert[‡] and Steven I. Reed^{*}

In most eukaryotic cells, DNA replication is confined to S phase of the cell cycle [1]. During this interval, S-phase checkpoint controls restrain mitosis until replication is complete [2]. In budding yeast, the anaphase inhibitor Pds1p has been associated with the checkpoint arrest of mitosis when DNA is damaged or when mitotic spindles have formed aberrantly [3,4], but not when DNA replication is blocked with hydroxyurea (HU). Previous studies have implicated the protein kinase Mec1p in S-phase checkpoint control [5]. Unlike *mec1* mutants, *pds1* mutants efficiently inhibit anaphase when replication is blocked. This does not, however, exclude an essential S-phase checkpoint function of Pds1 beyond the early S-phase arrest point of a HU block. Here, we show that Pds1p is an essential component of a previously unsuspected checkpoint control system that couples the completion of S phase with mitosis. Further, the S-phase checkpoint comprises at least two distinct pathways. A Mec1p-dependent pathway operates early in S phase, but a Pds1p-dependent pathway becomes essential part way through S phase.

Addresses: ^{*}Department of Molecular Biology, The Scripps Research Institute, 10550 North Torrey Pines Road, La Jolla, California 92037, USA. [‡]Synthelabo Recherche, Rueil-Malmaison, France.

[†]D.J.C. and M.S. contributed equally to this work.

Correspondence: Steven I. Reed
E-mail: sreed@scripps.edu

Received: 14 December 1998

Revised: 21 January 1999

Accepted: 15 February 1999

Published: 29 March 1999

Current Biology 1999, 9:365–368

<http://biomednet.com/elecref/0960982200900365>

© Elsevier Science Ltd ISSN 0960-9822

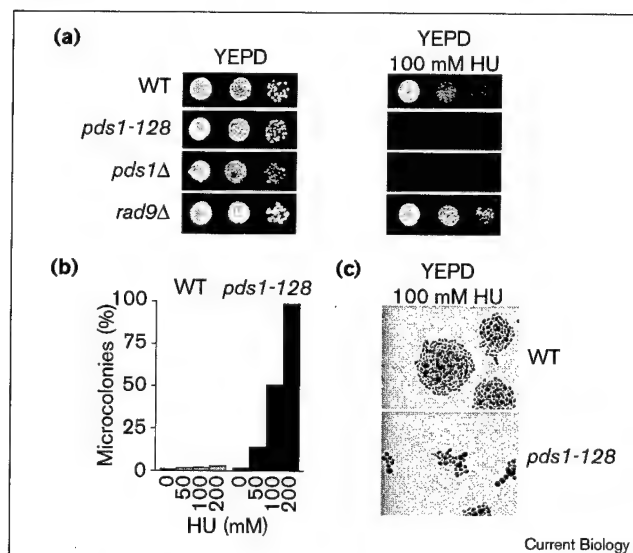
Results and discussion

In budding yeast, initiation of anaphase is controlled by the ubiquitin-dependent degradation of the anaphase inhibitor Pds1p. This process constitutes a target of late cycle checkpoint controls [6]. To address whether Pds1p is required for S-phase checkpoint control, we adopted two approaches. First, we used a hypomorphic *pds1* allele, *pds1-128*, that causes a less severe temperature sensitivity than a null allele and is, therefore, more amenable to the study of cell-cycle events in synchronous populations. Although the restrictive temperature for growth of *pds1-128* cells is 37°C, DNA damage and spindle assembly checkpoint defects are

apparent at 26°C, comparable to those previously described for the *pds1-1* mutant [3,4]. Although a replication block induced by 400 mM HU caused *pds1-128* and *pds1Δ* cells to checkpoint-arrest (data not shown), these mutants were highly sensitive to non-replication-arresting doses of HU (50–100 mM; Figure 1a). On solid medium containing 100 mM HU, *pds1-128* mutants formed microcolonies (Figure 1b,c). In liquid medium containing 100 mM HU, at least 50% of *pds1-128* cells lost viability per generation (see Supplementary material published with this article on the internet). Crucially, *rad9Δ* cells, defective for DNA damage checkpoint control, were not sensitive to 100 mM HU (Figure 1a). Hence, the sensitivity of *pds1* mutants does not result from a Rad9p-dependent DNA damage checkpoint defect.

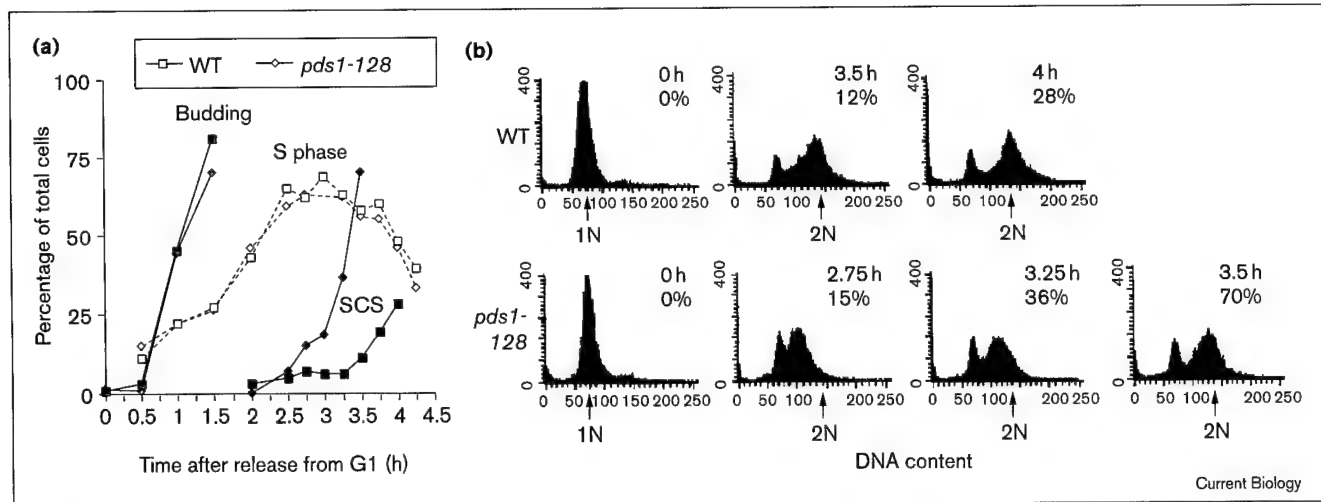
Second, we performed kinetic studies in which the coupling of S phase with mitosis was challenged by partial inhibition of replication. Normally, replication is completed before short G2 spindles form [7]. In the presence of 100 mM HU, replication proceeds at a reduced rate [7]. Only once cells have budded and formed short mitotic spindles must anaphase be delayed to allow the completion of replication. Under these conditions, loss of S-phase

Figure 1



Sensitivity of *pds1* mutants to HU. Serial dilutions of mid-log cells from wild type (WT), *pds1* or *rad9* mutants were spotted onto solid YEPD medium or onto YEPD containing HU and grown at 30°C (25°C for *pds1Δ*). (a) Spot growth was recorded after 2–3 days. After 24 h, microcolonies were (b) counted and (c) photographed.

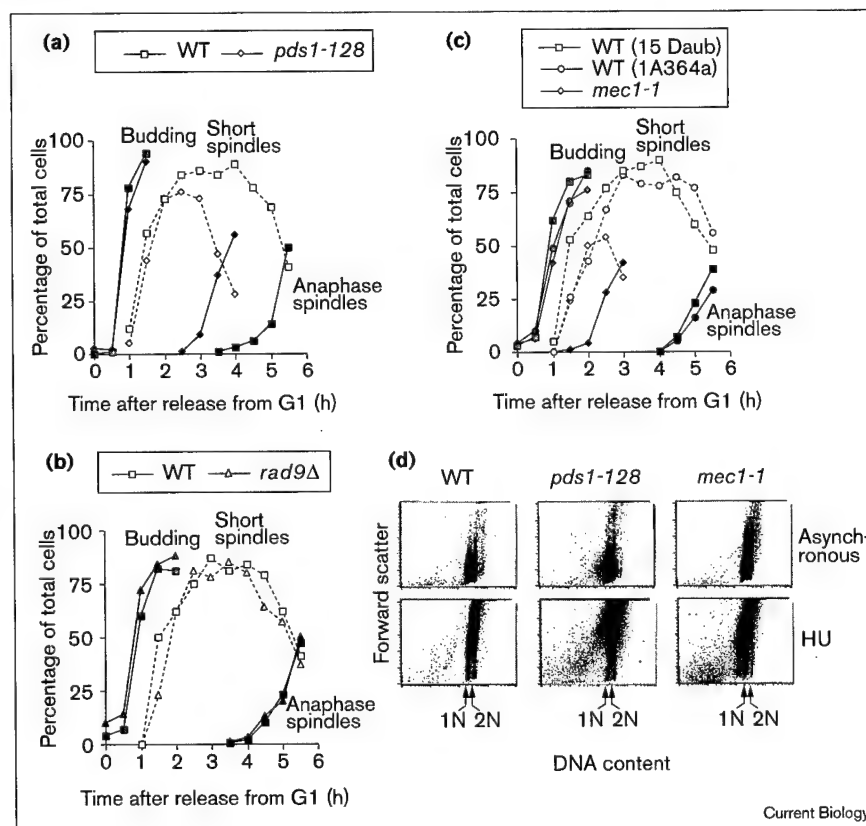
Figure 2



Loss of sister centromere cohesion during S phase in *pds1-128* cells. Wild-type (WT) and *pds1-128* cells were arrested in G1 with 200 ng/ml α factor (at least 90% unbudded cells), then released into rich medium containing 100 mM HU at 30°C. **(a)** Cell aliquots were taken at given time intervals for scoring budding index (gray symbols), sister centromere separation (SCS) for chromosome IV (black symbols), the percentage of cells in S phase (open symbols), and for FACS analysis of DNA content. **(b)** Histograms show the DNA

content of cells in samples at selected time points (the time following α factor release and the percentage of separated centromeres are indicated above the corresponding graph). When *pds1-128* cells divided before DNA replication was complete, nuclear division was unequal. This resulted in G1 cells with greater than 1N DNA content; the next S phase further increased the DNA content of these cells, a fact apparent late in this time course (notice the sub-2N peak for the *pds1-128* cells at 3.5 h).

Figure 3



Distinct checkpoint control defects in *pds1* and *mec1* mutants. Strains were G1-arrested as in Figure 2, then released into rich medium containing 100 mM HU at 26°C. Cell aliquots were taken at given time intervals to score budding index (gray symbols), short spindle formation (open symbols) and spindle elongation (black symbols), and for FACS analysis of DNA content. Each strain replicated DNA with similar kinetics (the kinetics of replication in *mec1-1* cells could not be determined because these cells began anaphase before much DNA had been replicated; data not shown). **(a)** Wild-type (WT) and *pds1-128* cells. **(b)** Wild-type and *rad9Δ* cells. **(c)** Wild-type (in both the 15Daub and A364a genetic backgrounds) and *mec1-1* (A364a genetic background) cells. **(d)** Dot plots of DNA content versus forward scatter for wild-type, *pds1-128* and *mec1-1* cells grown in rich media with or without 100 mM HU for three generations following release from α factor. The positions of 1N and 2N DNA content are indicated. In the presence of 100 mM HU, both *pds1-128* and *mec1-1* cultures contain populations of cells with less than 1N DNA content: about 10% of the total cells after the first division (7 h after release from α factor) of both mutants; 21% for *pds1-128* after three generations (14 h after release); and 31% for *mec1-1* after three generations (14 h after release).

checkpoint control can be unequivocally demonstrated by measuring the relative timing of budding, DNA replication, spindle assembly and the onset of anaphase. Others have identified proteins required for checkpoint arrest when replication has been blocked [5]; we examined checkpoint control during ongoing DNA replication.

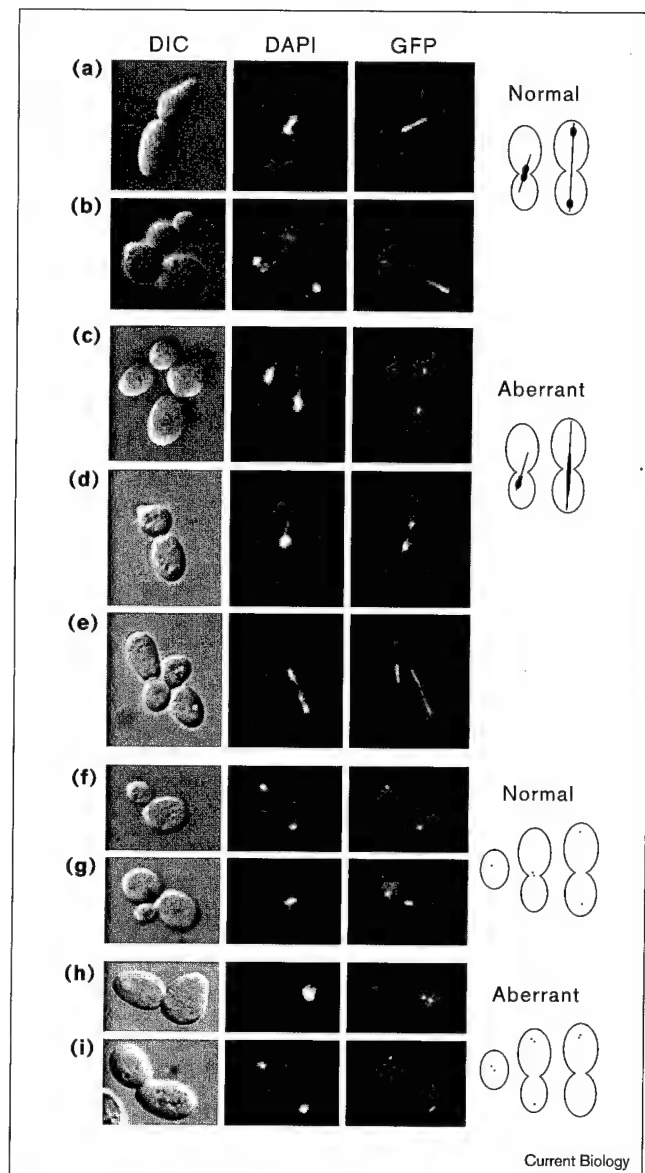
Wild-type and *pds1-128* cells were synchronized in G1 by adding α factor, then released into liquid YEPD medium containing 100 mM HU. To estimate the timing of the onset of anaphase, sister centromere separation was monitored (Figure 2a). Although both strains budded and progressed through S phase with similar timing, sister centromere separation was advanced in *pds1-128* cells. At least 36% of budded *pds1-128* cells had undergone sister centromere separation at a time when most cells were still in S phase, according to FACSscan analysis (Figure 2b). Thus, *pds1-128* cells engage in premature sister centromere separation when the coupling of S phase and mitosis is challenged.

Other aspects of anaphase also occurred prematurely in the *pds1-128* mutants. For example, *pds1-128* cells elongated mitotic spindles about 2 hours before wild-type cells (Figure 3a), even though both strains replicated DNA with similar timing (data not shown). Considering the relatively short G2 interval in budding yeast, the 2 hour advancement of spindle elongation indicates that most *pds1-128* cells must have initiated anaphase before replication was complete. Indeed, FACSscan profiles (data not shown, but see Figure 1) revealed that most cells had less than a 2N DNA content at a time when the bulk of the population had initiated spindle elongation. Wild-type and *pds1-128* cells progressed through S phase and began anaphase with indistinguishable timing in the absence of HU (see Supplementary material).

Uncoupling S phase from mitosis in *pds1-128* cells had several consequences. Following release from α factor in the presence of 100 mM HU, 50% of *pds1-128* cells engaged in an aberrant mitosis (Figure 4). After the first division, a population of cells with less than 1N DNA content was detectable by FACSscan analysis (Figure 3d), and 30% of the newly divided cells exhibited gain or loss of the centromere region of chromosome IV (17% of cells had no centromere region IV signal, 13% had a signal >1; Figure 4), indicating that many nuclei failed to segregate evenly. After three generation times in HU, 50% of cells had an excess of centromere region IV signals and 21% had <1N DNA content. These abortive attempts at anaphase closely resemble those described for *sec1* mutants, in which sister chromatid cohesion fails to become established during S phase [8].

The sensitivity of *pds1* mutants to HU could partly reflect the DNA damage checkpoint defect of these cells because,

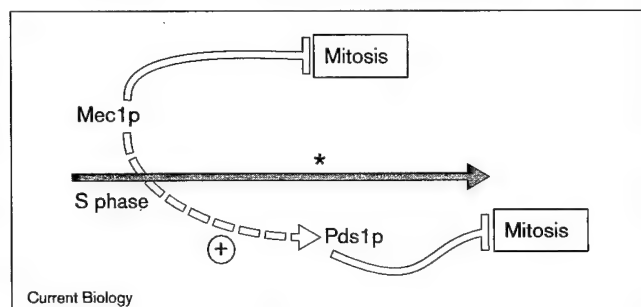
Figure 4



Aberrant mitosis part way through S phase in *pds1-128* cells.

(a,b,f,g) Wild-type and (c-e,h,i) *pds1-128* cells grown in medium containing 100 mM HU. (a-e) Images are from differential interference contrast (DIC) microscopy, 4,6-diamidino-2-phenylindole (DAPI) staining to visualize the chromosomes, and fluorescence microscopy to visualize spindles (using GFP-labeled TUB1). (f-i) Images are from DIC microscopy, DAPI staining and fluorescence microscopy to visualize the centrosome of chromosome IV (using GFP-labeled tetR). (a) Normal early anaphase: spindle partly elongated, nucleus stretched at bud neck. (b) Normal late anaphase: spindle fully elongated, nucleus divided. (c,d) Aberrant early anaphases: spindles partly elongated, nuclei abnormally positioned and stretched. (e) Aberrant late anaphase: spindle fully elongated, nucleus not divided. (f) Normal late anaphase: nuclei divided, each has one GFP signal. (g) Normal early anaphase: nucleus at bud neck, slightly separated centromeres (adjacent GFP signals). (h) Aneuploid *pds1-128* cell: undivided nucleus away from bud neck; two GFP signals. (i) Aneuploid late anaphase *pds1-128* cells; one nucleus has two GFP signals.

Figure 5



Model for coupling replication with mitosis. Possible modes of S-phase checkpoint regulation: Mec1p and Pds1p are essential components of distinct and sequential checkpoint pathways that block mitosis, one active in early S phase, the other active part way through S phase, either operating in parallel (solid lines) or operating in series (additional broken arrow). Part way through S phase (gray arrow), there is a switch (*) in the mode of checkpoint control.

during S phase, HU inevitably causes replicative stress. The severe aneuploidy induced by HU treatment in *pds1* mutants suggests, however, that loss of coordination between replication and mitosis is responsible for the lethality. Indeed, *rad9Δ* cells, defective for all known aspects of DNA damage checkpoint control [9] but not sensitive to HU (Figure 1), were proficient at coupling S phase with mitosis, using the same experimental conditions as described above (Figure 3b). Therefore, the S-phase Pds1p-dependent checkpoint system is Rad9p-independent.

We have shown that Pds1p is required to couple ongoing replication with mitosis. An outstanding issue is why *pds1* mutants arrest efficiently when replication is completely blocked. One intriguing explanation could be that S phase and mitosis are coupled by distinct checkpoint pathways that act sequentially. To test this, we compared the checkpoint defect of *pds1-128* with that of *mec1*, the prototypic S-phase checkpoint mutant [5]. When the *mec1* checkpoint defect was analysed during partial inhibition of replication, we observed that *mec1* cells initiated anaphase as soon as spindle assembly occurred (Figure 3c). In contrast, although *pds1-128* cells began anaphase prematurely, there was a distinct period in early S phase when mitosis was restrained. This was also true of the *pds1* null mutant (see Supplementary material).

Rather than regulating mitotic kinase activity, the budding yeast DNA damage and spindle assembly checkpoints inhibit anaphase directly by stabilizing the inhibitor Pds1p [6]. This work demonstrates that Pds1p, as well as Mec1p, is essential to coordinate ongoing DNA replication with mitosis. Although both of these proteins are required, they must act at different times in S phase and in distinct pathways (Figure 5). Mec1p must function either independently of Pds1p throughout S phase, or

independently of Pds1p in early S phase but upstream of Pds1p later in S phase. We propose that an event intrinsic to the progression of DNA replication elicits a switch in the mode of checkpoint regulation. As Pds1p is required for maintaining sister centromere cohesion, the Pds1p-dependent pathway may operate only once centromere cohesion has been established, an event that is likely to be completed by mid-S phase, when centromeric regions have been replicated [8,10]. Alternatively, Pds1p may be required following the initiation of late replication origins, because Mec1p was recently shown to be essential for an early S-phase checkpoint that inhibits late origin firing [11]. In response to DNA damage and spindle assembly checkpoint controls, Pds1p degradation is inhibited. By analogy, ongoing DNA replication may signal Pds1p stabilization in order to restrain anaphase until replication is completed.

Supplementary material

Additional methodological details, yeast strain genotypes and supplementary figures are published with this article on the internet.

Acknowledgements

We thank T. Weinert for yeast strains, A. Straight and A. Murray for TUB1-GFP constructs, M. Wolff for GFP:tet system construction, and M. Smeets, who originally observed that *pds1* mutants are sensitive to sub-arresting concentrations of HU. D.J.C. was funded by EMBO and US Army Breast Cancer Research fellowships. M.S. was funded by EMBO and HFSP fellowships.

References

1. Mitchison JM: *The Biology of the Cell Cycle*. Cambridge: Cambridge University Press; 1971.
2. Elledge SJ: **Cell cycle checkpoints: preventing an identity crisis**. *Science* 1996, **274**:1664-1672.
3. Yamamoto A, Guacci V, Koshland D: **Pds1p, an inhibitor of anaphase in budding yeast, plays a critical role in the APC and checkpoint pathway(s)**. *J Cell Biol* 1996, **133**:99-110.
4. Yamamoto A, Guacci V, Koshland D: **Pds1p is required for faithful execution of anaphase in the yeast *Saccharomyces cerevisiae***. *J Cell Biol* 1996, **133**:85-97.
5. Weinert TA, Kiser GL, Hartwell LH: **Mitotic checkpoint genes in budding yeast and the dependence of mitosis on DNA replication and repair**. *Genes Dev* 1994, **8**:652-665.
6. Cohen-Fix O, Peters JM, Kirschner MW, Koshland D: **Anaphase initiation in *Saccharomyces cerevisiae* is controlled by the APC-dependent degradation of the anaphase inhibitor Pds1p**. *Genes Dev* 1996, **10**:3081-3093.
7. Lew DJ, Weinert TA, Pringle JR: **Cell cycle control in *Saccharomyces cerevisiae***. In *The Molecular and Cellular Biology of the Yeast *Saccharomyces cerevisiae*: Cell Cycle and Cell Biology*. Edited by Pringle JR, Broach JR, Jones EW. Cold Spring Harbor, New York: Cold Spring Harbor Press; 1997:607-696.
8. Uhlmann F, Nasmyth K: **Cohesion between sister chromatids must be established during DNA replication**. *Curr Biol* 1998, **8**:1095-1101.
9. Weinert TA, Hartwell LH: **The *RAD9* gene controls the cell cycle response to DNA damage in *Saccharomyces cerevisiae***. *Science* 1988, **241**:317-241.
10. Campbell JL, Newlon CS: **Chromosomal DNA replication**. In *The Molecular and Cellular Biology of the Yeast *Saccharomyces cerevisiae*: Genome Dynamics, Protein Synthesis and Energetics*. Edited by Pringle JR, Broach JR, Jones EW. Cold Spring Harbor, New York: Cold Spring Harbor Press; 1991:41-146.
11. Santocanale C, Diffley JFX: **A Mec1- and Rad53-dependent checkpoint controls late-firing origins of DNA replication**. *Nature* 1998, **395**:615-618.

Checkpoints controlling mitosis

Duncan J. Clarke¹* and Juan F. Giménez-Abián²

Summary

Each year many reviews deal with checkpoint control.^(1–5) Here we discuss checkpoint pathways that control mitosis. We address four checkpoint systems in depth: budding yeast DNA damage, the DNA replication checkpoint, the spindle assembly checkpoint and the mammalian G2 topoisomerase II-dependent checkpoint. A main focus of the review is the organization of these checkpoint pathways. Recent work has elucidated the order-of-function of several checkpoint components, and has revealed that the S phase, DNA damage and spindle assembly checkpoints each have at least two parallel branches. These steps forward have largely come from kinetic studies of checkpoint-defective mutants. *BioEssays* 22:351–363, 2000.

© 2000 John Wiley & Sons, Inc.

Introduction

First, let us deal with the obligatory definition. A checkpoint is: "a mechanism that establishes a dependence relationship between two cellular processes that are biochemically unrelated". The cell cycle consists of a consecutive series of processes, generally invariant in their order, which successively double then halve the whole cell mass to produce almost identical daughter cells. Some of these processes must be controlled and monitored to ensure their accuracy. In particular, faithful replication and division of the genome, the basic events of genetic inheritance, are crucial for cell survival and integrity. Independently of checkpoint controls, the sequence of two specific events can be maintained during each cell cycle if the processes have a common starting point and require a minimum amount of time for their completion. This is a "timing" mechanism. For example, in budding yeast (*Saccharomyces cerevisiae*), DNA replication and mitotic spindle formation are initiated at a common cell cycle point, early in S phase. It is essential that the mitotic spindle does not elongate before DNA replication has been completed (the final result would be aneuploid daughter cells that are not viable), but DNA

replication takes only 20–30 minutes and spindle formation takes around 60 minutes. Thus, normally spindles cannot elongate until DNA replication has been completed. Such timing mechanisms can determine the order of two processes, but are not checkpoint controls. However, a checkpoint pathway does exist to ensure that the dependence between spindle elongation and DNA replication is maintained in budding yeast. This can be demonstrated by inhibiting DNA replication, for example with the ribonucleotide reductase inhibitor hydroxyurea (HU).⁽⁶⁾ In this case, these cells arrest with assembled short G2 spindles. After removal of the HU, spindle elongation does not proceed until replication is complete. Thus, the S-phase checkpoint establishes a dependence relationship between completion of DNA replication and anaphase in budding yeast. Checkpoint controls are required when a later event is not dependent on completion of an earlier event. In addition to maintaining dependence relationships, checkpoints modulate cell cycle progression in response to adverse conditions, such as when DNA becomes damaged.

If the classic definition is applied, such delay mechanisms can only be attributed to checkpoint controls if the later event is physically able to occur at a time when the earlier event is not yet complete. For the S-phase checkpoint in budding yeast, the question is whether spindle elongation can occur in the presence of HU (before DNA replication is complete). Therefore, the formal description of the S-phase checkpoint was based on the isolation of loss-of-function yeast mutants in which spindles elongated despite a replication block enforced by HU. However, the existence of checkpoint controls in mammalian cells had been inferred much earlier than these genetic analyses performed in yeast. Rao and Johnson fused mammalian cells that were at different cell cycle stages.⁽⁷⁾ A metaphase cell fused with an S-phase or G2 cell induced chromosome condensation in these interphase partners (Fig. 1). The conclusion was that a dominant factor in the mitotic cell could override the cell cycle stage in the S-phase or G2 cell. Mammalian checkpoint controls have been inferred more recently by showing that cell cycle arrest, induced for example by DNA damage or DNA replication inhibition, can be overridden by certain chemicals (e.g. caffeine; Fig. 1).

In this review, we discuss mitotic checkpoint control. As mentioned above, an elegant way to define checkpoint pathways has been by the analysis of loss-of-function mutants in yeast systems that can be genetically manipu-

¹The Scripps Research Institute, La Jolla, California, USA.

²Centro de Investigaciones Biológicas, Consejo Superior de Investigaciones Científicas, Velázquez, Madrid, Spain.

Funding agencies: US Army Medical Research; Materiel Command and Comunidad Autónoma de Madrid.

*Correspondence to: D. J. Clarke, The Scripps Research Institute, 10550 N. Torrey Pines Rd, La Jolla, CA 92037 USA. E-mail: duncs@scripps.edu

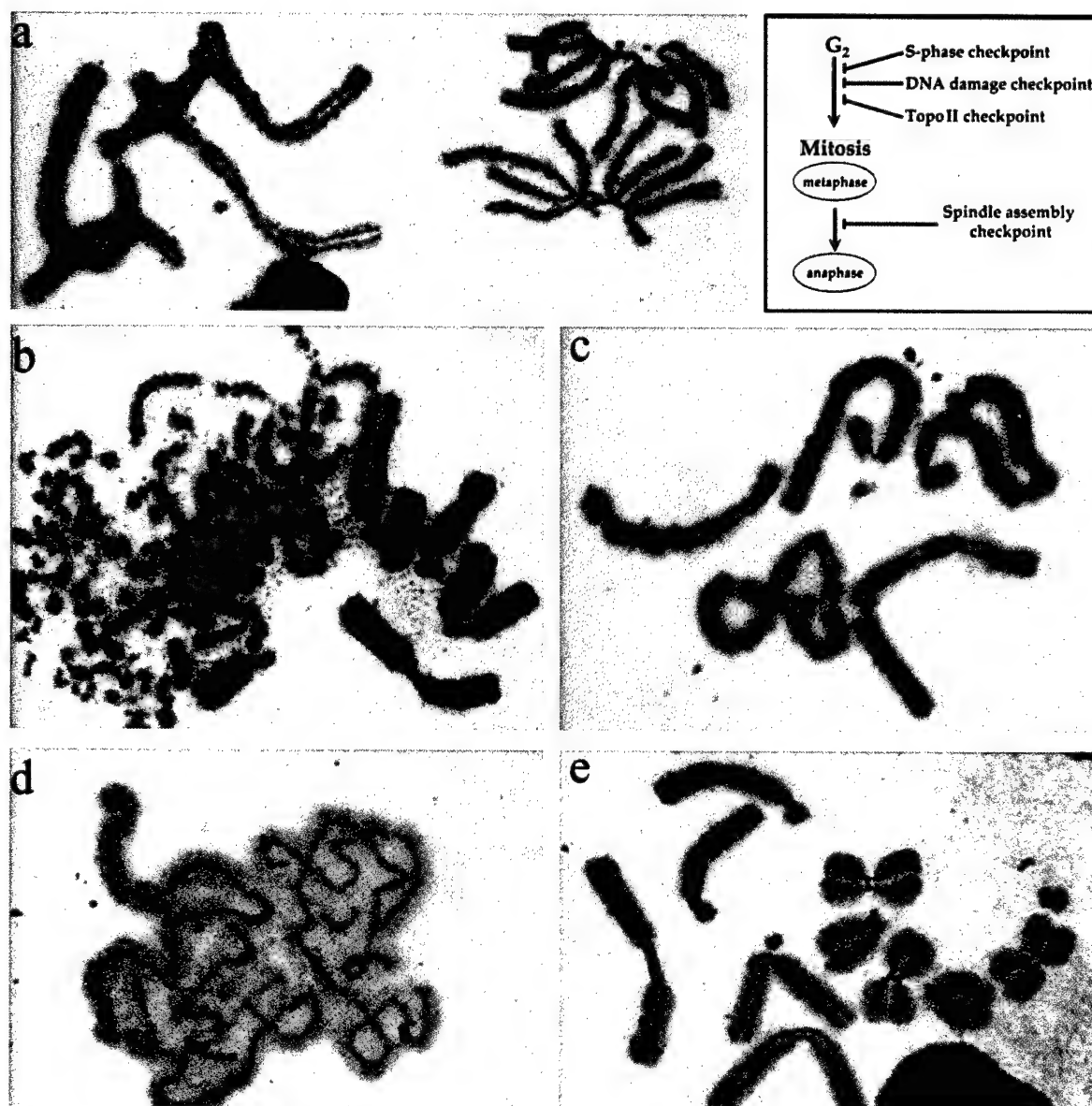


Figure 1. Checkpoints controlling mitosis. In mammals the G₂–M transition is regulated by at least three checkpoint pathways (line diagram, top right). These prevent the initiation of mitosis until DNA replication is complete, DNA damage has been repaired and DNA is sufficiently decatenated. In budding yeast, similar checkpoint controls inhibit the onset of anaphase rather than preventing passage beyond the G₂–M transition. Therefore, the G₂–M transition in mammals and the metaphase–anaphase transition in budding yeast are somewhat analogous. Indeed, sensor and signaling components of these checkpoint pathways are conserved. However, the checkpoint targets differ between mammals and budding yeast. In addition, both mammals and budding yeast use a spindle assembly checkpoint that delays the onset of anaphase until all the chromosomes of the karyotype have been aligned correctly, forming the metaphase plate. **a–e:** Photomicrographs of mammalian chromosomes (*Muntiacus muntjak*) depicting checkpoint control from the viewpoint of chromosome structure. **a:** The metaphase–anaphase transition. A metaphase cell is seen on the left. An anaphase cell, in which sister chromatids have separated irreversibly and are segregating to opposite poles of the mitotic spindle, is on the right. **b:** S-phase checkpoint override. Metaphase cell fused with an S-phase cell. Metaphase chromosomes are on the right, S-phase chromosomes induced to condense prematurely are on the left (notice that the S-phase chromosomes appear broken—“pulverized”—in regions that have not yet replicated). **c:** DNA damage checkpoint override. Metaphase chromosomes of a cell that entered mitosis (adapted) despite (continued)

lated. Mutants were isolated that begin mitosis before DNA replication has been completed, when DNA is damaged, or when mitotic spindles have assembled aberrantly. A fourth checkpoint, not functional in yeast, ensures that DNA topology has been correctly organized before mitosis in mammalian cells. Figure 1 summarizes the checkpoints discussed in this review and provides visual examples of how checkpoint failure can have disastrous results.

There is a general structure common to the known checkpoints. In simple terms there are three parts, which are defined as: (1) the sensor, (2) the transducer and (3) the target. The sensor monitors completion of the relevant process—for example, DNA replication—or detects an adverse condition such as DNA damage (then monitors the removal of damage in the latter case). The transducer transmits the signal from the sensor to the target of the checkpoint. So far, two distinct mechanisms have been identified that inhibit mitosis in eukaryotes. First, checkpoints can inhibit the activity of the mitotic kinase [cyclin/cyclin-dependent kinase (Cdk)], required for passage through the G2–M transition. Mitotic cyclin–Cdk activity is controlled by several factors including: (1) availability of the cyclin component, (2) binding of Cdk inhibitors and (3) Cdk

phosphorylation.⁽²⁾ This is the primary mode of regulation adopted by most eukaryotes including mammals. Second, checkpoints can act independently of mitotic cyclin–Cdk activity, by stabilizing inhibitors that prevent the onset of anaphase of mitosis. This mechanism is crucial in budding yeast cells, which checkpoint arrest at the metaphase–anaphase transition with high mitotic cyclin–Cdk activity.

A need for these two distinct modes of control has arisen primarily because of differences in the spindle assembly pathway. In many eukaryotes, including mammals and fission yeast, the mitotic spindle does not assemble until after mitosis has begun. However, in budding yeast, spindles assemble during S phase, and this process requires cyclin–Cdk activity. Therefore, the mitotic entry checkpoints must inhibit spindle elongation (one component of anaphase) independently of kinase activity. In addition, sister chromatid cohesion, established during DNA replication, must be maintained until the onset of anaphase. An inhibitor of anaphase, Pds1, has been identified in budding yeast.^(8–11) In most situations, Pds1 is both necessary and sufficient to prevent spindle elongation and loss of sister chromatid cohesion. Expression of a degradation-resistant *pds1* mutant blocks anaphase onset, whereas *pds1* null strains are

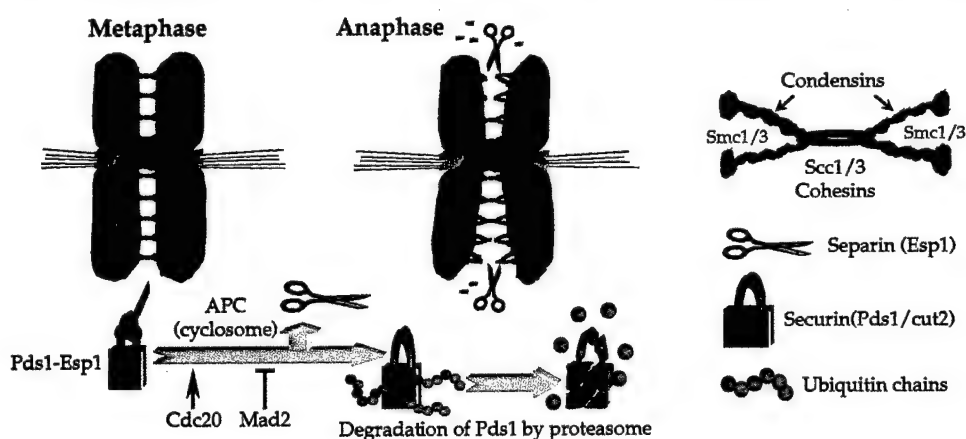


Figure 2. Regulation of anaphase in budding yeast. During DNA replication, sister DNA molecules become associated by the formation of protein complexes formed by the cohesins, Scc1 and Scc3, and the condensins, Smc1 and Smc3. Separation of sisters at anaphase requires loss of cohesion, initiated by Scc1 cleavage, and is dependent on the separin, Esp1. Before anaphase, Esp1 separin activity is inhibited by Pds1. At the onset of anaphase, Pds1 becomes ubiquitinated by the APC (cyclosome) and degraded by 26S proteasome complexes. Checkpoints maintain Pds1 stability, for example by inhibiting APC. (Based on Ref. 14.)

Figure 1. (caption continued)

the presence of chromosome damage. Chromatid breaks and recombination events are seen. **d:** Topoisomerase II (topo II)-dependent checkpoint override. Metaphase chromosomes that have failed to become individualized, have not resolved sister chromatids, and have not condensed fully—a cell arrested in G2 by inhibiting topo II activity was induced to enter mitosis by adding caffeine. **e:** Spindle assembly checkpoint arrest. Chromosomes of the cell on the right have become hyper-condensed owing to a prolonged metaphase arrest in the presence of nocodazole (a drug that inhibits spindle formation); the effects on chromosome morphology are more severe than in the cell on the left, which has arrested more recently in metaphase.

defective in anaphase checkpoint control. Before anaphase, Pds1 binds to Esp1 and thereby inhibits the anaphase-promoting activity of Esp1 (Fig. 2).⁽¹¹⁾ During an unperturbed cell cycle, Pds1 becomes polyubiquitinated at the metaphase to anaphase transition by a multisubunit enzyme complex known as the APC (anaphase promoting complex, also called the cyclosome); the modified forms are then recognized and degraded by 26S proteasomes.⁽⁹⁾ Once released from Pds1, Esp1 becomes active and this activity induces cleavage of Scc1. Scc1 is a cohesin, required to establish and maintain cohesion between sister chromatids during S phase.^(11–14) Concurrently with loss of sister cohesion, spindle elongation is initiated. Not surprisingly, Pds1 is a major target of the checkpoints controlling onset of anaphase in budding yeast. Checkpoint signals have the opportunity to regulate various aspects of the Pds1 degradation pathway including the APC, enzymes that de-ubiquitinate Pds1 and the 26S proteasome.

The fission yeast protein, cut2, is a partial functional homolog of Pds1.⁽¹⁵⁾ It inhibits anaphase and must be degraded for anaphase to be initiated. Vertebrate proteins, named securins, which are at least partial functional homologs of Pds1/cut2, have also been identified.⁽¹⁶⁾ Thus, control of anaphase by regulating degradation of inhibitors is likely to be a universal mechanism. Although most eukaryotes primarily regulate cyclin–Cdk activity to control entry into mitosis, parallel systems acting on the metaphase–anaphase transition might have been overlooked. It is important to remember that although S-phase and G2 checkpoints do not need to inhibit spindle elongation in many eukaryotes, sister chromatid cohesion must in all cases be maintained until the onset of anaphase.

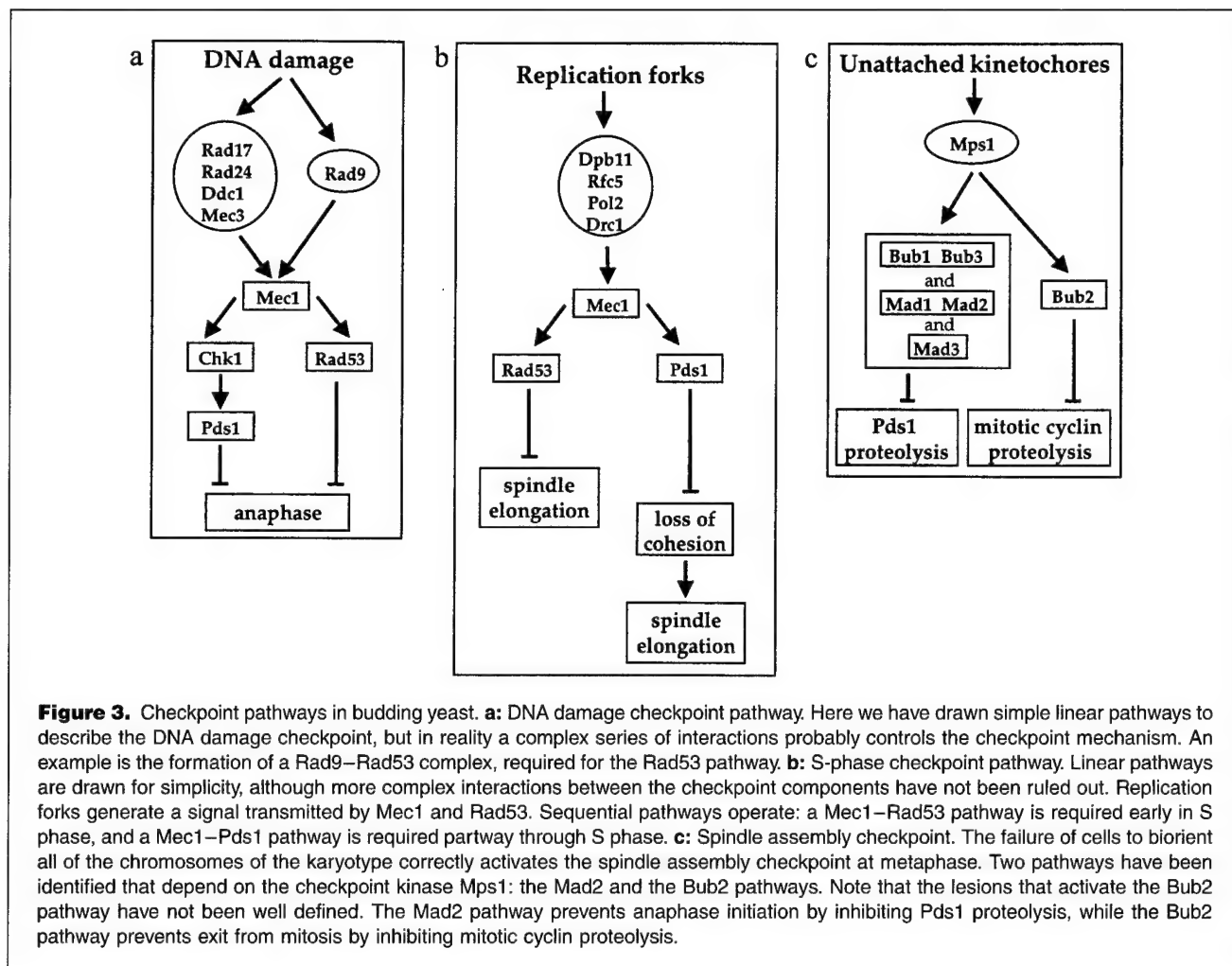
DNA damage checkpoint

The genetic definition of the DNA damage checkpoint in budding yeast led to our current appreciation of checkpoint controls.^(17,18) Over 10 years ago, Weinert and Hartwell hypothesized that dominant cellular mechanisms delay cycle progression when DNA is damaged. They demonstrated that a loss-of-function yeast mutant, *rad9*, was unable to inhibit anaphase when DNA had been damaged. Indeed, a single double-stranded DNA break is sufficient to activate the checkpoint response in budding yeast. The most important recent development has been the confirmation that the checkpoint consists of at least two parallel pathways. These experiments also directly investigated the order-of-function of several checkpoint components.⁽¹⁹⁾ Work with mammalian cells has confirmed that structural homologs of several yeast DNA damage checkpoint proteins are also functionally homologous. Novel targets of the mammalian DNA damage checkpoint have also been identified recently.

Evidence suggests that DNA damage checkpoint proteins sense single-stranded DNA.^(18,20,21) However, structurally

different DNA lesions can arrest cells before mitosis/anaphase. This discrepancy could be explained if different types of damage are recognized by repair systems, then during the process of repair, single-stranded DNA regions are formed that are detected by the checkpoint sensors. Indeed, some of the proteins that are thought to form the core of checkpoint sensors might also participate in the processing of DNA lesions in addition to initiating the checkpoint response.⁽¹⁸⁾ In budding yeast, the putative sensor components are Rad9, Rad24, Rad17, Mec3 and Ddc1 (Fig. 3).^(17,18,22–24) Based on additive sensitivities of the mutants to DNA-damaging agents, and differences in the processing of DNA lesions, these genes can be placed into two groups; the Rad9 class (just *rad9*), and the Rad24 class (*rad24*, *rad17*, *mec3*, and *ddc1*).^(18,24) For example, *rad24 rad9* double-mutant cells are far more sensitive to MMS (a DNA alkylating agent) than either of the single mutants. However, the mutants cannot be distinguished from one another based on the kinetics of entry into mitosis in the presence of DNA damage.⁽¹⁸⁾ A loss-of-function mutation in any one of the Rad9 or Rad24 group genes causes full penetrance of the checkpoint-defective phenotype: the timing of anaphase initiation is the same whether DNA damage is present or absent. Therefore, each protein is equally important for enforcing checkpoint arrest.

The sensor components activate checkpoint kinases Mec1, Rad53 and Chk1, which make up the signal transduction component of the checkpoint control system.^(6,23,25) Mec1, a member of the PI-kinase-like family of proteins, is probably the most upstream kinase of the transduction pathway,^(10,19,26,27) and therefore might be a mediator, acting between the sensor complexes and checkpoint targets such as Pds1. Like mutants of the Rad9 and Rad24 groups, *mec1* mutants have a fully penetrant checkpoint defect.^(19,25) When genes encoding components downstream of Rad9, Rad24 and Mec1, are mutated partial checkpoint defects are seen.^(19,25) Kinetic studies first demonstrated that *rad53* and *pds1* mutants can delay anaphase for about 90 minutes in the presence of irreparable DNA damage (compared with no delay in *mec1* mutants and an 8–10 hour delay in wild-type cells).⁽¹⁹⁾ This elegant study also showed that *rad53-pds1* double-mutant cells have a fully arrest-defective phenotype (similar to that of *mec1*), providing strong evidence that there are two parallel pathways that act downstream of Mec1 — the “Rad53 pathway” and the “Pds1 pathway” (Fig. 3). Biochemical studies revealed that the phosphorylation of Rad53, which is induced by DNA damage, depends on Mec1 activity,^(26,27) and similarly, that the phosphorylation of Pds1 depends on Mec1 but not on Rad53.⁽¹⁰⁾ These data suggest an order-of-function of the checkpoint components, although they do not demonstrate one. Firm conclusions regarding order-of-function cannot be based on phosphorylation studies because the phosphorylation event in question could



be part of a feedback mechanism. Moreover, in the case of Pds1 phosphorylation, the biological relevance of this modification has not been demonstrated. Nevertheless, the phosphorylation studies do provide a possible biochemical explanation for the order-of-function of Mec1, Rad53, and Pds1 established by the cell cycle kinetic studies described above. These crucial experiments were supplemented recently by biochemical and kinetic studies of *chk1* mutant cells.⁽²⁵⁾ This work placed Chk1 kinase in the Mec1–Pds1 branch of the DNA damage checkpoint pathway, and demonstrated that Chk1 phosphorylation, induced by DNA damage, depends on Mec1 and Rad9, but does not require Rad53. Pds1 phosphorylation required Chk1 kinase (Fig. 3).

In response to DNA damage, phosphorylation of several other checkpoint components depends on Mec1.^(22,24,28) Mec1 is partially required for phosphorylation of Rad9 and Ddc1 in response to DNA damage. Why should this be the case, as these are thought to be parts of the sensor complex and thus should be upstream of Mec1? One possibility is that Rad9 and Ddc1 are regulatory subunits of complexes

that operate in a Mec1-dependent manner. Activation of these complexes could involve autophosphorylation of some components including Rad9 and Ddc1. These data highlight the dangers of assuming order-of-function based solely on biochemical analysis, although they did reveal the nature of a key signaling component of the Rad53 pathway. DNA damage-induced Rad9 phosphorylation, dependent on Mec1, allows Rad9 to bind to Rad53.^(28,29) The Rad9–Rad53 complex is required for the checkpoint response, and is presumably the activating component of the Rad53 pathway.

Rad53 phosphorylation requires not only Rad9 and Mec1, but also the members of the Rad24 group.⁽²⁷⁾ In contrast, phosphorylation of Pds1 requires Rad9, but not members of the Rad24 class, indicating that distinct checkpoint-activating complexes operate in a Mec1-dependent manner.^(10,24) Ddc1 phosphorylation requires Mec1 and the Rad24 group, but not Rad9,⁽²⁴⁾ thus further separating the Rad9 and Rad24 classes. Clearly, multiple protein interaction and phosphorylation events participate ultimately to activate the Mec1–Rad53 and the Mec1–Pds1 pathways.

The mechanism by which the Mec1–Pds1 pathway prevents the initiation of anaphase has been resolved to some extent. Dependent on Chk1 kinase activity, Pds1 degradation is blocked and thus Esp1 activity is inhibited. However, the mechanism of anaphase delay enforced by the Mec1–Rad53 pathway is less well characterized. One checkpoint component that acts downstream of Mec1 and Rad53 is Dun1 protein kinase (damage uninducible).⁽⁶⁾ Activation of Dun1, in response to DNA damage, induces transcription of genes that promote efficient DNA repair.⁽⁶⁾ This transcription response, dependent on Mec1 and Rad53, is partially initiated by Crt1 hyperphosphorylation.⁽³⁰⁾ Crt1 represses transcription of DNA damage-inducible genes by binding to their promoter regions; binding is prevented by hyperphosphorylation. The transcription response presumably contributes towards inhibition of anaphase, because the kinetics of anaphase initiation in the presence of damage are similar in *dun1* mutants and *rad53* mutants.⁽¹⁹⁾ The partial checkpoint defect of *dun1* cells is fully penetrant in the *dun1-pds1* double mutant.⁽¹⁹⁾

There are structural and functional homologs of Mec1 and Rad53 in mammals. These are ATM and ATR,⁽³¹⁾ and Chk2 (checkpoint kinase), respectively.⁽³²⁾ ATM, the gene mutated in ataxia telangiectasia (AT) is a nuclear protein kinase and AT patients have an increased incidence of cancer. Cultured AT cells have checkpoint defects.⁽³³⁾ The ATR (ataxia telangiectasia and Rad3-related) protein kinase is structurally even more homologous to Mec1 than is ATM, and is itself likely to be involved in checkpoint control.⁽³⁴⁾ The mammalian Rad53 homolog, Chk2, becomes phosphorylated and activated after DNA damage in an ATM-dependent manner. Chk2 can phosphorylate Cdc25C on serine 216, and it is thought that this phosphorylation prevents Cdc25C from activating the mitotic kinase, cyclin B1–Cdc2.⁽³²⁾ Cdc25C is a protein phosphatase that promotes entry into mitosis by dephosphorylating Cdc2. The mammalian homolog of budding and fission yeast Chk1 (also named Chk1) can also phosphorylate Cdc25C on serine 216.⁽³⁵⁾ This phosphorylated residue seems to create a binding site for one of the 14-3-3 protein family members, resulting in Cdc25C inhibition.⁽³⁶⁾

Biochemical studies have also revealed several novel targets of the ATM and ATR kinases. Evidence suggests that, in response to DNA damage induction, the tumor suppressor protein p53 can become phosphorylated by ATM and ATR.^(37–39) In addition, ATM can exist in a complex with the Brca1 protein (breast cancer gene 1): gamma irradiation of cells induces phosphorylation of Brca1 that is dependent on ATM kinase.⁽⁴⁰⁾ If p53 and Brca1 are targets of the DNA damage checkpoint pathway in mammals, mutations in these proteins would be expected to result in checkpoint-defective phenotypes. Indeed, Brca1-deficient mouse cells are G2 checkpoint defective,⁽⁴¹⁾ and p53 is required to maintain

G2 DNA damage checkpoint arrest in human cells.⁽⁴²⁾ In response to gamma irradiation, p53 promotes the accumulation of p21, an inhibitor of several different cyclin–Cdk complexes. In addition, p53 transcriptionally activates another 14-3-3 family member, 14-3-3 σ , a protein that seems to sequester cyclin B1–cdc2 and thus prevent the onset of mitosis.^(43,44) Because p21 and 14-3-3 σ -deficient cells are similarly unable to maintain G2 arrest after DNA damage, these targets of p53 provide a likely mechanism by which prolonged arrest is enforced.^(42,43) The gene mutated in Nijmegen breakage syndrome (NBS) patients might also encode a DNA damage checkpoint protein, although a biochemical link to the known checkpoint kinases has not been established. This autosomal recessive disorder is characterized by increased cancer incidence and ionizing radiation sensitivity; cells from these patients are checkpoint defective in cell culture.⁽⁴⁵⁾

S-phase checkpoint

Some eukaryotic cells replicate much of their genome when chromatin is partially condensed, but on the whole, DNA replication is confined to S phase of the cell cycle. The S-phase checkpoint ensures that the onset of mitosis is dependent on the completion of DNA replication.⁽³⁾ It is worth remembering, however, that checkpoint control systems are largely defined empirically. For the replication checkpoint, loss-of-function mutations causing sensitivity to HU were identified. The relevant proteins encoded by these genes were determined to have an S-phase checkpoint control function by showing that the loss-of-function mutations allowed entry into mitosis when DNA replication was blocked with HU (Fig. 3). Thus, the S-phase checkpoint is defined as that which restrains entry into mitosis when replication is blocked with HU. However, kinetic analyses of various checkpoint mutants, grown in the presence of a concentration of HU that allows replication to proceed, but more slowly than in an unperturbed cell cycle, have revealed genetically distinct S-phase checkpoint systems (see below).

To monitor ongoing DNA replication, putative replication sensors are thought to reside at replication forks. In budding yeast, the putative sensor components include Pol2 (the replicative DNA polymerase, Pol ϵ),⁽⁴⁶⁾ Rfc5 (a replication factor C subunit involved in recruiting polymerases to replication forks),⁽⁴⁷⁾ Dpb11⁽⁴⁸⁾ and Drc1.⁽⁴⁹⁾ Because these proteins are also essential for DNA replication, it has been important to dissect these functions from their S-phase checkpoint functions.

Mec1 and Rad53 are components of the signal transduction pathway.^(6,23,27) As in the presence of DNA damage, Mec1 and Rad53 respond to replication inhibition by inducing transcription of genes involved in DNA repair, which help deal with the perturbed replication process.⁽⁶⁾ For the transcription pathway, Rad53-dependent phosphorylation of Dun1, and

hyperphosphorylation of Crt1, is required.^(6,30) However, it is not clear whether the transcriptional response contributes to cell cycle arrest in the presence of HU, because *dun1* mutants are not S-phase checkpoint defective.

The cell cycle checkpoint defects of *mec1* and *rad53* mutants are somewhat different. Both mutants elongate spindles when DNA replication is blocked with HU, so it seems that no checkpoint response remains in these cells. However, *rad53* mutants delay in anaphase, whereas *mec1* mutants exit mitosis. Thus, some aspects of mitotic progression are inhibited in *rad53* mutants. Mec1 and Rad53 also inhibit the firing of late replication origins during early S phase. Eukaryotic cells replicate their genomes by initiating DNA synthesis from multiple replication origins. Some fire early in S phase, whereas others are initiated partway through S phase. When cells are arrested in early S phase with HU, late firing origins are kept dormant by a dominant process that requires the Rad53–Mec1 pathway.⁽⁵⁰⁾ Rad53 regulates binding of RPA (replication protein A) to origins; RPA promotes origin firing by stabilizing unwound DNA and thus allowing recruitment of DNA polymerases.⁽⁵¹⁾

The target of the S-phase checkpoint is complex in budding yeast. In early S phase, Pds1 is not an essential target; *pds1* mutants can inhibit anaphase when replication is blocked. Kinetic analyses have determined that, partway through S phase, a crucial point is reached where Pds1 becomes essential; *pds1* mutants elongate spindles and lose sister chromatid cohesion when roughly a half to two-thirds of the genome has been replicated (in the presence of a nonreplication-arresting concentration of HU).⁽⁵²⁾ In these experiments, *mec1* or *rad53* mutant cells began anaphase when very little DNA had been replicated (as is the case when replication is blocked). Therefore, there must be a Pds1-independent system to restrain spindle elongation in early S phase, but later in S phase, Pds1 is required.

Extrapolating from what is known about DNA damage checkpoint organization, a reasonable prediction is that Pds1 and Rad53 function downstream of Mec1 in the context of S-phase checkpoint control (Fig. 3). These pathways must run in parallel, and be temporally regulated; one being necessary in early S phase, whereas the other is needed partway through S phase. Therefore, it would be expected that Mec1, but not Rad53, controls Pds1 stability in late S phase. Indeed, the fact that *pds1* null mutants can restrain spindle elongation when replication is blocked with HU suggests that Esp1 activity is inhibited by a mechanism independent of Pds1 binding in early S phase. Regulation of Esp1 could be mediated by the Mec1–Rad53 pathway. Alternatively, inhibition of spindle elongation in early S phase might be achieved by a mechanism other than blocking Esp1 activity.

An explanation for the duality of S-phase checkpoint control in budding yeast is the linkage of spindle elongation

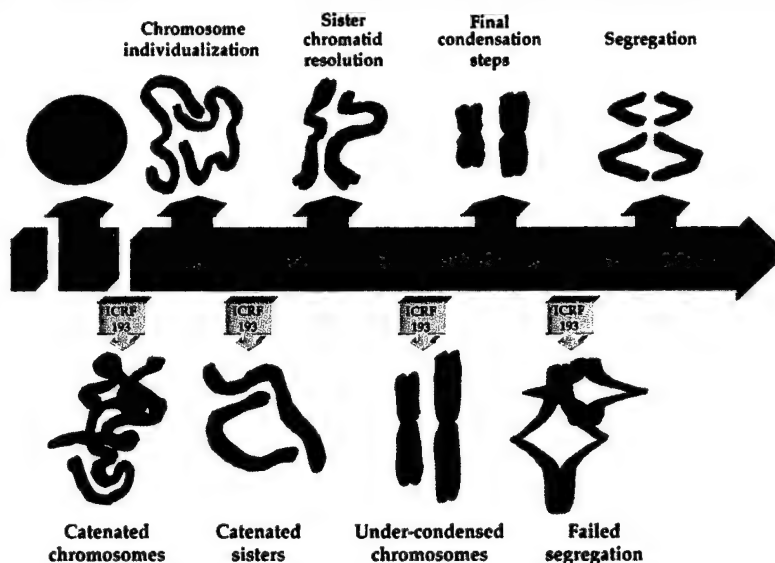
with the regulation of sister cohesion. Sister cohesion is established during DNA replication, and must be maintained until the onset of anaphase.^(13,14) Once centromere cohesion is established, partway through S phase,⁽⁵³⁾ checkpoint control of anaphase must coordinate release of cohesion with spindle elongation. Early in S phase, before replication of centromeric regions and concomitant establishment of centromere cohesion, spindle elongation must be regulated independently of cohesion. Therefore, the switch in the mode of checkpoint control from the Mec1–Rad53 pathway, to the Mec1–Pds1 pathway might be controlled by the establishment of sister chromatid cohesion.

Topoisomerase II-dependent checkpoint

DNA topoisomerase II (topo II) activity is required for chromosome condensation and segregation in eukaryotes. Although these are mitotic processes, their successful completion depends partly on pre-mitotic topo II activity during DNA replication and in G2 phase (Fig. 4). Chromosome replication creates two identical sister DNA molecules that are knotted together (catenated). Topo II removes these tangles; in higher eukaryotes, the majority must be resolved before entry into mitosis to allow accurate chromosome condensation.^(54,55) Not surprisingly, in mammals a G2 checkpoint ensures that DNA catenations have been resolved sufficiently before cells enter mitosis.⁽⁵⁴⁾

As described in the introduction, a crucial part of the definition of a checkpoint arrest states that cells must inhibit a subsequent process despite being physically capable of carrying out that process. The description of the topo II-dependent checkpoint is an example where this criterion was important. The non-DNA-damaging topo II inhibitor, ICRF-193, blocks mammalian cells in G2 (as judged by the lack of chromosome condensation), yet topo II is required for chromosome condensation (albeit a requirement at a late step in the process).⁽⁵⁴⁾ Therefore, it was necessary to prove that cells were physically capable of initiating chromosome condensation when topo II activity was absent. Such evidence could not be sought by isolating loss-of-function budding or fission yeast mutants because the topo II-dependent checkpoint seems to be absent in yeast. Temperature-sensitive mutants of fission or budding yeast topo II enter an abortive mitosis, apparently without delay.^(56,57) Therefore, the checkpoint was first described in mammals, by demonstrating checkpoint bypass induced with caffeine or kinase and phosphatase inhibitors.⁽⁵⁴⁾ In the presence of topo II inhibitors and caffeine, cells began to condense chromosomes without delay. Fully condensed chromosomes were not formed, consistent with the essential role of topo II late in the condensation process. Thus, the topo II-dependent checkpoint prevents the onset of a process that cells can begin, but cannot complete. As a result, cells finally enter an abortive anaphase.

Figure 4. Mitotic processes that require DNA topoisomerase II activity. DNA topoisomerase II (topo II) is required for several mitotic processes in mammals. In G2, topo II decatenatory activity allows chromosomes to become individualized as they condense. Continued topo II activity is required for sister chromatid resolution in prometaphase, and for the final stages of chromosome condensation that take place in metaphase. Finally, topo II is needed at the metaphase–anaphase transition to allow sister chromatid separation. The upper panel of sketches (in red) depicts these dynamic chromosomal changes in an unperturbed cell cycle. The lower panel illustrates the consequences inflicted on chromosomes when progression through mitosis continues despite a lack of topo II activity (chromosomes seen at metaphase are represented after the addition of a topo II inhibitor, ICRF-193, to cells at various cell cycle stages, indicated by the yellow arrows.) The results of cycle progression in the absence of topo II activity are severe; thus, cells guard against such aberrations by means of a G2 checkpoint sensitive to topo II activity or to the catenation state of DNA.



It is not known whether topo II levels are sensed directly, or whether physical structures within chromosomes, such as chromosome tangles, are monitored by the topo II-dependent checkpoint. However, the target of the checkpoint is presumed to be mitotic cyclin–Cdk activity: recent work has shown that a topo II-dependent checkpoint exists in plant cells that can be overridden by overexpressing a mitotic cyclin (Juan F. Giménez-Abián, unpublished observations).

It remains a possibility that ICRF-193 inhibits topo II activity and independently induces DNA damage, thus activating the DNA damage checkpoint. Several pieces of evidence indicate that this is not the case. In a variety of assays that measured DNA damage, ICRF-193 did not induce DNA breaks *in vivo* and *in vitro* (Ref. 54 and Refs therein). Nevertheless, it is possible that these methods of measurement are not sensitive enough to detect small amounts of DNA damage, and as mentioned above, a single double-stranded DNA break is sufficient to activate the DNA damage checkpoint in budding yeast. However, the background level of damage detected in these assays can be compared with the level of damage induced by DNA-damaging topo II inhibitors such as etoposide. Up to 40–60 μM etoposide is required to delay cells in G₂,⁽⁵⁴⁾ whereas breaks can be detected after treatment with only 5 μM etoposide (six times the background level of breaks in the assay). In contrast, doses of ICRF-193 that blocked cells in G₂ did not induce a measurable amount of DNA damage in these assays. Therefore, it is unlikely that ICRF-193 triggers the DNA damage checkpoint. In addition, the DNA

damage and topo II-dependent checkpoints have been distinguished genetically. One particular mammalian cell line (DM87) that becomes blocked in G₂ in response to ICRF-193 treatment or gamma irradiation differs from all other cell lines that have been studied. As is the case for most cell lines, DM87 cells are forced into mitosis, in the presence of ICRF-193, by the checkpoint-evading drug caffeine. However, caffeine cannot induce premature mitosis after gamma irradiation in DM87 cells. Therefore, the mechanism of the block induced by gamma irradiation is distinct from the block enforced by ICRF-193. One signaling pathway is sensitive to override by caffeine, whereas the other is not.

However, it is possible that the DNA damage and topo II-dependent checkpoint pathways are closely linked. One way to address this issue will be to test whether components of the DNA damage checkpoint, such as Chk1, Chk2, p53 and 14-3-3 σ , are activated in the context of ICRF-193-induced G₂ arrest. These diagnostic hallmarks of DNA damage checkpoint activation have only been identified recently, and should be useful additional tools with which to distinguish G₂ checkpoint mechanisms.

Spindle assembly checkpoint

The spindle assembly checkpoint monitors the process of bipolar attachment of all the chromosomes to the mitotic spindle. Every chromosome of the karyotype becomes bioriented on the metaphase plate by amphitelic attachment of kinetochores to the spindle.^(4,58) Detailed biology of the checkpoint has been described in higher eukaryotes including mammalian cells, and genetic analyses have been

performed in yeast.^(3,4) Here, we describe the main findings from both of these complementary approaches.

Eukaryotic cells have long been known to arrest in metaphase when microtubule polymerization is disturbed. In higher eukaryotes, cells also arrest (with a normal spindle) if just one chromosome has failed to become bioriented and has therefore not congressed to the metaphase plate.⁽⁵⁹⁾ Other defects such as spindle pole body, kinetochore and centromere abnormalities also activate the checkpoint.⁽⁴⁾ In animals and in yeast, evidence suggests that the checkpoint has a role in unperturbed cell cycles.^(60,61) Biorientation of a chromosome on the mitotic spindle forms a stable structure;^(58,62) thus, the correct alignment of chromosomes, creating the metaphase plate, is favored. Nevertheless, the process of chromosome capture by the spindle occurs more or less randomly.⁽⁵⁸⁾ Within the same species and cell type, it is accomplished quickly in some cells, but takes much longer in others.⁽⁵⁹⁾ Thus, there should be a need to activate the checkpoint every cell cycle. In contrast, the time period between biorientation of the last chromosome and the initiation of anaphase is astonishingly constant.⁽⁵⁹⁾

The checkpoint signal emanates from unattached kinetochores.⁽⁶³⁾ Indeed, yeast strains harboring extra kinetochores delay progression through mitosis.⁽⁶⁴⁾ In higher eukaryotes, a phosphoepitope (recognized by the 3F3/2 antibody) is present specifically on unattached kinetochores.^(58,65) Thus, in theory, attachment of microtubules to a kinetochore induces dephosphorylation (or loss) of the

3F3/2 phosphoepitopes at that kinetochore: once all the chromosomal 3F3/2 epitopes are dephosphorylated (or lost), the checkpoint becomes inactive (Fig. 5). Exactly how this comes about is unknown, although one possibility is that the checkpoint sensors are tension-sensitive complexes residing within the kinetochores.^(58,59,63,66) Elegant studies have shown that tension exerted on kinetochores, applied by manipulating chromosomes with a micro-needle, induces loss of the kinetochore 3F3/2 epitope (Fig. 5).⁽⁶⁷⁾ Therefore, a lack of tension might generate the checkpoint signal. To digress momentarily from mitotic checkpoint control, a dramatic example of the importance of tension for the spindle assembly checkpoint comes from praying mantid spermatocyte meiosis.⁽⁵⁸⁾ In these cells, the three sex chromosomes (connected by distal chiasmata) usually form a trivalent, allowing them to form a stable bioriented alignment on the metaphase spindle (2X/1Y). When this connection fails, resulting in an XY bivalent and an unpaired X chromosome (as happens in about 10% of the spermatocytes), anaphase is blocked for five to seven hours, and such cells do not form mature sperm.^(58,68)

The "phosphorylated kinetochores" are recognized by a component of the checkpoint pathway (Mad2, see below), leading to inhibition of anaphase.⁽⁶⁹⁾ But how is the checkpoint signal mobilized? How does a single unattached kinetochore generate a signal that inhibits anaphase spindle elongation and prevents loss of sister chromatid cohesion of all the other chromosomes? One study has revealed impor-

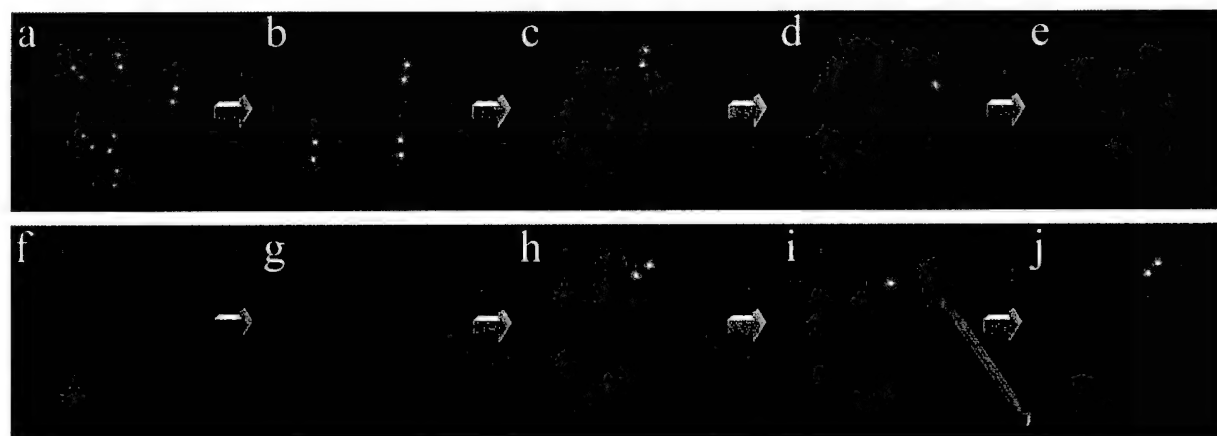
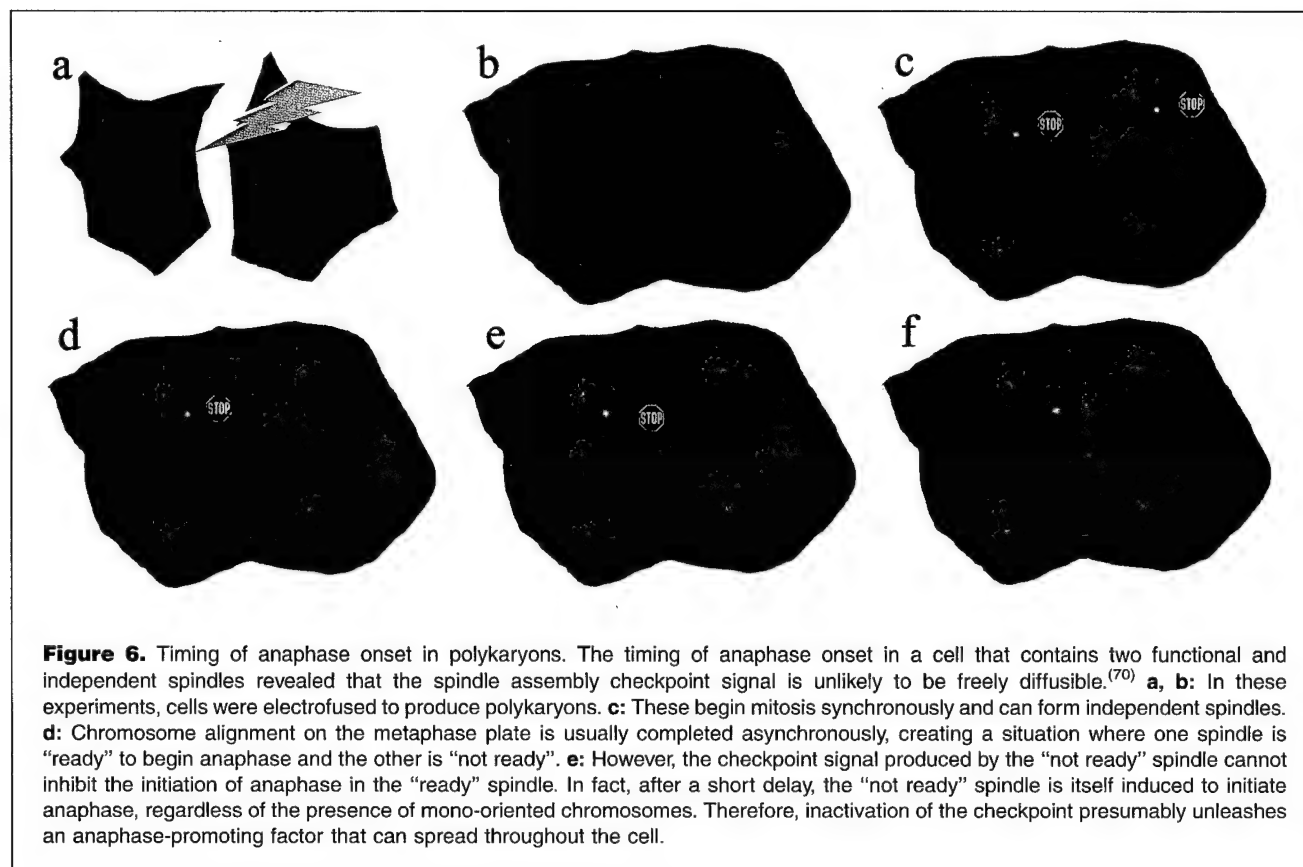


Figure 5. Tension-sensitive kinetochore phosphorylation. The upper panel illustrates that **a**: kinetochores of prometaphase chromosomes become phosphorylated forming a 3F3/2 antibody-reactive epitope (yellow dots). **b–e**: The phosphoepitope is lost (blue dots) as chromosomes attach to the mitotic spindle forming the metaphase plate. The lower panel describes an experiment on first meiotic metaphase cells, showing that phosphorylation of the epitope is sensitive to tension.⁽⁶⁷⁾ **h**: When both pairs of homologous sister kinetochores (each pair represented by a single blue or yellow dot) of a bivalent are forced to attach to the same spindle pole, these kinetochores become phosphorylated and anaphase is blocked. **i**: The application of tension to only one chromosome of the bivalent, via a micro-needle (shown in silver), induces loss of the phosphoepitope from its sister kinetochores. **j**: The phosphoepitope reappears when the tension is released.



tant information that should help to resolve this question (Fig. 6). Rieder *et al.* examined the timing of anaphase onset in cells that contain two functional and independent spindles.⁽⁷⁰⁾ Such polykaryons are generated by cell fusion. When two cells at different stages of the cell cycle are fused, cell cycle progression of their nuclei soon becomes synchronized, allowing measurements of anaphase timing in independent spindles that share a common cytoplasm. This analysis revealed that the inhibitor emanating from a single unattached kinetochore is not freely diffusible, but rather is likely to be associated with the spindle itself.

In contrast to work with higher eukaryotes, yeast genetic studies have revealed molecular components of the checkpoint. Several groups of yeast spindle assembly checkpoint proteins were identified in genetic screens designed to find mutants sensitive to microtubule antagonists (Fig. 3). These are Mad1, Mad2, Mad3 (mitotic arrest defective)⁽⁶⁰⁾ and Bub1, Bub2, Bub3 (budding uninhibited by benzimidazole).⁽⁷¹⁾ In addition, Mps1 is required.⁽⁷²⁾ Rapidly moving back to higher eukaryotes, a recent *in vitro* study revealed that vertebrate Mad2 binds selectively to phosphorylated kinetochores.⁽⁶⁹⁾ Conversely, Mad2 binding is inhibited by kinetochore-microtubule attachment.⁽⁷³⁾ This information allowed a satisfying model of the checkpoint pathway to be described.⁽⁶⁹⁾ First, attachment- or tension-sensitive kine-

chore components become phosphorylated. Second, these are recognized by Mad2, leading to the formation of an active checkpoint complex. But what is the nature and function of this active complex? In yeast, spindle defects activate Mps1 kinase, resulting in Mad1 hyperphosphorylation (perhaps directly by Mps1).^(72,74) Overexpression of Mps1 alone can activate the checkpoint. This induced arrest is (at least partly) dependent on Mad1, Mad2, Mad3 and Bub1, Bub2, Bub3, tentatively placing all of these components downstream of Mps1. Mad1 phosphorylation also requires Bub1, Bub3 and Mad2.^(74,75) This modified form of Mad1 is required to mediate metaphase arrest. Significantly, Mad1 has been shown to bind to Mad2; in this complex, Mad1 is a better substrate for Mps1 kinase than is unbound Mad1. Together, the yeast genetic data and studies in higher eukaryotes indicate that checkpoint activation relies on the recognition of unattached kinetochores by Mad2, and the formation of an activated Mad1–Mad2 complex in which Mad1 is hyperphosphorylated. Cell cycle arrest is brought about by inhibition of APC activity, which prevents Pds1 ubiquitination. The link with APC activity comes from studies showing that yeast Mad2 can bind to Cdc20, a component of APC required for Pds1 degradation.^(76,77) It seems that this binding might inhibit APC-dependent ubiquitination of APC substrates.⁽⁷⁶⁾ Overexpression of Cdc20, or expression of a Cdc20 mutant

that cannot bind to Mad2, bypasses the spindle assembly checkpoint arrest.⁽⁷⁷⁾

Animal homologs of Mad1, Mad2, Mad3, Bub1 and Bub3 are found at the kinetochores of prophase-prometaphase (not yet bioriented) chromosomes. After congression to the metaphase plate, these proteins seem to dissociate.⁽⁷⁸⁾ In mono-oriented chromosomes, only the unattached kinetochore contains Mad2 protein.⁽⁷⁹⁾ These localization studies suggest that formation of an active checkpoint complex within kinetochores is likely to be a conserved mechanism that activates the checkpoint pathway.

Recently, parallel branches of the spindle assembly checkpoint were identified.^(80–83) These have been called the “Mad2” and “Bub2” pathways. In the presence of nocodazole, *mad2 bub2* mutant cells entered a new cell cycle (re-budded) much more rapidly than *mad2* or *bub2* single-mutant cells did. The Mad2 pathway is essentially that described above, ultimately targeting Pds1p and preventing spindle elongation and loss of sister chromatid cohesion. In contrast, the Bub2 pathway inhibits mitotic cyclin proteolysis, and thus prevents exit from mitosis (and therefore might not be part of mitotic entry control). Mps1 kinase can activate the Bub2 pathway, suggesting that this pathway is a component of the spindle assembly checkpoint.⁽⁸⁰⁾

Adaptation

In yeast, checkpoints are counter-balanced by adaptation responses. Adaptation is: “the re-initiation of cell cycle progression, subsequent to checkpoint arrest, without inactivation of the checkpoint and despite the incomplete resolution of the cause of the arrest”. This is in contrast to checkpoint inactivation (or “recovery”), which occurs after the cause of the arrest has been corrected. Like checkpoint controls, adaptation signals are dominant processes. One pathway has been defined genetically for the DNA damage checkpoint by the isolation of loss-of-function budding yeast mutants.⁽⁸⁴⁾ An irreparable double-stranded DNA break induces a Rad9-dependent checkpoint response that arrests cells at metaphase for 8–10 hours before cell cycle progression resumes. However, adaptation-defective mutants remain arrested in metaphase and this prolonged arrest is dependent on Rad9. The decision to arrest or to adapt might depend on the amount of single-stranded DNA at repair sites.⁽²¹⁾ Yeast cells also adapt after prolonged arrest induced by the spindle assembly checkpoint, and in this case adaptation involves inhibitory phosphorylation of the mitotic kinase, Clb2/Cdc28.^(4,85)

Conclusions

Many elements of the complex regulation of cell cycle events by checkpoint controls are now understood. Kinetic analyses of cell cycle progression in checkpoint defective mutants have recently elucidated the order-of-function of several

checkpoint components, and have revealed points at which the checkpoint pathways become branched. Although many details remain unresolved, a solid appreciation of the organization of these intricate pathways has been gained and, importantly, early suspicions regarding the conserved nature of checkpoint components have been confirmed. To a large extent, investigators are able to leap between the yeast and mammalian systems to do studies that are complementary; a very fruitful exercise that will help our knowledge of the field to grow rapidly. It is significant that key checkpoint components, initially identified through yeast genetic screens, have mammalian homologs that have been strongly implicated in the etiology of cancer.

Acknowledgments

We are indebted to Nick Rhind, Adrian Smith, Consuelo De la Torre and Catherine Andrews for comments on the MS and for many invaluable discussions.

References

1. Skibbens RV, Hieter P. Kinetochores and the checkpoint mechanism that monitors for defects in the chromosome segregation machinery. *Annu Rev Genet* 1998;32:307–337.
2. Rhind N, Russell P. Mitotic DNA damage and replication checkpoints in yeast. *Curr Opin Cell Biol* 1998;10:749–758.
3. Elledge SJ. Cell cycle checkpoints: preventing an identity crisis. *Science* 1996;274:1664–1672.
4. Rudner AD, Murray AW. The spindle assembly checkpoint. *Curr Opin Cell Biol* 1996;8:773–780.
5. Weinert T. DNA damage checkpoints update: getting molecular. *Curr Opin Genet Dev* 1998;8:185–193.
6. Allen JB, Zhou Z, Siede W, Friedberg EC, Elledge SJ. The SAD1/RAD53 protein kinase controls multiple checkpoints and DNA damage-induced transcription in yeast. *Genes Dev* 1994;8:2401–2415.
7. Rao PN, Johnson RT. Mammalian cell fusion: studies on the regulation of DNA synthesis and mitosis. *Nature* 1970;225:159–162.
8. Yamamoto A, Guacci V, Koshland D. Pds1p is required for faithful execution of anaphase in the yeast, *Saccharomyces cerevisiae*. *J Cell Biol* 1996;133:85–97.
9. Cohen-Fix O, Peters JM, Kirschner MW, Koshland D. Anaphase initiation in *Saccharomyces cerevisiae* is controlled by the APC-dependent degradation of the anaphase inhibitor Pds1p. *Genes Dev* 1996;10:3081–3093.
10. Cohen-Fix O, Koshland D. The anaphase inhibitor of *Saccharomyces cerevisiae* Pds1p is a target of the DNA damage checkpoint pathway. *Proc Natl Acad Sci U S A* 1997;94:14361–14366.
11. Ciosk R, Zachariae W, Michaelis C, Shevchenko A, Mann M, Nasmyth K. An ESP1/PDS1 complex regulates loss of sister chromatid cohesion at the metaphase to anaphase transition in yeast. *Cell* 1998;93:1067–1076.
12. Michaelis C, Ciosk R, Nasmyth K. Cohesins: chromosomal proteins that prevent premature separation of sister chromatids. *Cell* 1997;91:35–45.
13. Uhlmann F, Nasmyth K. Cohesion between sister chromatids must be established during DNA replication. *Curr Biol* 1998;8:1095–1101.
14. Uhlmann F, Lottspeich F, Nasmyth K. Sister-chromatid separation at anaphase onset is promoted by cleavage of the cohesin subunit Scc1. *Nature* 1999;400:37–42.
15. Funabiki H, Kumada K, Yanagida M. Fission yeast Cut1 and Cut2 are essential for sister chromatid separation, concentrate along the metaphase spindle and form large complexes. *EMBO J* 1996;15:6617–6628.
16. Zou H, McGarry TJ, Bernal T, Kirschner MW. Identification of a vertebrate sister-chromatid separation inhibitor involved in transformation and tumorigenesis. *Science* 1999;285:418–422.

17. Weinert TA, Hartwell LH. The *RAD9* gene controls the cell cycle response to DNA damage in *S. cerevisiae*. *Science* 1988;241:317–322.
18. Lydall D, Weinert T. Yeast checkpoint genes in DNA damage processing: implications for repair and arrest. *Science* 1995;270:1488–1491.
19. Gardner R, Putnam CW, Weinert T. *RAD53*, *DUN1* and *PDS1* define two parallel G2/M checkpoint pathways in budding yeast. *EMBO J* 1999;18:3173–3185.
20. Garvik B, Carson M, Hartwell L. Single-stranded DNA arising at telomeres in *cdc13* mutants may constitute a specific signal for the *RAD9* checkpoint. *Mol Cell Biol* 1995;15:6128–6138.
21. Lee SE, Moore JK, Holmes A, Umez K, Kolodner RD, Haber JE. *Saccharomyces* Ku70, mre11/rad50 and RPA proteins regulate adaptation to G2/M arrest after DNA damage. *Cell* 1998;94:399–409.
22. Longhese MP, Paciotti V, Franchini R, Zaccarini R, Plevani P, Lucchini G. The novel DNA damage checkpoint protein ddc1p is phosphorylated periodically during the cell cycle and in response to DNA damage in budding yeast. *EMBO J* 1997;16:5216–5226.
23. Weinert TA, Kiser GL, Hartwell LH. Mitotic checkpoint genes in budding yeast and the dependence of mitosis on DNA replication and repair. *Genes Dev* 1994;8:652–665.
24. Paciotti V, Lucchini G, Plevani P, Longhese MP. Mec1p is essential for phosphorylation of the yeast DNA damage checkpoint protein Ddc1p, which physically interacts with Mec3p. *EMBO J* 1998;17:4199–4209.
25. Sanchez Y, Bachant J, Wang H, Hu F, Liu D, Tetzlaff M, Elledge S. Control of the DNA damage checkpoint by Chk1 and Rad53 protein kinases through distinct mechanisms. *Science* 1999;286:1166–1171.
26. Sun Z, Fay DS, Marini F, Foiani M, Stern DF. Spk1/Rad53 is regulated by Mec1-dependent protein phosphorylation in DNA replication and damage checkpoint pathways. *Genes Dev* 1996;10:395–406.
27. Sanchez Y, Desany BA, Jones WJ, Liu Q, Wang B, Elledge SJ. Regulation of *RAD53* by the ATM-like kinases *MEC1* and *TEL1* in yeast cell cycle checkpoint pathways. *Science* 1996;271:357–360.
28. Emili A. *MEC1*-dependent phosphorylation of Rad9p in response to DNA damage. *Mol Cell* 1998;2:183–189.
29. Sun Z, Hsiao J, Fay DS, Stern DF. Rad53 FHA domain associated with phosphorylated Rad9 in the DNA damage checkpoint. *Science* 1998;281:272–274.
30. Huang M, Zhou Z, Elledge SJ. The DNA replication and damage checkpoint pathways induce transcription by inhibition of the Crt1 repressor. *Cell* 1998;94:595–605.
31. Savitsky K, Bar SA, Gilad S, Rotman G, Ziv Y, Vanagaite L, Tagle DA, Smith S, Uziel T, Sfez S, et al. A single ataxia telangiectasia gene with a product similar to PI-3 kinase. *Science* 1995;268:1749–1753.
32. Matsuoka S, Huang M, Elledge SJ. Linkage of ATM to cell cycle regulation by the Chk2 protein kinase. *Science* 1998;282:1893–1897.
33. Kastan MB, Zhan Q, el DW, Carrier F, Jacks T, Walsh WV, Plunkett BS, Vogelstein B, Fornace AJ. A mammalian cell cycle checkpoint pathway utilizing p53 and GADD45 is defective in ataxia-telangiectasia. *Cell* 1992;71:587–597.
34. Wright JA, Keegan KS, Herendeen DR, Bentley NJ, Carr AM, Hoekstra MF, Concannon P. Protein kinase mutants of human ATR increase sensitivity to UV and ionizing radiation and abrogate cell cycle checkpoint control. *Proc Natl Acad Sci USA* 1998;95:7445–7450.
35. Sanchez Y, Wong C, Thoma RS, Richman R, Wu Z, Piwnica WH, Elledge SJ. Conservation of the Chk1 checkpoint pathway in mammals: linkage of DNA damage to Cdk regulation through Cdc25. *Science* 1997;277:1497–1501.
36. Peng CY, Graves PR, Thoma RS, Wu Z, Shaw AS, Piwnica WH. Mitotic and G2 checkpoint control: regulation of 14-3-3 protein binding by phosphorylation of Cdc25C on serine-216. *Science* 1997;277:1501–1505.
37. Tibbetts RS, Brumbaugh KM, Williams JM, Sarkaria JN, Cliby WA, Shieh SY, Taya Y, Prives C, Abraham RT. A role for ATR in the DNA damage-induced phosphorylation of p53. *Genes Dev* 1999;13:152–157.
38. Banin S, Moyal L, Shieh S, Taya Y, Anderson CW, Chessa L, Smorodinsky NI, Prives C, Reiss Y, Shiloh Y, Ziv Y. Enhanced phosphorylation of p53 by ATM in response to DNA damage. *Science* 1998;281:1674–1677.
39. Canman CE, Lim DS, Cimprich KA, Taya Y, Tamai K, Sakaguchi K, Appella E, Kastan MB, Siliciano JD. Activation of the ATM kinase by ionizing radiation and phosphorylation of p53. *Science* 1998;281:1677–1679.
40. Cortez D, Wang Y, Qin J, Elledge S. Requirement of ATM-dependent phosphorylation of Brca1 in the DNA damage response to double-strand breaks. *Science* 1999;286:1162–1166.
41. Xu X, Weaver Z, Linke SP, Li C, Gotay J, Wang XW, Harris CC, Ried T, Deng CX. Centrosome amplification and a defective G2–M cell cycle checkpoint induce genetic instability in BRCA1 exon 11 isoform-deficient cells. *Mol Cell* 1999;3:389–395.
42. Bunz F, Dutriaux A, Lengauer C, Waldman T, Zhou S, Brown JP, Sedivy JM, Kinzler KW, Vogelstein B. Requirement for p53 and p21 to sustain G2 arrest after DNA damage. *Science* 1998;282:1497–1501.
43. Chan TA, Hermeking H, Lengauer C, Kinzler KW, Vogelstein B. 14-3-3Sigma is required to prevent mitotic catastrophe after DNA damage. *Nature* 1999;401:616–620.
44. Hermeking H, Lengauer C, Polyak K, He TC, Zhang L, Thiagalingam S, Kinzler KW, Vogelstein B. 14-3-3 Sigma is a p53-regulated inhibitor of G2/M progression. *Mol Cell* 1997;1:3–11.
45. Carney JP, Maser RS, Olivares H, Davis EM, Le BM, Yates JR, Hays L, Morgan WF, Petrini JH. The hMre11/hRad50 protein complex and Nijmegen breakage syndrome: linkage of double-strand break repair to the cellular DNA damage response. *Cell* 1998;93:477–486.
46. Navas TA, Zhou Z, Elledge SJ. DNA polymerase epsilon links the DNA replication machinery to the S phase checkpoint. *Cell* 1995;80:29–39.
47. Sugimoto K, Shimomura T, Hashimoto K, Araki H, Sugino A, Matsumoto K. Rfc5, a small subunit of replication factor C complex, couples DNA replication and mitosis in budding yeast. *Proc Natl Acad Sci USA* 1996;93:7048–7052.
48. Araki H, Leem SH, Phongdara A, Sugino A. Dpb11, which interacts with DNA polymerase II(epsilon) in *Saccharomyces cerevisiae*, has a dual role in S-phase progression and at a cell cycle checkpoint. *Proc Natl Acad Sci USA* 1995;92:11791–11795.
49. Wang H, Elledge SJ. DRC1, DNA replication and checkpoint protein 1, functions with DPB11 to control DNA replication and the S-phase checkpoint in *Saccharomyces cerevisiae*. *Proc Natl Acad Sci USA* 1999;96:3824–3829.
50. Santocanale C, Diffley JF. A Mec1- and Rad53-dependent checkpoint controls late-firing origins of DNA replication. *Nature* 1998;395:615–618.
51. Tanaka T, Nasmyth K. Association of RPA with chromosomal replication origins requires an mcm protein, and is regulated by rad53, and cyclin- and Dbf4-dependent kinases. *EMBO J* 1998;17:5182–5191.
52. Clarke DJ, Segal M, Mondesert G, Reed SI. The Pds1 anaphase inhibitor and Mec1 kinase define distinct checkpoints coupling S phase with mitosis in budding yeast. *Curr Biol* 1999;9:365–368.
53. Blat Y, Kleckner N. Cohesins bind to preferential sites along yeast chromosome III, with differential regulation along arms versus the centric region. *Cell* 1999;98:249–259.
54. Downes CS, Clarke DJ, Mullinger AM, Giménez-Abián JF, Creighton AM, Johnson RT. A topoisomerase II-dependent G2 cycle checkpoint in mammalian cells. *Nature* 1994;372:467–470.
55. Giménez-Abián JF, Clarke DJ, Mullinger AM, Downes CS, Johnson RT. A postprophase topoisomerase II-dependent chromatid core separation step in the formation of metaphase chromosomes. *J Cell Biol* 1995;131:7–17.
56. Uemura T, Ohkura H, Adachi Y, Morino K, Shiozaki K, Yanagida M. DNA topoisomerase II is required for condensation and separation of mitotic chromosomes in *S. pombe*. *Cell* 1987;50:917–925.
57. Holm C, Goto T, Wang JC, Botstein D. DNA topoisomerase II is required at the time of mitosis in yeast. *Cell* 1985;41:553–563.
58. Nicklas RB. How cells get the right chromosomes. *Science* 1997;275:632–637.
59. Rieder CL, Schultz A, Cole R, Sluder G. Anaphase onset in vertebrate somatic cells is controlled by a checkpoint that monitors sister kinetochore attachment to the spindle. *J Cell Biol* 1994;127:1301–1310.
60. Li R, Murray AW. Feedback control of mitosis in budding yeast. *Cell* 1991;66:519–531.
61. Taylor SS, McKeon F. Kinetochore localization of murine Bub1 is required for normal mitotic timing and checkpoint response to spindle damage. *Cell* 1997;89:727–735.

62. Hyman AA, Karsenti E. Morphogenetic properties of microtubules and mitotic spindle assembly. *Cell* 1996;84:401-410.
63. Rieder CL, Cole RW, Khodjakov A, Sluder G. The checkpoint delaying anaphase in response to chromosome monoorientation is mediated by an inhibitory signal produced by unattached kinetochores. *J Cell Biol* 1995;130:941-948.
64. Wells WA, Murray AW. Aberrantly segregating centromeres activate the spindle assembly checkpoint in budding yeast. *J Cell Biol* 1996;133:75-84.
65. Gorbisky GJ, Ricketts WA. Differential expression of a phosphopeptide at the kinetochores of moving chromosomes. *J Cell Biol* 1993;122:1311-1321.
66. McIntosh JR. Structural and mechanical control of mitotic progression. *Cold Spring Harb Symp Quant Biol* 1991;56:613-619.
67. Nicklas RB, Ward SC, Gorbisky GJ. Kinetochore chemistry is sensitive to tension and may link mitotic forces to a cell cycle checkpoint. *J Cell Biol* 1995;130:929-939.
68. Callan HG, Jacobs PA. The meiotic process in *Mantis religiosa* L. Males. *J Genet* 1957;55:200-217.
69. Waters JC, Chen RH, Murray AW, Gorbisky GJ, Salmon ED, Nicklas RB. Mad2 binding by phosphorylated kinetochores links error detection and checkpoint action in mitosis. *Curr Biol* 1999;9:649-652.
70. Rieder CL, Khodjakov A, Paliulis LV, Fortier TM, Cole RW, Sluder G. Mitosis in vertebrate somatic cells with two spindles: implications for the metaphase/anaphase transition checkpoint and cleavage. *Proc Natl Acad Sci U S A* 1997;94:5107-5112.
71. Hoyt MA, Totis L, Roberts BT. *S. cerevisiae* genes required for cell cycle arrest in response to loss of microtubule function. *Cell* 1991;66:507-517.
72. Weiss E, Winey M. The *Saccharomyces cerevisiae* spindle pole body duplication gene *MPS1* is part of a mitotic checkpoint. *J Cell Biol* 1996;132:111-123.
73. Waters JC, Chen RH, Murray AW, Salmon ED. Localization of Mad2 to kinetochores depends on microtubule attachment, not tension. *J Cell Biol* 1998;141:1181-1191.
74. Hardwick KG, Weiss E, Luca FC, Winey M, Murray AW. Activation of the budding yeast spindle assembly checkpoint without mitotic spindle disruption. *Science* 1996;273:953-956.
75. Hardwick KG, Murray AW. Mad1p, a phosphoprotein component of the spindle assembly checkpoint in budding yeast. *J Cell Biol* 1995;131:709-720.
76. Li Y, Gorbea C, Mahaffey D, Rechsteiner M, Benezra R. MAD2 associates with the cyclosome/anaphase-promoting complex and inhibits its activity. *Proc Natl Acad Sci USA* 1997;94:12431-12436.
77. Hwang LH, Lau LF, Smith DL, Mistrot CA, Hardwick KG, Hwang ES, Amon A, Murray AW. Budding yeast Cdc20: a target of the spindle checkpoint. *Science* 1998;279:1041-1044.
78. Nasmyth K. Separating sister chromatids. *Trends Biochem Sci* 1999;24:98-104.
79. Chen RH, Waters JC, Salmon ED, Murray AW. Association of spindle assembly checkpoint component XMad2 with unattached kinetochores. *Science* 1996;274:242-246.
80. Fesquet D, Fitzpatrick PJ, Johnson AL, Kramer KM, Toyn JH, Johnston LH. A Bub2p-dependent spindle checkpoint pathway regulates the Dbf2p kinase in budding yeast. *EMBO J* 1999;18:2424-2434.
81. Alexandru G, Zachariae W, Schleiffer A, Nasmyth K. Sister chromatid separation and chromosome re-duplication are regulated by different mechanisms in response to spindle damage. *EMBO J* 1999;18:2707-2721.
82. Fraschini R, Formenti E, Lucchini G, Piatti S. Budding yeast Bub2 is localized at spindle pole bodies and activates the mitotic checkpoint via a different pathway from Mad2. *J Cell Biol* 1999;145:979-991.
83. Li R. Bifurcation of the mitotic checkpoint pathway in budding yeast. *Proc Natl Acad Sci USA* 1999;96:4989-4994.
84. Toczyski DP, Galgoczy DJ, Hartwell LH. CDC5 and CKII control adaptation to the yeast DNA damage checkpoint. *Cell* 1997;90:1097-1106.
85. Minshull J, Straight A, Rudner AD, Dernburg AF, Belmont A, Murray AW. Protein phosphatase 2A regulates MPF activity and sister chromatid cohesion in budding yeast. *Curr Biol* 1996;6:1609-1620.

Coordinated Spindle Assembly and Orientation Requires Clb5p-dependent Kinase in Budding Yeast

Marisa Segal,* Duncan J. Clarke,* Paul Maddox,[‡] E.D. Salmon,[‡] Kerry Bloom,[‡] and Steven I. Reed*

*Department of Molecular Biology, MB7, The Scripps Research Institute, La Jolla, California, 92037; and [‡]Department of Biology, CB3280, University of North Carolina, Chapel Hill, North Carolina, 27599

Abstract. The orientation of the mitotic spindle along a polarity axis is critical in asymmetric cell divisions. In the budding yeast, *Saccharomyces cerevisiae*, loss of the S-phase B-type cyclin Clb5p under conditions of limited cyclin-dependent kinase activity (*cdc28-4 clb5Δ* cells) causes a spindle positioning defect that results in an undivided nucleus entering the bud. Based on time-lapse digital imaging microscopy of microtubules labeled with green fluorescent protein fusions to either tubulin or dynein, we observed that the asymmetric behavior of the spindle pole bodies during spindle assembly was lost in the *cdc28-4 clb5Δ* cells. As soon as a spindle formed, both poles were equally likely to interact with the bud cell cortex. Persistent dynamic interac-

tions with the bud ultimately led to spindle translocation across the bud neck. Thus, the mutant failed to assign one spindle pole body the task of organizing astral microtubules towards the mother cell. Our data suggest that Clb5p-associated kinase is required to confer mother-bound behavior to one pole in order to establish correct spindle polarity. In contrast, B-type cyclins, Clb3p and Clb4p, though partially redundant with Clb5p for an early role in spindle morphogenesis, preferentially promote spindle assembly.

Key words: spindle polarity • astral microtubules • cell cycle • cyclin • *Saccharomyces cerevisiae*

Introduction

Development of a spindle in *Saccharomyces cerevisiae* is initiated upon progression through START, before the G1/S transition (Byers, 1981; Hoyt and Geiser, 1996; Lew et al., 1997). As cells proceed through START, the yeast microtubule organizing center, the spindle pole body (SPB)¹ is duplicated. SPBs are embedded in the nuclear envelope throughout the cell cycle and are responsible for organizing astral microtubules in the cytosol, as well as the mitotic spindle within the nucleus. After duplication, SPBs separate to assemble a spindle. Before anaphase, the spindle positions at the bud neck with one SPB directed towards the mother and the other towards the daughter cell. As the spindle assembles, astral microtubules dynamically interact with the cell cortex of the mother or daughter cell to ultimately establish spindle orientation along the mother-daughter polarity axis (Yeh et al., 1995; Carminati and Stearns, 1997; Shaw et al., 1997b). Thus, spindle assembly and orientation are normally tightly linked pro-

cesses contributing to the asymmetric nature of the spindle pathway. Asymmetry is also reflected in the fact that the newly synthesized spindle pole is destined for the daughter cell (Vallen et al., 1992).

The kinetics of spindle assembly has been previously characterized by time-lapse video-enhanced differential interference contrast (DIC) microscopy (Yeh et al., 1995). This study identified a two-step process. SPB separation initially occurs rapidly, creating a 1- μ m long spindle, followed by a second slower phase to produce a 2- μ m long spindle oriented along the mother-bud axis. Overall, this process takes \sim 30 min, followed by an additional period in which spindle length remains constant until onset of anaphase. This study, however, could not correlate these kinetics with astral microtubule behavior during spindle assembly.

A separate study in which astral microtubules were visualized by labeling with dynein fused to green fluorescent protein (GFP) provided further support to the notion that the spindle pathway is inherently asymmetric. The asymmetry was revealed by sequential association of the dynein fusion, first with astral microtubules emanating from the daughter-bound SPB (SPB_{daughter}), then, once spindle poles were \sim 1 μ m apart, with astral microtubules emanating from the mother-bound pole (SPB_{mother}). Temporal as-

Address correspondence to S.I. Reed, Department of Molecular Biology, MB7, The Scripps Research Institute, 10550 N. Torrey Pines Road, La Jolla, CA 92037. Tel.: (858) 784-9836. Fax: (858) 784-2781. E-mail: sreed@scripps.edu

¹Abbreviations used in this paper: DIC, differential interference contrast; GFP, green fluorescent protein; SPB, spindle pole body.

sociation of dynein-GFP reflected astral microtubule organization by the SPBs rather than a consequence of microtubule orientation into the bud. Thus, the dynein-GFP label provides valuable information on SPB polarity and astral microtubule behavior in a variety of processes, including spindle orientation and karyogamy (Shaw et al., 1997b; Maddox et al., 1999).

Genetic analysis has implicated B-type cyclin function in spindle assembly. Strains containing multiple *CLB* deletions (e.g., *clb1-4Δ*, *clb3-5Δ*), fail to form a bipolar spindle (Surana et al., 1991; Fitch et al., 1992; Schwob and Nasmyth, 1993). Yet, due to functional redundancy, the relative contribution of individual Clbs in the various aspects of the spindle pathway has not been precisely determined.

We have previously described a spindle positioning defect associated with loss of the S-phase cyclin Clb5p under conditions in which the cyclin-dependent kinase Cdc28p is partially impaired (*cdc28-4 clb5Δ* cells). The *cdc28-4* allele, hypomorphic at permissive temperature, confers a sensitized environment for the genetic analysis of loss of individual cyclins (Segal et al., 1998). This strategy circumvents the problem of functional redundancy among the Clbs (Fitch et al., 1992; Richardson et al., 1992; Schwob and Nasmyth, 1993). The positioning defect in *cdc28-4 clb5Δ* cells ultimately perturbed spindle dynamics at the metaphase to anaphase transition, resulting in a terminal phenotype characterized by an undivided nucleus migrating into the bud. The Clb5p requirement for correct spindle positioning, however, was restricted to a temporal window at the G1/S boundary, coincident with the normal time of Clb5p-associated Cdc28p kinase activation (Segal et al., 1998).

In the present study, we have investigated the primary defect that results in nuclear mispositioning in *cdc28-4 clb5Δ* cells. We show that spindle polarity is normally established at the time of SPB separation and that Clb5p kinase is required to correctly coordinate these two processes. Based on time-lapse microscopy of microtubules labeled with GFP fusions to either tubulin or dynein, the asymmetric behavior of SPBs during spindle assembly was lost in the *cdc28-4 clb5Δ* cells: the mutant failed to assign one SPB the task of organizing astral microtubules towards the mother cell. At the same time, the kinetics of spindle assembly was altered in these cells. The combination of both defects results in symmetric spindles with astral microtubules from both poles initially interacting with the bud. Thus, Clb5p-associated kinase coordinates spindle assembly and orientation to confer mother-bound behavior to one SPB to establish correct spindle polarity. In contrast, Clb3p and -4 were not required for polarity establishment; these B-type cyclins contributed to spindle morphogenesis by promoting spindle assembly. These results indicate that both establishment of spindle polarity and spindle assembly are differentially subjected to cell cycle control.

Materials and Methods

Yeast Strains, Genetic Procedures, Media, and Growth Conditions

Strains MYT1010, *MATa/α cdc28-4/cdc28-4 GAL1:CLB5-TRP1/trp1*

HIS3::GFP:TUB1-URA3/ura3; MYT1416, *MATa/α cdc28-4/cdc28-4 clb5::ARG4/clb5::ARG4 GAL1:CLB5-TRP1/trp1 HIS3::GFP:TUB1-URA3/ura3*; and MYT2426, *MATa/α cdc28-4/cdc28-4 clb3::TRP1/clb3::TRP1 clb4::HIS2/clb4::HIS2 GAL1:CLB5-LEU2/leu2 HIS3::GFP:TUB1-URA3/ura3*, or isogenic versions carrying a *MET3:CLB5* construct instead of the *GAL1:CLB5* plasmid were previously described (Segal et al., 1998). Deletion of *DHC1* was constructed as previously described (Li et al., 1993). Standard yeast media and genetic procedures were used (Sherman et al., 1986). Yeast cultures were grown at 23°C unless indicated.

Digital Imaging Microscopy in Live Cells Expressing GFP-TUB1

Cells were grown to $\sim 5 \times 10^6$ cells/ml in selective 3% galactose/0.1% dextrose medium and collected by filtration for a 2-h shift on selective glucose medium at 23°C to repress *CLB5* expression. Cells were then mounted in the same medium containing 25% gelatin to perform time-lapse recordings at room temperature as described (Shaw et al., 1997a; Maddox et al., 1999). In brief, a total of five fluorescence images were acquired at a Z-distance of 0.75 μ m between each plane. A single bright-field image was taken in the middle focal plane. This acquisition regime was repeated at 30- or 60-s intervals. Images were processed as previously described (Shaw et al., 1997a,b; Maddox et al., 1999) using Metamorph software (Universal Imaging). Quantitation of oriented astral microtubules organized by the SPB_{mother} or SPB_{daughter} was carried out by scoring single digital images corresponding to cells at metaphase with ~ 2 - μ m spindles observed in 22 independent time-lapse series.

Still cell images (see Figs. 4 and 5) were captured using 100% incident light intensity and 500-ms exposures to optimize visualization of astral microtubules. Spindle measurements in digital images were carried out as previously described (Segal et al., 1998).

Digital Imaging Microscopy in Live Cells Expressing DHC1-GFP

Recordings were performed in cells transformed with pKBY701. This construct expresses a dynein-GFP fusion under the control of the *GAL1* promoter (Shaw et al., 1997b). Strains MY1010GD, *MATa/α cdc28-4/cdc28-4 MET3:CLB5-TRP1/trp1 [GAL1:DHC1-GFP]*; or mutant MY1416GD, *MATa/α cdc28-4/cdc28-4 clb5::ARG4/clb5::ARG4 MET3:CLB5-TRP1/trp1 [GAL1:DHC1-GFP]* were grown to midlog phase in selective dextrose lacking methionine (for expression of *CLB5* under the control of the *MET3* promoter). Cells were then transferred to selective galactose medium supplemented with methionine (to induce *DHC1-GFP* expression and repress *CLB5*) for 2 h at room temperature. Recordings and image processing were performed as described (Shaw et al., 1997b).

Results

Astral Microtubule Behavior during Spindle Assembly

We have previously assigned a role for Clb5p-dependent kinase at an early step of the spindle pathway. Loss of Clb5p under conditions of limiting Cdc28p activity (*cdc28-4 clb5Δ* at permissive temperature) resulted in a spindle positioning defect before anaphase (Segal et al., 1998).

Dynamic astral microtubule interactions play a critical role in the establishment of spindle orientation (Carminati and Stearns, 1997; Shaw et al., 1997b). To determine the possible contribution of Clb5p to this process, we undertook a detailed analysis of astral microtubule behavior throughout spindle assembly by time-lapse microscopy in live cells.

Recordings were carried out in parental *cdc28-4* and mutant *cdc28-4 clb5Δ* diploids expressing a GFP-Tub1 fusion (Straight et al., 1997) to visualize both astral microtubules and spindle structures. Fig. 1 shows a representative recording ($n = 15$) of parental *cdc28-4* cells. A budded cell oriented astral microtubules towards and into the bud (Fig. 1, 9 min, arrowhead) while the SPBs remained side

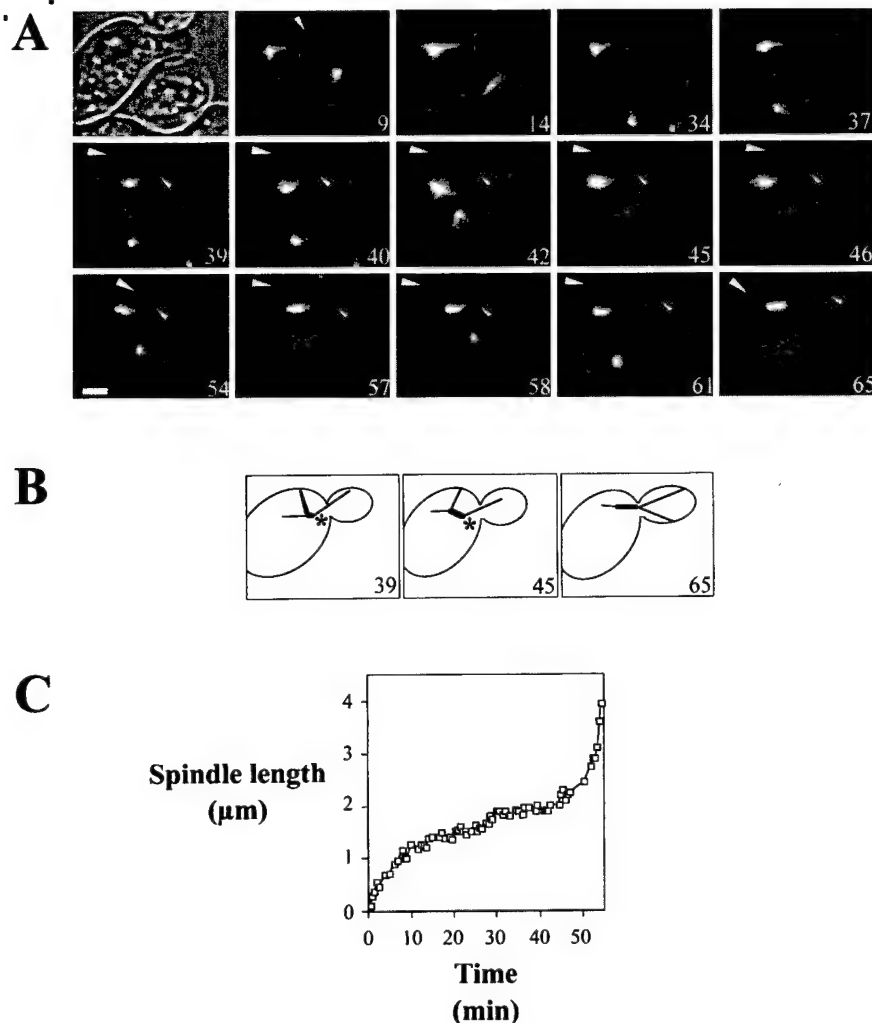


Figure 1. Spindle assembly in a *cdc28-4* diploid cell expressing a GFP-Tub1 fusion. **A**, Time-lapse series showing formation of a mitotic spindle in a *cdc28-4* cell. Astral microtubule interactions with the bud and with the vicinity of the neck cortex (organized by the SPB_{daughter} and SPB_{mother}, respectively) contribute to spindle orientation. Selected frames from a 65-min time-lapse experiment are shown. Numbers correspond to the time elapsed in minutes relative to bud emergence. Arrowheads are described in the text. Bar, 2 μ m. **B**, Cartoon of microtubule structures and cell outline for the indicated frames. Asterisk indicates SPB_{daughter}. **C**, Kinetics of spindle assembly in a *cdc28-4* cell. A representative time-lapse series was plotted from onset of SPB separation to initiation of spindle elongation at anaphase. For statistical information, see Table I.

by side facing the bud neck (Fig. 1, 9–37 min). During SPB separation, astral microtubules emanating from one SPB dynamically interacted preferentially with the bud cortex (SPB_{daughter}; Fig. 1, 39–40 min, small arrowhead). At the same time, astral microtubules from the SPB_{mother} first interacted with the mother cortex in the vicinity of the bud neck (Fig. 1, 39–40 min, large arrowhead). Therefore, spindle polarity is already evident during SPB separation. As spindle development progressed, the astral microtubules of the SPB_{mother} dynamically interacted with the mother cell cortex at points progressively further away from the bud neck (Fig. 1, 42–58 min, large arrowhead). As a result of these interactions, the SPB_{mother} was pushed away from the bud neck, promoting rotation of the spindle into the mother cell as the spindle assembled, thus ultimately orienting the spindle along the mother–bud axis (Fig. 1, 58–65 min). Once oriented, mobility of the spindle was restricted along the mother–bud axis. This sequence of events suggests that the initial astral microtubule interactions in the vicinity of the neck may be important for correct orientation of the SPB_{mother}.

The kinetics of SPB separation and spindle formation were consistent with the previous analysis of DIC time-lapse series that identified a two-step process (Yeh et al., 1995). From our data (Fig. 1 C; Table I), an ~ 1 - μ m spindle

(1.2 ± 0.2 μ m) was formed initially. This step took ~ 12 min. During this first phase, astral microtubules emanating from the SPB_{mother} interacted primarily with the cortex near the bud neck. Then, SPB separation proceeded to produce an ~ 2 - μ m spindle oriented along the mother–daughter axis (Fig. 1 C; Table I). During this second phase, microtubules emerging from the SPB_{mother} grew into the mother cell and interacted further away from the neck. Once spindles became oriented along the mother–bud axis, astral microtubules from the SPB_{mother} grew exclusively into the mother cell (100%, $n = 39$), whereas astral microtubules from the SPB_{daughter} mainly grew into the bud (88%, $n = 42$).

We conclude that spindle polarity is specified soon after, or concomitant with, SPB separation, leading to differential astral microtubule interactions: either with the bud cortex or the bud neck region, respectively. Thus, the resulting asymmetric behavior of the two SPBs is a critical determinant of spindle polarity and orientation.

Spindle Assembly and Orientation in *cdc28-4 clb5 Δ* Cells

In contrast to parental cells, in *cdc28-4 clb5 Δ* diploids, astral microtubules from both SPBs dynamically interacted

Table I. Analysis of Spindle Morphogenesis in Parental and *clb*– Mutants

Strain	Onset of spindle assembly	Spindle Assembly [‡]		Preanaphase spindle length
		~1 μ m	~2 μ m	
	<i>min</i> *	<i>min</i>	<i>min</i>	μ m
<i>cdc28-4</i>	$37 \pm 5, n = 15$	$12 \pm 3, n = 15$	$19 \pm 5, n = 13$	$2.0 \pm 0.2, n = 24$
<i>cdc28-4 clb5</i>	$34 \pm 7, n = 22$	$7 \pm 3, n = 26$	$7 \pm 3, n = 26$	$2.2 \pm 0.5, n = 31$
<i>cdc28-4 clb3 clb4</i>	$72 \pm 9, n = 6$	$11 \pm 2, n = 6$	$12 \pm 4, n = 8$	$2.3 \pm 0.4, n = 11$

*Timing was relative to bud emergence.

[‡]~1 μ m, Time from initiation of spindle assembly until length remained constant for at least 5 min; ~2 μ m, additional time to produce a preanaphase spindle.

with the bud cortex as soon as SPB separation occurred (Fig. 2). Astral microtubules from both SPBs at onset of SPB separation were more evident in cells expressing a dynein–GFP fusion, since the strong fluorescence of Tub1–GFP label associated with the spindle makes visualization of astral microtubules particularly difficult (Fig. 2, 39 min,

and Fig. 3 C). Astral microtubules from both SPBs entering the bud can be clearly seen in the time-lapse series shown in Fig. 2 at 42 min after bud emergence. The interactions with the bud cortex continued throughout the process of spindle assembly (90%, $n = 22$; Fig. 2, cell A). Overall, both poles seemed equally likely to establish dy-

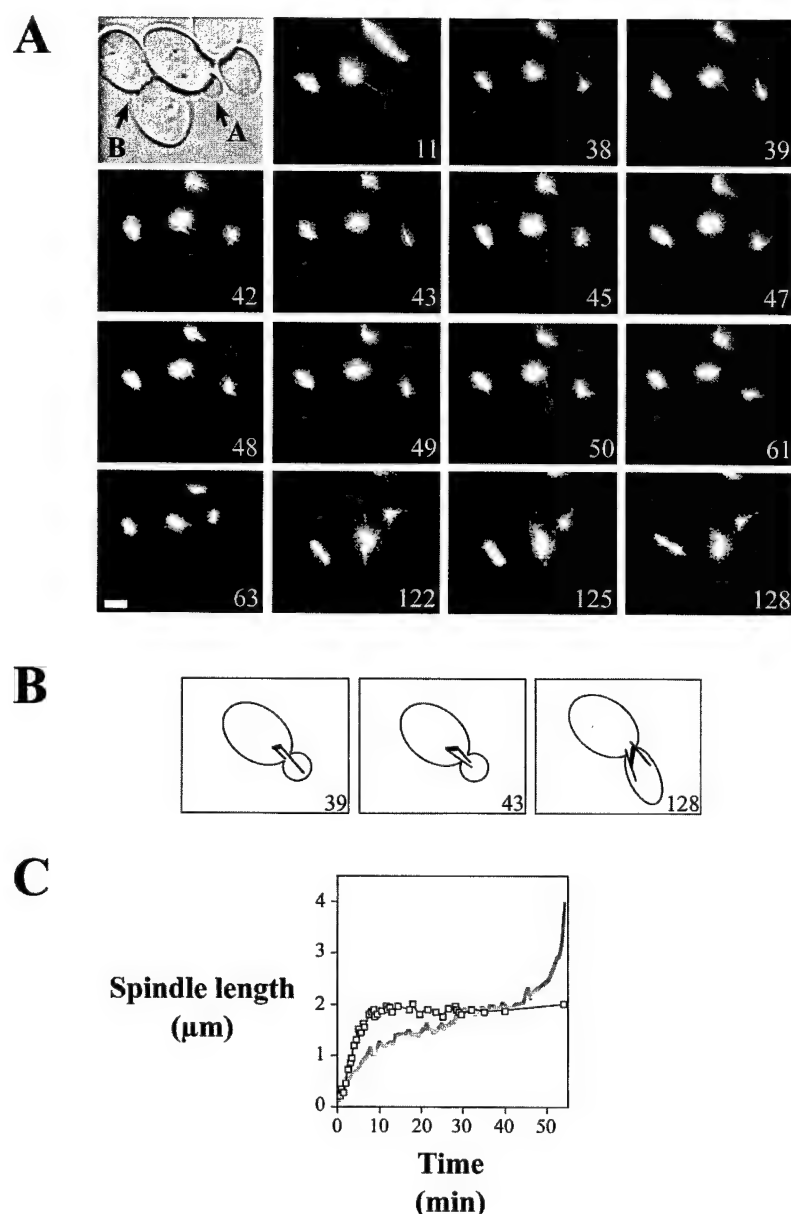


Figure 2. Spindle assembly in a *cdc28-4 clb5Δ* diploid cell expressing a GFP–Tub1 fusion. A, Time-lapse series showing formation of a mitotic spindle (cell A) in a *cdc28-4 clb5Δ* cell. During spindle assembly both SPBs organize astral microtubules interacting with the bud cortex. Microtubules from both poles entering the bud are seen at 42 min after bud emergence. A second cell already blocked late at metaphase is shown (cell B). Notice the large bud size of this cell (top) already in the first frame. In this cell, microtubules from both poles are directed towards the bud (visible in frames 49 and 50). Selected frames from a 145-min time-lapse experiment are shown. Numbers correspond to the time elapsed in minutes relative to bud emergence for cell A. Bar, 2 μ m. B, Cartoon of microtubule structures and cell outline for the indicated frames (cell A). C, Kinetics of spindle assembly in a *cdc28-4 clb5Δ* cell (\square) from onset of SPB separation. For reference, the kinetics of the parental cell shown in Fig. 1 C has been overlaid (gray line). For statistical information, see Table I.

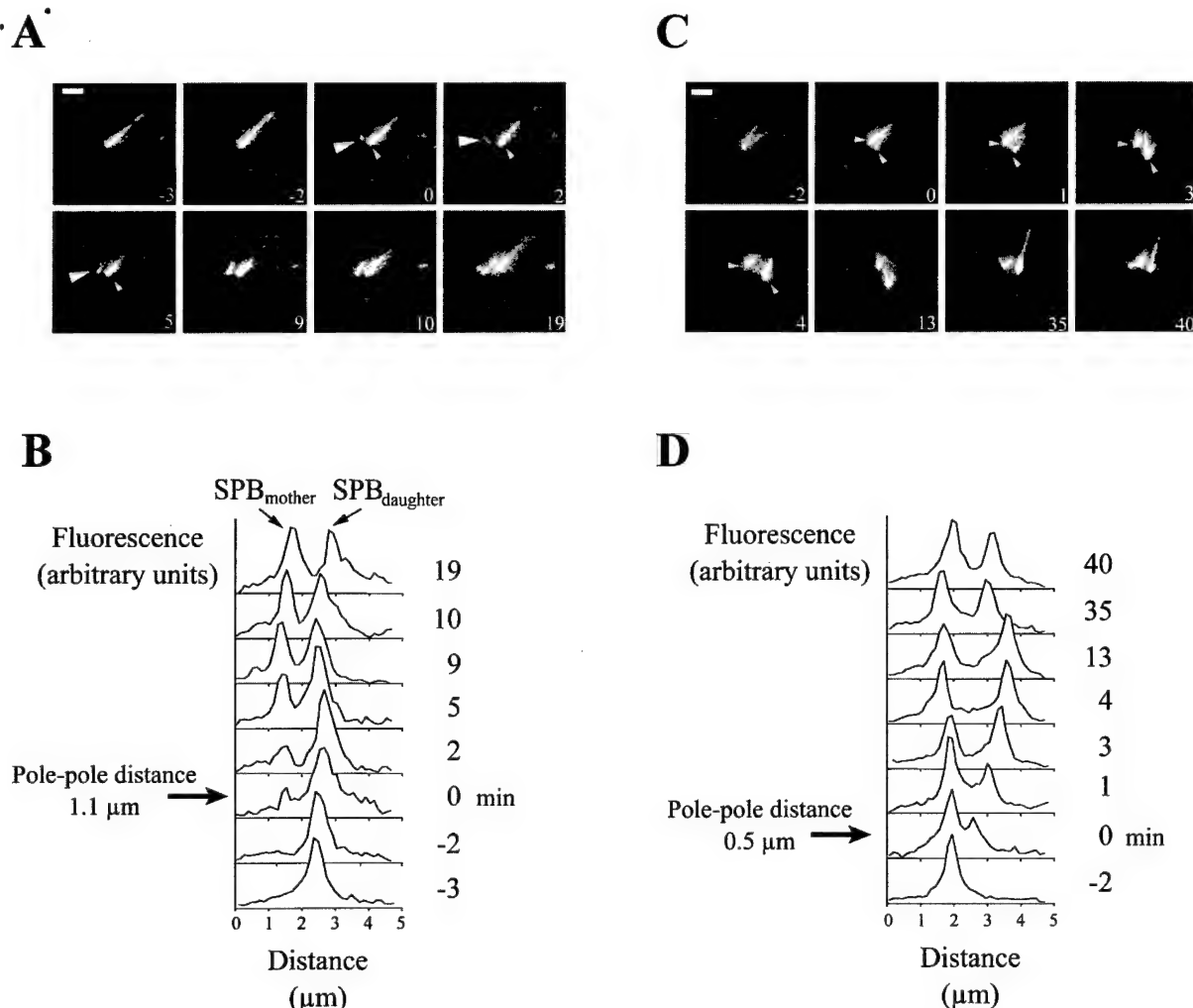


Figure 3. Dynein-GFP accumulation at the SPBs and astral microtubule behavior during spindle assembly. **A** and **B**, SPBs and astral microtubules visualized with a dynein-GFP fusion during spindle assembly in a *cdc28-4* cell. **A**, Initially the SPB_{daughter} is labeled. The second SPB (large arrowhead, 0–5 min) acquires fluorescence once SPB separation has occurred. Small arrowhead, SPB_{daughter}. **B**, Plot showing line scans through the axis of the spindle corresponding to each time frame in **A**. Pole to pole distance at time 0 was 1.1 μm and increased to 1.3 μm by 19 min. **C** and **D**, Symmetric behavior of SPBs during spindle assembly in a *cdc28-4 clb5Δ* cell. **C**, Both SPBs are already labeled at onset of SPB separation (arrowheads, 0–4 min). Microtubules from both poles enter the bud as the spindle forms, corresponding to the behavior observed in cells expressing the GFP-Tub1 fusion. **D**, Plot showing line scans through the axis of the spindle corresponding to each time frame in **C**. Pole to pole distance was 0.5 μm at 0 min and increased to 2.0 μm by 4 min. Poles appear closer at time points 35–40 min due to spindle rotation away from the axis of measurement. Numbers indicate time elapsed in minutes relative to the first frame in which the two SPBs become visible. Bars, 2 μm .

namic interactions with the daughter cell cortex >40 min after SPB separation. The dynamic nature of these interactions with the bud was evident from the fact that assembled spindles were abnormally mobile and initially tended to orient orthogonally relative to the mother–bud axis. This reflected net force between both SPBs and the bud cortex. Due to these pulling forces, spindles eventually translocated across the neck into the bud (Fig. 2, 122 min), as has been previously described (Segal et al., 1998).

The kinetics of SPB separation was dramatically affected in this mutant. Contrary to the two-step spindle assembly observed in parental *cdc28-4* diploids (Fig. 1 C) or wild-type cells (not shown; Yeh et al., 1995), *cdc28-4 clb5* mutants appeared to assemble a spindle in one step (Fig. 2

C). While parental cells completed spindle assembly in ~30 min, the mutant formed ~2- μm spindles in seven minutes (Table I).

After spindle assembly, most cells failed to proceed with spindle elongation. During the block, spindles tended to become aligned with respect to the mother–bud axis. This was due to the restrictions in orientation imposed by occasional transits of the spindle across the bud neck. However, polarity was still disrupted since both poles continued to interact with the bud cortex (Fig. 2, cell B). After a prolonged block, astral microtubules directed towards the daughter cell cortex seemed functional, but those growing into the mother cell became abnormally long and curved. It is possible that this behavior resulted from lack of initial

interactions between these mother-bound microtubules and the neck cortex. This corresponded to the terminal phenotype previously described for this mutant.

These data suggest that Clb5p-dependent kinase ensures that SPBs become asymmetric regarding their ability to promote specific astral microtubule interactions either with the mother or daughter cell cortex in tight coordination with spindle assembly. In addition, our results suggest a direct or indirect role for Clb5p in regulating the kinetics of spindle assembly.

Dynein-GFP Labeling and Spindle Symmetry

Differential association of dynein fusion proteins with each SPB throughout the cell cycle has demonstrated the inherent asymmetry of the SPBs during spindle morphogenesis (Yeh et al., 1995; Shaw et al., 1997b). The fact that both SPBs in *cdc28-4 clb5Δ* cells appeared to organize astral microtubules that interacted with the bud cortex during spindle assembly suggested that the inherent polarity of the spindle might be disrupted in *cdc28-4 clb5Δ* cells. To address this issue, parental and *cdc28-4 clb5Δ* mutant cells expressing a dynein-GFP fusion were studied by time-lapse digital imaging microscopy. As previously reported (Shaw et al., 1997b), otherwise wild-type diploids displayed the characteristic lag in dynein-GFP acquisition to the SPB_{mother} (delayed acquisition in ten out of ten events; not shown). Parental *cdc28-4* diploids behaved like wild-type cells (delayed acquisition 11 out of 13 events; Fig. 3, A and B). In other words, the SPB_{mother} was not labeled until the spindle was at least 1 μm long ($1.1 \pm 0.2 \mu\text{m}$, $n = 11$). At this time, the SPB_{mother} was weakly labeled (Fig. 3 A, 0 min) as in wild-type cells. Label gradually increased until it reached comparable intensities to the SPB_{daughter} (Fig. 3 B).

This asymmetric behavior, however, was lost in *cdc28-4 clb5Δ* diploids. Both SPBs were labeled and visible as soon as SPBs separated (no lag in eight out of eight events, pole to pole distance $0.45 \pm 0.1 \mu\text{m}$; Fig. 3, C and D, 0 min). The absence of any observable lag in the acquisition of dynein-GFP correlated with the fact that both SPBs promoted interactions with the bud cortex.

Previous digital imaging microscopy studies using the same fusion have indicated that astral microtubules mediate dynein-GFP labeling of the SPB (Shaw et al., 1997b; Maddox et al., 1999). Thus, dynein-GFP label acts as a "read out" for the delayed presence of microtubules emerging from the SPB_{mother}. Such built-in delay in astral microtubule organization, relative to SPB separation, may constitute the basis for correct spindle orientation, as previously suggested by Shaw et al. (1997b).

Consistent with dynein not being a direct mediator of daughter-bound polarity, deletion of *DHC1*, the gene encoding dynein heavy chain (Eshel et al., 1993; Li et al., 1993), did not suppress the polarity defect observed in *cdc28-4 clb5Δ* cells. Astral microtubule behavior was examined after a four-hour shift of a *cdc28-4 clb5Δ dhc1Δ* *GAL1-CLB5* strain to glucose. Initial symmetric astral microtubule interactions with the bud occurred in *cdc28-4 clb5Δ dhc1Δ* as in *cdc28-4 clb5Δ DHC1* cells (Fig. 4). In addition, 10% of cells displayed a combination of the polarity defect of *cdc28-4 clb5Δ* and the astral microtubule

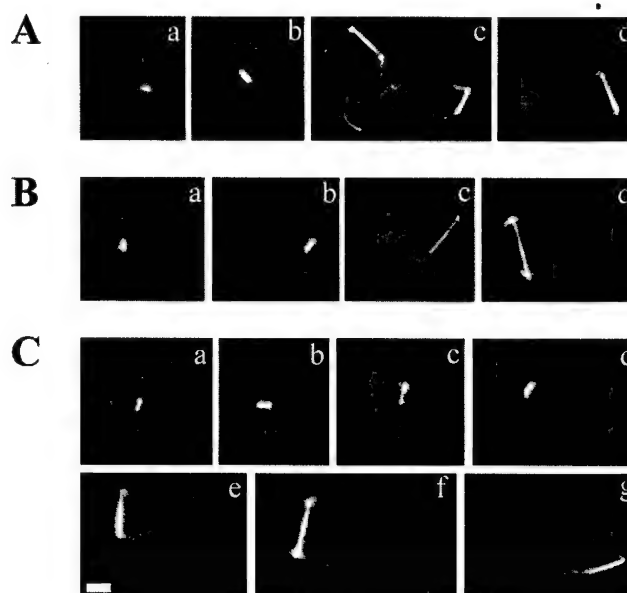


Figure 4. Definition of spindle polarity is not affected in *dhc1Δ* mutants. Cells were grown on 3% galactose–0.1% glucose synthetic medium followed by a 4-h shift to glucose synthetic medium to repress *GAL1-CLB5* expression necessary for viability of *cdc28-4 clb5* diploids. Cells were examined microscopically and scored for defects in apparent polarity definition after spindle assembly, irrespective of position or orientation (i.e., astral microtubule interactions with the bud from both poles). Images of cells expressing the GFP-Tub1 fusion were captured as previously described (Segal et al., 1998). Percentages represent the average of two independent counts of 500 cells containing a spindle for the indicated strains. **A**, Representative stages in *dhc1Δ* diploids. Spindle polarity is evident as soon as a spindle forms (a and b), as well as in cells undergoing anaphase without the spindle translocating across the neck (c and d). Anaphases in the mother occurred in 12% of cells under the experimental conditions. 98% of cells carrying a spindle exhibited astral microtubules from a single pole interacting with the bud. **B**, Representative stages in a *cdc28-4 dhc1Δ* diploid. a, Cell with a short spindle. One pole is interacting with the bud. Also, prominent interactions with the neck are evident. b, Cell containing a short spindle away from the bud neck. c and d, Mispositioned anaphase spindles. Astral microtubules from a single pole interacted with the bud in 95% of cells. **C**, Representative stages in a *cdc28-4 clb5 dhc1Δ* diploid. a–c, As a spindle forms, both poles interact with the bud as described in Fig. 2. d, Cell with spindle mispositioned in the bud (20% of cells). e–g, Mispositioned anaphase spindles. Both poles still interact with the bud (10% of cells). Bar, 2 μm.

behavior characteristic of *dhc1Δ* mutants. Comparable behavior of astral microtubules from both SPBs was observed even in cells with spindles positioned in the mother (Fig. 4 C). In contrast, *cdc28-4 dhc1Δ* cells displayed correct spindle polarity regardless of spindle positioning, i.e., only a single SPB seemed to associate with the bud via abnormally long astral microtubules.

Overall, the *dhc1Δ* mutation seemed to exacerbate the polarity defect of *cdc28-4 clb5* cells. Presumably, due to the decreased microtubule dynamic instability characteristic of *dhc1Δ* cells (Carminati and Stearns, 1997), misdirected microtubule attachments were even harder to rectify after spindle assembly. The mutation also increased

the proportion of spindles remaining in the mother cell (irrespective of orientation of astral microtubules into the bud), consistent with dynein's importance in spindle translocation. However, a new spindle-dynamic behavior resulted in this situation. Occasional anaphases in the mother cell stalled, apparently, as a consequence of lack of functional attachments into the mother cell (not shown).

Taken together, these results suggest that the Clb5p-dependent kinase effect on inherent spindle polarity was not mediated by dynein activity. However, the resulting genetic interaction emphasizes the contribution of microtubule dynamic instability as a factor in the establishment of correct spindle orientation. The *dhc1Δ* mutation, however, did not alter the fact that both SPBs ultimately displayed the characteristic daughter-bound behavior of the *cdc28-4 clb5Δ* mutant, even though translocation across the neck was partially suppressed.

Contribution of Clb3p and Clb4p to Spindle Morphogenesis

A redundant function early in the spindle pathway has been genetically assigned to Clb5p, Clb3p, and Clb4p. A triple *clb3 clb4 clb5* mutant fails to form a bipolar spindle and arrests with a 2C DNA content (Schwob and Nasmyth, 1993). Nevertheless, the precise role played by each of these cyclins in spindle development has not been addressed.

Using our genetic approach of sensitizing cells to cyclin deficiencies with a mutant Cdc28p kinase, we constructed a strain carrying a *cdc28-4* allele in combination with disruptions at the *CLB3* and *CLB4* loci and expressing the GFP-Tub1 fusion (Segal et al., 1998). The diploid mutant was viable at permissive temperature and displayed comparable temperature sensitivity to a parental *cdc28-4* diploid (data not shown). However, elimination of Clb3p and Clb4p had a profound effect on the cell cycle timing of spindle development. Fluorescence microscopy of cells from an asynchronous culture indicated that a high proportion of large budded cells was apparently delayed for spindle assembly. The percentage of large budded cells that had not initiated spindle assembly was $21 \pm 2\%$ for parental cells, whereas in *cdc28-4 clb3Δ clb4Δ* diploids, it was $54 \pm 6\%$. Yet, in the *cdc28-4 clb3 clb4* cells, astral microtubules projecting from the unseparated SPBs were oriented correctly, one bundle towards the mother and one towards the bud, a behavior normally characteristic of cells that have already assembled a spindle (Fig. 5). The fact that *cdc28-4 clb3 clb4* diploids can establish correct spindle polarity, even though SPB separation is delayed, was confirmed by time-lapse microscopy (Fig. 6). The timing of SPB separation was significantly delayed relative to bud emergence (72 min, compared with 37 min in *cdc28-4* cells or 34 min in *cdc28-4 clb5* cells; Table I). Yet, astral microtubule behavior followed a cell cycle pattern comparable to that of parental *cdc28-4* cells (Fig. 1). Since attachments appeared to orient before SPB separation (Fig. 5 C and Fig. 6, 41–73 min), spindle orientation along the mother–bud axis could be rapidly established upon assembly (Fig. 6, 88 min). Kinetics of spindle formation in this mutant, while delayed with respect to bud emergence, was more comparable to that of parental cells (Fig. 6 C; Table

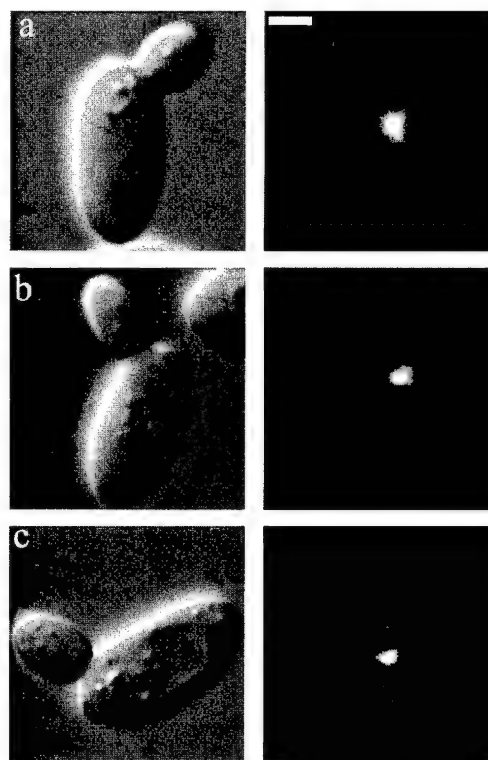


Figure 5. Definition of spindle polarity in a *cdc28-4 clb3Δ clb4Δ* diploid. Comparison of astral microtubule behavior in *cdc28-4* (a), *cdc28-4 clb5Δ* (b), and *cdc28-4 clb3Δ clb4Δ* (c) cells expressing the GFP-Tub1 fusion. Notice that in a and b, SPB separation has already started, whereas in c, SPBs remain side by side. Pairs of DIC and single fluorescence images are shown. Bar, 2 μ m.

I). Formation of a 2- μ m long spindle took place over a period of ~ 20 min. Then, spindle length continued to increase until onset of anaphase. As a result, anaphase occurred with a slight delay, relative to bud emergence (110 min vs. 92 min in parental cells).

The distinct contributions of Clb3p, Clb4p, and Clb5p, respectively, in spindle morphogenesis suggests that nuclear and astral microtubules are regulated differentially by the cell cycle machinery. In addition, Clb5p may be directly or indirectly responsible for the two-step kinetics of spindle assembly.

Discussion

Clb5p-dependent Kinase Contributes to Spindle Polarity

Our analysis of spindle development by time-lapse digital imaging microscopy indicates that the inherent asymmetry of SPBs can dictate the correct orientation of astral microtubules so that they interact with the bud or mother cell cortex, respectively, during spindle assembly (Figs. 1 and 3 A). This asymmetric behavior was lost in *cdc28-4 clb5Δ* cells, causing astral microtubules, emanating from both SPBs, to primarily orient towards the bud (Figs. 2 and 3 C). Therefore, Clb5p-associated kinase is required to impart polarity to the spindle during assembly, by regulating,

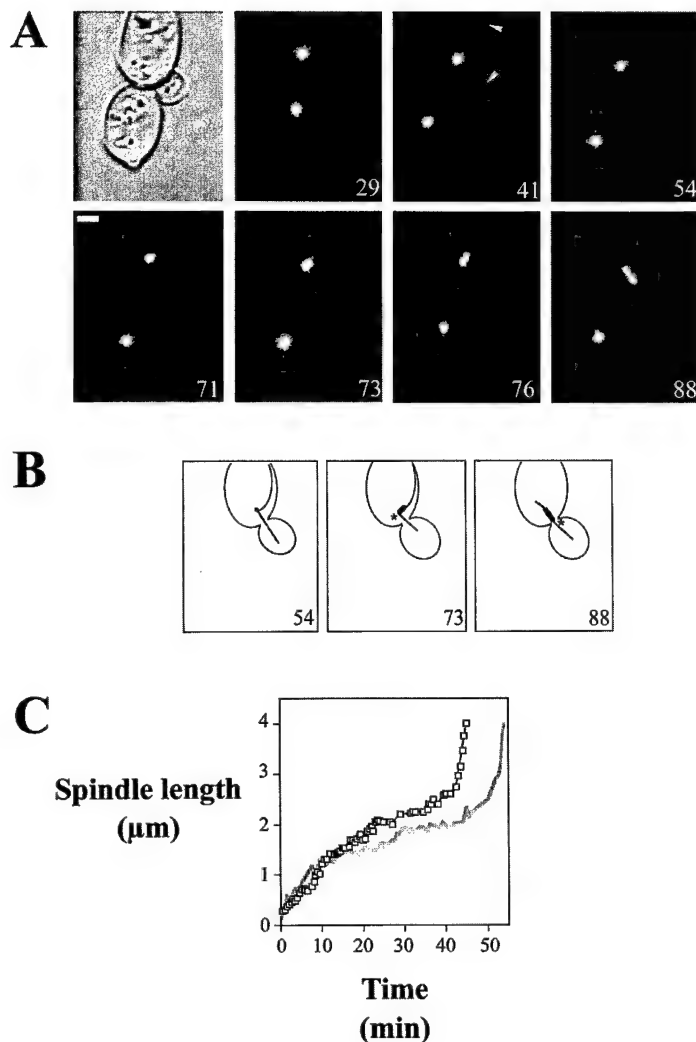


Figure 6. Spindle assembly and orientation in a *cdc28-4 clb3Δ clb4Δ* cell expressing the GFP-Tub1 fusion. **A**, Time-lapse series showing delayed spindle assembly in a *cdc28-4 clb3Δ clb4Δ* cell. SPB separation started at 73 min after bud emergence. Spindle orientation along the mother-bud axis was achieved by 88 min, before anaphase. Though astral microtubules are difficult to distinguish in this series, frame 41 corresponds approximately to the cell cycle stage of the cell shown in Fig. 5 C, suggesting that attachments to the mother and bud cell cortex occurred approximately on schedule (arrowheads), even though SPBs remained side by side for an additional 32 min. Numbers indicate time elapsed in minutes relative to bud emergence for the upper cell. Bar, 2 μ m. **B**, Cartoon of microtubule structures and cell outline for the indicated frames. Asterisk indicates SPB_{daughter}. **C**, Kinetics of spindle assembly from pole separation to initiation of anaphase in a *cdc28-4 clb3 clb4* cell. For reference, the kinetics of the parental cell shown in Fig. 1 C has been overlaid (gray line). For statistical information, see Table I.

at least, SPB_{mother} function. This event must occur within a restricted temporal window (Segal et al., 1998), possibly related to changes in astral microtubule dynamic properties during the cell cycle. Before spindle development, astral microtubules display fast turnover rates (Carminati and Stearns, 1997; Shaw et al., 1997b; Tirnauer et al., 1999). Failure within this restricted period to specify spindle polarity appears to compromise spindle orientation, suggesting that misoriented astral microtubule contacts might be difficult to rectify once microtubule turnover rates decrease later in the cell cycle. Alternatively, Clb5p activity may only ensure correct spindle polarity if present before SPB separation.

Two additional B-type cyclins, Clb3p and Clb4p, were dispensable for correct spindle polarity (Figs. 5 and 6). However, these cyclins were important for correct timing of spindle assembly (Fig. 6; Table I).

Spindle Assembly and Orientation Are Tightly Linked Processes

Our studies of spindle assembly in cells expressing a Tub1-GFP fusion enabled us to correlate astral microtubule behavior with spindle assembly. Our conclusions,

while consistent with previous studies dealing separately with either kinetics of SPB separation (Kahana et al., 1995; Yeh et al., 1995) or astral microtubule behavior (Carminati and Stearns, 1997; Shaw et al., 1997b), convey an integrated view of spindle assembly and initial orientation as tightly linked processes.

After bud emergence, side by side SPBs orient facing the bud neck, a process that depends on a microtubule-based search mechanism (Shaw et al., 1997b). Both in wild-type (not shown) and parental *cdc28-4* diploids (Fig. 1), we observed that formation of a short, <1.2- μ m spindle was accompanied by interactions between one pole (SPB_{mother}) and the vicinity of the neck via astral microtubules. Individual spindles spent a variable time (5–15 min) at this stage before proceeding to the second phase of spindle assembly (not shown). During the second phase, astral microtubules from the SPB_{mother} continued to grow into the mother cell and interacted with points further away from the neck as the spindle oriented along the mother-bud axis and reached a constant size of \sim 2 μ m.

Interestingly, dynein-GFP label is first acquired by the SPB_{mother} when the poles were \sim 1 μ m apart (Fig. 3 B). As label gradually increased, the distance between the poles remained approximately constant (Fig. 3, A and B). This

suggests that acquisition of dynein-GFP label by the SPB_{mother} occurs coincident with the transition between the first and second phase of spindle assembly.

In view of these results, it is striking that *cdc28-4 clb5Δ* cells displayed a spindle polarity defect, as well as altered kinetics of spindle assembly (Fig. 2). The simultaneous labeling by dynein-GFP at onset of SPB separation and the perturbed kinetics of spindle assembly might represent independent defects resulting from loss of Clb5p-dependent kinase. Yet, it is tempting to suggest that both defects are somehow related. The wild-type program of dynein-GFP acquisition and the kinetics of SPB separation may indicate that spindle orientation (i.e., astral microtubule organization and/or interactions with the neck) and spindle morphogenesis can cross-talk at the transition between the first and second step of spindle assembly.

It is unlikely that the spindle polarity and morphogenesis defects in *cdc28-4 clb5Δ* cells are a consequence of Clb5p normally antagonizing Clb3p and Clb4p function. First, these three cyclins have been suggested to play a redundant function in the spindle pathway (Schwob and Nasmyth, 1993). Second, *CLB3* is a high dosage suppressor of the *cdc28-4 clb5Δ* lethality and spindle positioning defect (Segal et al., 1998). In addition, our kinetic studies of spindle assembly in the context of S-phase checkpoint activation by 0.1 M hydroxyurea (Clarke et al., 1999; Clarke, D.J., M. Segal, and S.I. Reed, unpublished results), do not favor a relationship between the biphasic kinetics of spindle assembly discussed here and events associated with completion of DNA replication.

Previously, we have reported that in *cdc28-4 clb5Δ* cells, nuclear division in the bud was blocked (Segal et al., 1998). The combination of defects in spindle morphogenesis described in the present study may account for this observation. Whether the inability of spindles to elongate results from the triggering of a checkpoint or from a mechanical defect remains to be determined.

A Model for Clb5p Role in Spindle Morphogenesis

At present, our understanding at the molecular level of structures and events associated with astral microtubule organization is too limited to suggest a defined target(s) for Clb5p kinase relevant to SPB asymmetry. After SPB duplication, astral microtubules emerge from the bridge region (Byers and Goetsch, 1975; Byers, 1981). Throughout the rest of the cell cycle, however, astral microtubules seem to organize from the outer plaques of the SPBs. In addition, a model to explain establishment of asymmetry upon SPB separation must incorporate the fact that it is the old SPB inherited from the previous cell cycle that is destined to the mother cell (Vallen et al., 1992). Interestingly, it was a Kar1-LacZ fusion (mistargeted to the outer plaque) that revealed the asymmetric nature of SPBs. Wild-type Kar1, which localizes to the half-bridge, associates with both SPBs throughout the cell cycle (Spang et al., 1995). Thus, the mechanistic implications for the differential association of this protein fusion remain unclear.

The asymmetric acquisition of a dynein-GFP fusion by the SPBs correlates with the promotion of asymmetric dynamic contacts towards the bud and mother cell. This suggests that timing of microtubule organization by SPBs

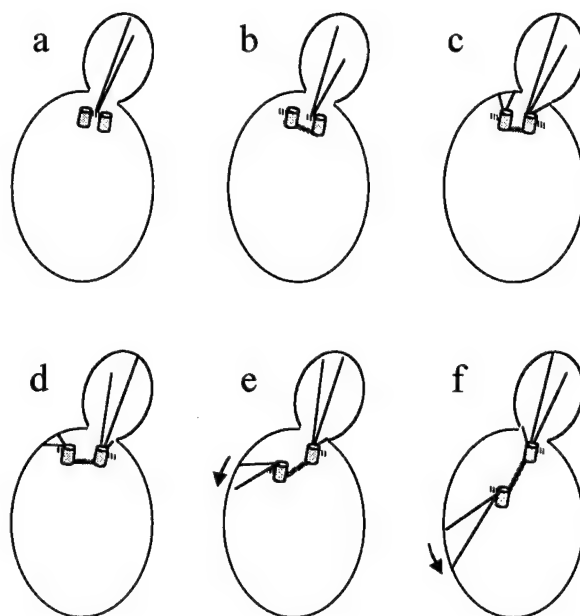


Figure 7. A model for coordinated spindle assembly and orientation. After bud emergence, the duplicated SPBs orient facing the bud neck via astral microtubules emanating from the bridge (a). Once oriented, one pole, the SPB_{daughter}, inherits these astral microtubules as the bridge divides between the two SPBs (b). A "fast" phase of spindle assembly occurs and, coordinate with this event, astral microtubules initiate interactions from each pole with the mother cortex at the neck area (c). These interactions may initiate a transition to a second, slower phase of spindle formation. While spindle assembly continues, astral microtubules from the SPB_{mother} are crucial to impart correct orientation to the spindle along the mother-bud axis (d-f). Spindle morphogenesis in *cdc28-4 clb5* cells is deregulated in step (c), leading to inherent symmetry of the spindle already at this point.

is crucial for microtubule orientation, as anticipated by Shaw et al. (1997b). Thus, dividing spindle morphogenesis into two temporally distinct steps might ensure the asymmetric behavior of SPBs. The first step would commit the SPB_{daughter} to interact with the bud cortex. The second step would impart mother-bound behavior to the remaining pole (Fig. 7). Initially, astral microtubules emanating from the bridge interact with the bud cell cortex (Fig. 7 a). Based on time-lapse microscopy, astral microtubules interact continuously with the bud before and during SPB separation. This may indicate that, as the poles separate, the microtubules initially present on the bridge are inherited by a single pole, the SPB_{daughter} (Fig. 7 b). Regardless of the mechanistic details, however, this event cannot solely regulate spindle polarity. As SPBs separate, microtubule organization at the respective outer plaques must be delayed until a temporal window, when initial contacts with the mother cell at the neck area, would be favored. Since one pole is initially committed to be the SPB_{daughter}, the delay in microtubule organization could actually be imparted to both poles with the net result of ensuring correct fate to the SPB_{mother} (Fig. 7 c).

Dynein-GFP labeling is consistent with such a model. The intensity of label remains constant through initial orientation of the microtubule bundle into the bud and the

early steps of SPB separation. Thus, the bundle of microtubules associated with the bud seems to be inherited by the SPB_{daughter}. As a short spindle forms, delayed acquisition is only evident on the SPB_{mother}. Microtubule organization by the SPB_{daughter}, however, is not revealed because of the already existing label at this pole.

The pattern of dynein-GFP labeling in a *cdc28-4 clb5Δ* cell (Fig. 3 C) suggests that the initial partition of microtubules associated with the bud occurs correctly since only one pole seemed to retain contacts to the bud cortex at onset of SPB separation (Fig. 3 C, 0 min). However, this mutant presumably organized microtubules at the outer plaque of the SPBs prematurely and/or uncoordinated with respect to SPB separation. The net result is that the SPB_{mother} lacks the normal lag in dynein-GFP acquisition that reflects correct fate. Thus, both poles become equally likely to be daughter-bound. This model can explain how Clb5p regulates correct asymmetry at a point in which two poles are already present. It is possible that Clb6-dependent kinase in this strain may be sufficient to bring about clipping of the bridge with correct timing relative to bud emergence. This event also requires B-type cyclin-dependent Cdc28p activity since it is blocked in a *cdc4* mutant, which arrests before Clb-dependent kinase activation at the restrictive temperature (Byers, 1981; Schwob et al., 1994). Yet, Clb6p activity may be unable to regulate outer plaque function unless grossly overexpressed (Segal et al., 1998). Thus, Clb5p/Cdc28p kinase activity may be necessary to inhibit or delay astral microtubule organization from the SPB outer plaque until the cell is permissive for mother cortex interaction.

It is not known what triggers initial organization of astral microtubules at the outer plaque or how the process might be coordinated during SPB separation. Yet this, or a closely related event, remains a likely target in imparting Clb5p-dependent SPB asymmetry. For example, association of the γ -tubulin complex to the outer plaque target, Spc72p (Knop and Schiebel, 1998), may be subjected to regulation by cyclin-dependent kinases. Cortical cues are important in establishment of correct spindle orientation (Lee et al., 1999; Miller et al., 1999). Their contribution to the *cdc28-4 clb5* phenotype, however, is mostly reflected in the different penetrance of the nuclear positioning defect in haploids and diploids (Segal et al., 1998; Segal, M., K. Bloom, and S.I. Reed, manuscript in preparation). However, our genetic analysis does not support a primary role for known cortical cues in mediating the initially symmetric behavior of spindles in *cdc28-4 clb5Δ* cells described here (Segal, M., K. Bloom, and S.I. Reed, unpublished results).

Development of a multicellular organism entails the ability to generate a variety of cell types beginning from a single cell. Diversity arises primarily from asymmetric divisions, resulting in daughter cells that differ in developmental fates (Rhyu and Knoblich, 1995). The strategy, which relies on regulating the orientation of cell divisions in response to positional cues, has been characterized in a variety of systems, including the early divisions of *Caenorhabditis elegans* (Rhyu and Knoblich, 1995) and mammalian neurogenesis (Hyman and White, 1987). The mechanism for spindle orientation shares common features with the yeast system (Chenn and McConnell, 1995; Rhyu and Knoblich, 1995; Skop and White, 1998). The

role of Clb5p in the definition of inherent spindle polarity, in yeast suggests that the cell cycle machinery may also play a crucial role in early development, by regulating centrosome asymmetry. In turn, alternative modes of spindle orientation might contribute to specify symmetric versus asymmetric divisions and, eventually, cell fate.

We thank A.F. Straight and D. Stuart for the generous gift of plasmids and strains. Thanks to C. Wittenberg and K. Sullivan for stimulating discussions and members of the Reed, Wittenberg, Russel, Bloom, and Salmon labs for the supporting environment.

M. Segal acknowledges fellowships from the European Molecular Biology Organization and the Human Frontiers in Science Program. D.J. Clarke was supported by a United States Army Medical Research Materiel Command Breast Cancer Research Fellowship. This work was supported by a United States Public Health Service grant GM38328 to S.I. Reed.

Submitted: 2 November 1999

Revised: 30 December 1999

Accepted: 5 January 2000

References

- Byers, B. 1981. Cytology of the yeast life cycle. In *The Molecular Biology of the Yeast Saccharomyces: Life Cycle and Inheritance*. J.N. Strathern, E.W. Jones, and J.R. Broach, editors. Cold Spring Harbor Laboratory Press, Cold Spring Harbor, NY. 59–96.
- Byers, B., and L. Goetsch. 1975. Behavior of spindles and spindle plaques in the cell cycle and conjugation of *Saccharomyces cerevisiae*. *J. Bacteriol.* 124:511–523.
- Carminati, J.L., and T. Stearns. 1997. Microtubules orient the mitotic spindle in yeast through dynein-dependent interactions with the cell cortex. *J. Cell Biol.* 138:629–641.
- Chenn, A., and S.K. McConnell. 1995. Cleavage orientation and the asymmetric inheritance of Notch1 immunoreactivity in mammalian neurogenesis. *Cell.* 82:631–641.
- Clarke, D.J., M. Segal, G. Mondésert, and S.I. Reed. 1999. The Pds1 anaphase inhibitor and Mec1 kinase define distinct checkpoints coupling S phase with mitosis in budding yeast. *Curr. Biol.* 9:365–368.
- Eshel, D., L.A. Urrestarazu, S. Vissers, J.C. Jauniaux, J.C. Van Vliet-Reedijk, R.J. Planta, and I.R. Gibbons. 1993. Cytoplasmic dynein is required for normal nuclear segregation in yeast. *Proc. Natl. Acad. Sci. USA.* 90:11172–11176.
- Fitch, I., C. Dahmann, U. Surana, A. Amon, K. Nasmyth, L. Goetsch, B. Byers, and B. Futcher. 1992. Characterization of four B-type cyclin genes of the budding yeast *Saccharomyces cerevisiae*. *Mol. Biol. Cell.* 3:805–818.
- Hoyt, M.A., and J.R. Geiser. 1996. Genetic analysis of the mitotic spindle. *Annu. Rev. Genet.* 30:7–33.
- Hyman, A.A., and J.G. White. 1987. Determination of cell division axes in the early embryogenesis of *Caenorhabditis elegans*. *J. Cell Biol.* 105:2123–2135.
- Kahana, J.A., B.J. Schnapp, and P.A. Silver. 1995. Kinetics of spindle pole body separation in budding yeast. *Proc. Natl. Acad. Sci. USA.* 92:9707–9711.
- Knop, M., and E. Schiebel. 1998. Receptors determine the cellular localization of a γ -tubulin complex and thereby the site of microtubule formation. *EMBO (Eur. Mol. Biol. Organ.) J.* 17:3952–3967.
- Lee, L., S.K. Klee, M. Evangelista, C. Boone, and D. Pellman. 1999. Control of mitotic spindle position by the *Saccharomyces cerevisiae* formin Bni1p. *J. Cell Biol.* 144:947–961.
- Lew, D.J., T. Weinert, and J.R. Pringle. 1997. Cell cycle control in *Saccharomyces cerevisiae*. In *The Molecular and Cellular Biology of the Yeast Saccharomyces*. J.R. Pringle, J.R. Broach, and E.W. Jones, editors. Cold Spring Harbor Laboratory Press, Cold Spring Harbor, NY. 607–695.
- Li, Y.-Y., E. Yeh, T. Hays, and K. Bloom. 1993. Disruption of mitotic spindle orientation in a yeast dynein mutant. *Proc. Natl. Acad. Sci. USA.* 90:10096–10100.
- Maddox, P., E. Chin, A. Mallavarapu, E. Yeh, E.D. Salmon, and K. Bloom. 1999. Microtubule dynamics from mating through the first zygotic division in the budding yeast *Saccharomyces cerevisiae*. *J. Cell Biol.* 144:977–987.
- Miller, R.K., D. Matheos, and M.D. Rose. 1999. The cortical localization of the microtubule orientation protein, Kar9p, is dependent upon actin and proteins required for polarization. *J. Cell Biol.* 144:963–975.
- Rhyu, M.S., and J.A. Knoblich. 1995. Spindle orientation and asymmetric cell fate. *Cell.* 82:523–526.
- Richardson, H., D.J. Lew, M. Henze, K. Sugimoto, and S.I. Reed. 1992. Cyclin-B homologs in *Saccharomyces cerevisiae* function in S phase and in G2. *Genes Dev.* 6:2021–2034.
- Schwob, E., and K. Nasmyth. 1993. *CLB5* and *CLB6*, a new pair of B cyclins involved in DNA replication in *Saccharomyces cerevisiae*. *Genes Dev.* 7:1160–1175.

- Schwöb, E.T. Böhm, M.D. Mendenhall, and K. Nasmyth. 1994. The B-type cyclin kinase inhibitor p40^{STC1} controls the G1 to S transition in *S. cerevisiae*. *Cell*. 79:233–244.
- Segal, M., D.J. Clarke, and S.I. Reed. 1998. Clb5-associated kinase activity is required early in the spindle pathway for correct preanaphase nuclear positioning in *Saccharomyces cerevisiae*. *J. Cell Biol.* 143:135–145.
- Shaw, S.L., E. Yeh, K. Bloom, and E.D. Salmon. 1997a. Imaging green fluorescent protein fusion proteins in *Saccharomyces cerevisiae*. *Curr. Biol.* 7:701–704.
- Shaw, S.L., E. Yeh, P. Maddox, E.D. Salmon, and K. Bloom. 1997b. Astral microtubule-based searching mechanism for spindle orientation and nuclear migration into the bud. *J. Cell Biol.* 139:985–994.
- Sherman, F., G. Fink, and J.B. Hicks. 1986. *Methods in Yeast Genetics*. Cold Spring Harbor Laboratory Press, Cold Spring Harbor, NY.
- Skop, A.R., and J.G. White. 1998. The dynactin complex is required for cleavage plane specification in early *Caenorhabditis elegans* embryos. *Curr. Biol.* 8:1110–1116.
- Spang, A., I. Courtney, K. Grein, M. Matzner, and E. Schiebel. 1995. The Cdc31p-binding protein Kar1p is a component of the half bridge of the yeast spindle pole body. *J. Cell Biol.* 128:863–877.
- Straight, A.F., W.F. Marshall, J.W. Sedat, and A.W. Murray. 1997. Mitosis in living budding yeast: anaphase A but no metaphase plate. *Science*. 277:574–578.
- Surana, U., H. Robitsch, C. Price, T. Schuster, I. Fitch, A.B. Futcher, and K. Nasmyth. 1991. The role of *CDC28* and cyclins during mitosis in the budding yeast *S. cerevisiae*. *Cell*. 65:145–161.
- Tirnauer, J.S., E. O'Toole, L. Berrueta, B.E. Bierer, and D. Pellman. 1999. Yeast Bim1p promotes the G1-specific dynamics of microtubules. *J. Cell Biol.* 145:993–1007.
- Vallen, E.A., T.Y. Scherson, T. Roberts, K. van Zee, and M.D. Rose. 1992. Asymmetric mitotic segregation of the yeast spindle pole body. *Cell*. 69:505–515.
- Yeh, E., R.V. Skibbens, J.W. Cheng, E.D. Salmon, and K. Bloom. 1995. Spindle dynamics and cell cycle regulation of dynein in the budding yeast, *Saccharomyces cerevisiae*. *J. Cell Biol.* 130:687–700.

**Mec1-Dependent Regulation of Pds1 Levels in response to S phase
checkpoint activation**

Duncan J. Clarke^{*}, Marisa Segal^{*}, Sanne Jensen^{†*}
and Steven I. Reed[‡]

Department of Molecular Biology,
The Scripps Research Institute,
10550 North Torrey Pines Road,
La Jolla,
California 92037,
USA

Tel: +1 (858) 784 9836

Fax: +1 (858) 784 2781

[†] Present address: Division of Yeast Genetics, National Institute for Medical Research,
Mill Hill, London NW7 1AA, UK

[‡] Corresponding author; sreed@scripps.edu

^{*} Equal contribution

Running title: S-phase checkpoint regulates Pds1p stability

Abstract

Background

The yeast anaphase inhibitor Pds1p is stabilised in response to DNA damage and spindle assembly checkpoint controls. We have previously provided genetic evidence that Pds1p also functions in a novel late S-phase checkpoint pathway that couples mitotic progression to completion of DNA replication. *pds1* mutants lose sister chromatid cohesion and initiate spindle elongation during S-phase. However, it is not known whether this Pds1p-dependent control system is biochemically linked to the well established S-phase checkpoint machinery, defined by Mec1 and Rad53 protein kinases.

Results

Here we show that Pds1 protein is maintained in response to S-phase checkpoint activation, and that this depends on Mec1p kinase. In contrast, Rad53p is dispensable for Pds1 persistence, demonstrating that S-phase checkpoint control operates by two distinct sequential branches downstream of Mec1p. We further demonstrate that Pds1p cannot regulate spindle elongation in early S-phase, and that the inhibitory target of Pds1p, separin Esp1, is dispensable for spindle elongation in early S-phase.

Conclusions

We conclude that Mec1p kinase maintains anaphase inhibitor Pds1p levels under S-phase checkpoint conditions. Distinct “Mec1p/Rad53p” and “Mec1p/Pds1p” S-phase checkpoint pathway branches operate in yeast. This duality reflects the need for coordinate regulation of sister cohesion and spindle elongation in late S, via Pds1 stabilization, while only inhibition of spindle elongation is necessary in early S-phase.

Background

Onset of anaphase in yeast is preceded by ubiquitin-dependent proteolysis of the yeast anaphase inhibitor Pds1p [1, 2]. Pds1p inhibits Esp1p, a separin that promotes loss of sister chromatid cohesion and elongation of the mitotic spindle [3]. Pds1p proteolysis is antagonized by checkpoint controls that regulate mitotic progression in response to either DNA damage or aberrantly formed spindles [4-6]. More recently, Pds1p has also been implicated in S-phase checkpoint control, a surveillance system that prevents mitosis when DNA replication is perturbed [7]. In yeast, distinct early and late S-phase checkpoints have been genetically defined, which operate to ultimately couple completion of DNA replication with mitotic progression [7]. Several proteins associated with these checkpoints, including Rad53p and Mec1p on the one hand (the homologues of human Chk2 kinase and ATM/ATR kinase) [8, 9], and Pds1p on the other, have been classified as early and late signaling elements, respectively, based on genetic analysis [7].

In the unperturbed yeast cell cycle, replication is completed before assembly of the mitotic spindle. Thus, cells usually coordinate DNA replication with mitosis solely on the basis of timing. However, when replication is perturbed, spindles still form and become competent to elongate while replication is ongoing. In this case, S-phase checkpoint controls delay anaphase (loss of sister chromatid cohesion and spindle elongation) until replication is complete. *mec1* and *rad53* mutants are unable to prevent spindle elongation when DNA replication is blocked in early S-phase with the ribonucleotide reductase inhibitor, hydroxyurea HU [8, 9]. Under the same conditions, *pds1* mutants are competent to prevent spindle elongation [4, 5]. But, in the presence of sub-replication-arresting amounts of HU, *pds1* mutants lose sister chromatid cohesion and initiate spindle elongation part-way through S-

phase [7]. These data suggest that separate S-phase checkpoint systems operate in yeast, one acting early in S (depending upon Mec1p and Rad53p), and a second pathway needed only in late S-phase (dependent on Pds1p). It remains questionable whether these pathways function independently, or if they might be biochemically linked. A second question is why two distinct control systems should be needed to couple DNA replication with mitosis. To address these issues, we analysed the phenotypes of S-phase checkpoint mutants and have monitored changes in Pds1p levels in response to HU treatment.

Results

Pds1 protein levels are maintained during a prolonged S-phase

We determined whether Pds1p-dependent delay in loss of cohesion and spindle elongation, in the presence of 100 mM HU (a dose that allows replication to proceed at a reduced rate), relied on persistent Pds1p levels. The kinetics of anaphase onset in wild type and HU-sensitive *pds1-128* cells expressing epitope tagged versions of Pds1p or mutant Pds1-128p, respectively, were compared (Fig. 1 A-B). Both strains were synchronised in G1 with mating pheromone, then released into rich medium containing 100 mM HU at 26°C (the restrictive temperature for *pds1-128* cells is 37°C). Cell cycle progression was monitored by scoring budding index, mitotic spindle formation and elongation (using a GFP-TUB1 construct) and by FACScan analysis. Wild type cells began anaphase 5 h following release from G1, when the genome had been fully replicated (Fig. 1 A and data not shown). Under these conditions of slow DNA replication, Pds1[HA]p persisted for about 3 hours longer than in cells released from G1 into rich medium without HU (Fig. 1 B and data not shown), and its degradation occurred coincidentally with the onset of anaphase. Thus, Pds1p levels are maintained while DNA replication is ongoing in yeast. *pds1-128* mutant cells began anaphase 3 h after release from G1, when approximately 2/3 of bulk DNA replication was complete (Fig. 1 A and data not shown). Epitope tagged Pds1-128[HA]p was undetectable after 2.5 h suggesting that the mutant protein could not be stabilized in response to S-phase checkpoint activation. This was consistent with the checkpoint defect observed in *pds1-128* cells [7].

The Pds1p-dependent Late S-phase checkpoint control becomes essential once the genome has been partially replicated

Our experiments have not addressed what factor determines the timing of establishment of the Pds1p-dependent S-phase checkpoint. *pds1-128* mutants consistently initiated anaphase 3 1/2 hours after release from G1 in the presence of 100 mM HU. However, the timing of anaphase onset could be due to the length of time spent in S-phase, or more interestingly, it could be dependent on the actual extent of DNA replication. Moreover, it is possible that the primary defect of *pds1* cells is an inability to respond to DNA damage in late S-phase, rather than to a failure to perceive ongoing DNA replication itself. A prevailing view of S-phase checkpoint signaling is that replication fork components generate the checkpoint response [10]. Replication fork stalling, after prolonged exposure to HU, might interfere with the generation of the checkpoint signal. In this case, wild type cells would be prevented from initiating anaphase by an operational DNA damage checkpoint, since HU causes DNA damage as well as inhibiting replication. To distinguish between these possibilities, *pds1-128* cells released from G1 arrest, were grown with various HU concentrations, and the timing of loss of cohesion monitored using a GFP-tagged sub-centromere-linked probe [7]. In these experiments, cells progressed from G1 (budded) at a similar rate, regardless of the HU concentration. In contrast, loss of cohesion occurred at different times following entry into S-phase, dependent on the concentration of HU (Figure 1 C). The higher the HU dose, the longer the delay before cohesion was lost. Thus, the timing of loss of cohesion correlated with the extent of DNA replication accomplished (Figure 1D). These data provided good evidence that *pds1-128* cells are unable to perceive that DNA replication has not been completed during the latter part of S-phase. Since the requirement for Pds1p correlated with the extent of ongoing replication, we speculate that

the Pds1p-dependent checkpoint becomes critical once sister chromatid cohesion has been established.

Mec1p kinase maintains Pds1p levels under S-phase checkpoint conditions

Taken together our results indicated that maintenance of functional Pds1p is critical for coupling mitotic progression with the completion of DNA replication under conditions where replication is impaired. An outstanding question is whether the early S-phase, Mec1p/Rad53p-dependent, pathway is biochemically linked to the Pds1p-dependent late S-phase pathway. To address this, we compared the kinetics of anaphase initiation and Pds1p destruction in *mec1* and *rad53* mutant cells, released from an α factor-induced G1 block, in the presence of 100 mM HU (Fig. 2). Both mutants budded and formed short G2 spindles with similar timing. In *mec1* mutant cells, Pds1[HA]p was degraded during S-phase, indicating that Mec1p is required to prevent Pds1[HA]p proteolysis when replication is perturbed (Fig. 2 A). This result placed Mec1p upstream of Pds1p in the late S-phase checkpoint (see model; Figure 5). In contrast, Pds1[HA]p levels were maintained in *rad53* cells (Fig. 2 A). Therefore, Rad53p is not required to inhibit Pds1[HA]p proteolysis in S-phase. These data revealed that Rad53p does not perform all of the Mec1p-dependent S-phase checkpoint functions, and demonstrated that separate S-phase checkpoint pathways can be distinguished biochemically. In agreement with this proposal, the phenotype of *mec1* and *rad53* mutants differed with regard to cell cycle progression once spindle elongation had taken place in the presence of HU. Indeed, *mec1* mutants exited mitosis and eventually re-budded, whereas *rad53* cells became arrested with elongated mitotic spindles (Fig. 2 and Fig. 3). (Under the same conditions, *pds1-128* cells also

exited mitosis and rebudded; see Fig. 3.) Still, the kinetic analyses also showed that both *mec1* and *rad53* mutants initiated spindle elongation with similar timing in early S-phase (1.5 - 2 h following release from G1), when very little DNA had been replicated (Fig. 2 B-C and data not shown). Thus, *rad53* and *mec1* mutants similarly failed to prevent spindle elongation in response to S-phase checkpoint activation. This is consistent with biochemical analyses suggesting that Rad53p and Mec1p function in the same pathway [11]. Thus, we propose that Rad53p and Pds1p define distinct branches of the S-phase checkpoint, both acting downstream of Mec1p (see model; Figure 5).

Pds1p is not required for spindle elongation in early S-phase

The above data suggested that Mec1p controls the S-phase checkpoint by dual mechanisms, targeting Rad53p in early S-phase, and Pds1p in late S-phase. It follows that, in early S-phase, the Mec1p/Rad53p-dependent checkpoint pathway inhibits spindle elongation without targeting Pds1p. This is consistent with the fact that, unlike *mec1* and *rad53* mutants, *pds1* mutant cells do not attempt anaphase when replication is blocked early in S-phase [4, 5, 7]. However, an alternative explanation could be that *pds1* mutants are not capable of initiating spindle elongation early in S-phase, reflecting an underlying requirement for Pds1p for normal spindle function. Pds1p and Esp1p, as well as the fission yeast homologues Cut2 and Cut1, localize to mitotic spindles, and Pds1p is required for the association of Esp1p with the spindle [12, 13 and SJ, MS, DJC & SIR unpublished data]. In fact, *pds1* mutants are unable to initiate spindle elongation during mitosis, if shifted to the non-permissive temperature in G1 of the cell cycle [4]. We therefore compared the kinetics of cell cycle progression and spindle elongation in *rad53* and *pds1-128 rad53* mutant cells in the presence of 100 mM HU. After release from G1

arrest, both mutants budded and formed short G2 spindles with similar timing. Onset of anaphase also occurred with comparable kinetics in both mutants (Fig. 3 A). (*rad53 pds1Δ* mutant cells behaved comparably; data not shown.) Clearly, cells that lack Pds1p are competent to initiate spindle elongation in early S-phase. Thus, deregulated spindle elongation in *rad53* cells is indeed independent of a Pds1p requirement for spindle function. Given this result, we can safely conclude that Pds1p is only required for the S-phase checkpoint part way through S-phase. Moreover, these data demonstrate unequivocally that the S-phase checkpoint is composed of dual mechanisms that are employed sequentially (see Model in Fig. 5).

Esp1p is needed for spindle elongation in mitosis but not in Early S-phase

We have shown that Pds1p is not required for spindle elongation in early S-phase. Perhaps more surprisingly, our data also show that the presence of Pds1p is not sufficient to inhibit spindle elongation in early S-phase (see Fig. 2). Both *mec1* and *rad53* cells began anaphase well before Pds1p was degraded in the presence of HU (Fig. 2 A-B). Further, *rad53* mutants initiated spindle elongation in the presence of HU, even when a non-degradable Pds1p mutant (lacking its destruction box motif; Pds1p^{Δdb}) was overexpressed from the *GAL1* promoter (data not shown); note that this allele can, however, block anaphase in *rad53* mutants in an unperturbed cell cycle (data not shown) and in the context of the G2 DNA damage checkpoint [14]. Thus, although Pds1p must be stabilized to prevent premature initiation of anaphase during late S-phase, the presence of Pds1p in early S is not sufficient to inhibit spindle elongation in HU-treated *mec1* or *rad53* cells. This could be explained by any of several mechanisms. First, Pds1p might be unable to bind and/or inhibit Esp1p in early S-phase upon checkpoint activation in *rad53* cells. To test this, we immunoprecipitated Pds1p-Esp1p

complexes from wild type and *rad53* cells treated with HU (Fig. 3 B). We analysed samples of budded wild type and *rad53* cells that had short G2 spindles, and samples of budded *rad53* cells with anaphase spindles. In each sample taken from the kinetic experiments in Fig. 2, similar amounts of Pds1p-Esp1p complexes were isolated. Therefore, the ability of *rad53* cells to initiate spindle elongation in the presence of Pds1p cannot be explained by a lack of Pds1p binding to Esp1p.

This result suggested that Pds1p is incapable of inhibiting Esp1p in early S-phase, and that Rad53p might inhibit Esp1p directly. An alternative possibility is that Esp1p activity is not required for spindle elongation in early S-phase. This would seem to be an unlikely scenario, however, since Esp1p activity is absolutely required for spindle elongation in mitosis [15]. Still, we tested this hypothesis by generating a novel *esp1* mutant (*esp1-B3*), temperature sensitive at a relatively low temperature (30°C), making it suitable for analysis of the kinetics of spindle elongation in synchronous cell cycles. After release from G1 into rich medium at 31°C, *esp1-B3* and *esp1-B3 rad53* could not elongate spindles when these cells reached mitosis (Fig. 3 C). Therefore, the *rad53* mutation could not relieve the inability of *esp1-B3* cells to elongate spindles in mitosis. In the presence of HU, *esp1-B3* cells arrested with short G2 spindles while DNA replication was ongoing, confirming that *esp1-B3* cells are S-phase checkpoint proficient. However, *esp1-B3 rad53* cells and *rad53* cells initiated spindle elongation with similar timing when grown in the presence of HU (Fig. 3 C). Thus, while Esp1p is needed for spindle elongation at mitosis, spindle elongation in early S-phase, upon checkpoint activation, occurs by a mechanism that involves neither Pds1p nor Esp1p. This result mechanistically explains the need for distinct and sequential branches of the S-phase

checkpoint system. While the late S-phase checkpoint targets Pds1p/Esp1p, the early S-phase checkpoint must have a novel target.

Discussion

We have shown that distinct “Mec1p/Rad53p” and “Mec1p/Pds1p” S-phase checkpoint pathway branches operate in yeast; one necessary in early S and manifest in the presence of a replication block [8, 9], and another novel pathway operating part-way through S (Figure 5). We show that the late S-phase checkpoint couples DNA replication with mitosis by Mec1p-dependent maintenance of Pds1p anaphase inhibitor levels. Interestingly, the *mec1* and *rad53* phenotypes in 100 mM HU were not identical, indicating that Rad53p mediates only a subset of Mec1p-dependent functions. Under conditions of slow DNA replication, *rad53* cells were proficient at maintaining Pds1p levels, did not exit mitosis, but accumulated with long anaphase spindles (Fig. 2 B-C and Fig. 3). This arrest phenotype could be accounted for by the persistence of Pds1p, which is sufficient to block the release of Cdc14p from nucleoli, an event that is needed for mitotic exit [16-21]. In contrast, following spindle elongation, *mec1* cells disassembled mitotic spindles and exited mitosis with similar timing to wild type or *pds1-128* cells (Fig. 2-C and Fig. 3). Remarkably, *mec1* mutants even re-budded following mitotic exit, despite suffering a catastrophic mitosis with an unreplicated genome (Fig. 2 and Fig. 3). Based on these phenotypes and the differential abilities of *mec1* and *rad53* mutants to maintain Pds1p levels during S-phase, we conclude that Mec1p controls two distinct S-phase checkpoint pathways that are defined by Rad53p and Pds1p.

An explanation for the duality of S-phase checkpoint control is the linkage of spindle elongation with regulation of sister chromatid cohesion (Fig. 1). Eukaryotes establish cohesion during replication, and must maintain it until the onset of anaphase [3, 22-24]. Once cohesion is established, checkpoint controls must coordinate release of cohesion with spindle elongation. Early in S-phase, prior to the replication of a significant portion of the genome and concomitant

establishment of cohesion, spindle elongation is presumably regulated independently of the machinery monitoring and regulating the status of cohesion (see Fig. 5). However, once cohesion is established, part-way through S-phase, a coordinate regulatory system becomes critical. The novel finding that the separin Esp1p is needed for spindle elongation once cohesion is established, but not in early S-phase, supports this hypothesis.

CONCLUSIONS

We conclude that Pds1 protein levels are maintained in a Mec1p kinase-dependent manner until DNA replication is complete. This checkpoint pathway ensures that late S-phase cells do not attempt mitotic progression before the genome has been replicated. Although Rad53p activity is also controlled by Mec1p, Rad53p is dispensable for Pds1p persistence in S-phase, demonstrating that the S-phase checkpoint comprises two distinct sequential branches downstream of Mec1p. The persistence of Pds1p inhibits the onset of anaphase during late S-phase, but not in early S-phase. In early S, a distinct Mec1p/Rad53p pathway prevents spindle elongation independently of the mechanism that maintains chromatid cohesion. We propose that the duality of S-phase checkpoint control is based on the need for coordinate regulation of spindle elongation and sister chromatid separation once cohesion is established.

Materials and Methods

Yeast strain genotypes and construction

All strains are isogenic derivatives of BF264-15 15DU: **a** *ura3 Δ ns ade1 his2 leu2-3,112 trp1-1^a* [25] and were grown at 26°C unless otherwise indicated. Gene disruptions were performed by PCR-targeting technique [26]. The *esp1-B3* allele was generated by error-prone PCR followed by *in vivo* gap repair [27]. Genotypes: DCY1723, **MATa** *bar1 Δ* *ura3::HIS3:GFP:TUB1(URA3) PDS1::PDS1[HA]X3(LEU2)*; DCY1817, **MATa** *bar1 Δ* *ura3::HIS3:GFP:TUB1(URA3) pds1-128::pds1-128[HA]X3(LEU2)*. DCY1791, **MATa** *bar1 Δ* *ura3::HIS3:GFP:TUB1(URA3) rad53 PDS1::PDS1[HA]X3(LEU2)*. Strains DCY1832, **MATa** *bar1 Δ mec1-1 ura3::HIS3:GFP:TUB1(URA3) PDS1::PDS1[HA]X3(LEU2)* and DCY1698, **MATa** *bar1 Δ his3::HIS3:GFP-TUB1(HIS3)* were derived from A364a wild type and A364a *mec1-1*. DCY1672, **MATa** *bar1 Δ pds1-128 ura3::HIS3:GFP:TUB1 (URA3)*; DCY1775, **MATa** *bar1 Δ ura3::HIS3:GFP:TUB1(URA3) rad53 pds1-128*. DCY1871, **MATa** *bar1 Δ* *ura3::HIS3:GFP:TUB1(URA3) PDS1::PDS1[HA]X3(LEU2) pep4::URA3 ESP1::[MYC]X18ESP1(TRP1)*; DCY1872, **MATa** *bar1 Δ ura3::HIS3:GFP:TUB1(URA3) PDS1::PDS1[HA]X3(LEU2) pep4::URA3 ESP1::[MYC]X18ESP1(TRP1) rad53*. DCY1898, **MATa** *bar1::LEU2 ura3::HIS3:GFP:TUB1(URA3) esp1::KAN^R (esp1-B3:TRP1:CEN)*; DCY1905, **MATa** *bar1::LEU2 ura3::HIS3:GFP:TUB1(URA3) esp1::KAN^R (esp1-B3:TRP1:CEN) rad53*.

Cellbiology

General procedures relating to the handling and cell cycle synchronisation of yeast cultures were as previously described [7]. Sister centromere separation was monitored using the tetO/tetR-GFP

system [7]. Fluorescence and differential interference contrast (DIC) microscopy of live or fixed (3.75 % formaldehyde, 30 min) cells was performed using an Eclipse E800 microscope (Nikon Inc., Melville, NY) with a 100X objective. Cell images were captured with a Quantix CCD (Photometrics, Tuscon, AZ) camera using IPLab Spectrum software (Signal Analytics Co., Vienna, VA). Use of the GFP-Tub1 fusion construct was described previously [28, 29]. Cell cycle progression, estimated by FACScan analysis, was performed according to a previous description [30], except that the DNA dye sytox was used rather than propidium iodide [31]. Detection of epitope-tagged Pds1p and Cdc28p after SDS PAGE and Western blotting were as described [32].

Immunoprecipitation and Immunostaining

Proteins were isolated in NP-40 buffer as described [33]. 750 µg protein extract were used for immunoprecipitation with myc9E10 antibody pre-bound to protein A-sepharose or with 12CA5 antibody cross-linked to protein A-sepharose. Immunocomplexes were washed with extraction buffer and bound proteins were eluted by boiling in SDS sample buffer. Samples were separated by SDS-PAGE (7.5% protein gels), Western blotted, then analyzed by immunostaining with anti-HA antibody (12CA5, BabCO), anti-myc antibody (9E10) and anti-PSTAIRES antibody.

Acknowledgements

We thank D. Koshland and O. Cohen-Fix for the Pds1p tagging vector, T. Weinert for strains, and P. Russell and N. Rhind for critical reading of the manuscript. DJC was funded by EMBO and US Army Breast Cancer Research fellowships. MS was funded by EMBO and HFSP fellowships, SJ by the Danish Medical Research Council. Correspondence and requests for materials should be addressed to SI Reed, sreed@scripps.edu

References

1. Cohen-Fix O, Peters JM, Kirschner MW, Koshland D: **Anaphase initiation in *Saccharomyces cerevisiae* is controlled by the APC-dependent degradation of the anaphase inhibitor Pds1p.** *Genes Dev* 1996, **10**: 3081-93.
2. Visintin R, Prinz S, Amon A: **CDC20 and CDH1: a family of substrate-specific activators of APC- dependent proteolysis.** *Science* 1997, **278**: 460-3.
3. Uhlmann F, Lottspeich F, Nasmyth K: **Sister-chromatid separation at anaphase onset is promoted by cleavage of the cohesin subunit Scc1.** *Nature* 1999, **400**: 37-42.
4. Yamamoto A, Guacci V, Koshland D: **Pds1p, an inhibitor of anaphase in budding yeast, plays a critical role in the APC and checkpoint pathway(s).** *J Cell Biol* 1996, **133**: 99-110.
5. Yamamoto A, Guacci V, Koshland D: **Pds1p is required for faithful execution of anaphase in the yeast, *Saccharomyces cerevisiae*.** *J Cell Biol* 1996, **133**: 85-97.
6. Hwang LH, *et al*: **Budding yeast Cdc20: a target of the spindle checkpoint.** *Science* 1998, **279**: 1041-4.
7. Clarke DJ, Segal M, Mondesert G, Reed SI: **The Pds1 anaphase inhibitor and Mec1 kinase define distinct checkpoints coupling S phase with mitosis in budding yeast.** *Curr Biol* 1999, **9**: 365-8.
8. Allen JB, Zhou Z, Siede W, Friedberg EC, Elledge SJ: **The SAD1/RAD53 protein kinase controls multiple checkpoints and DNA damage-induced transcription in yeast.** *Genes Dev* 1994, **8**: 2401-15.

9. Weinert TA, Kiser GL, Hartwell LH: **Mitotic checkpoint genes in budding yeast and the dependence of mitosis on DNA replication and repair.** *Genes Dev* 1994, **8**: 652-65.
10. Rhind N, Russell P: **Mitotic DNA damage and replication checkpoints in yeast.** *Curr Opin Cell Biol* 1998, **10**: 749-58.
11. Sanchez Y, Desany BA, Jones WJ, Liu Q, Wang B, Elledge SJ: **Regulation of RAD53 by the ATM-like kinases MEC1 and TEL1 in yeast cell cycle checkpoint pathways.** *Science* 1996, **271**: 357-60.
12. Funabiki H, Kumada K, Yanagida M: **Fission yeast Cut1 and Cut2 are essential for sister chromatid separation, concentrate along the metaphase spindle and form large complexes.** *Embo J* 1996, **15**: 6617-28.
13. Ciosk R, Zachariae W, Michaelis C, Shevchenko A, Mann M, Nasmyth K: **An ESP1/PDS1 complex regulates loss of sister chromatid cohesion at the metaphase to anaphase transition in yeast.** *Cell* 1998, **93**: 1067-76.
14. Sanchez Y, *et al*: **Control of the DNA damage checkpoint by chk1 and rad53 protein kinases through distinct mechanisms.** *Science* 1999, **286**: 1166-71.
15. McGrew JT, Goetsch L, Byers B, Baum P: **Requirement for ESP1 in the nuclear division of *Saccharomyces cerevisiae*.** *Mol Biol Cell* 1992, **3**: 1443-54.
16. Jaspersen SL, Charles JF, Tinker KR, Morgan DO: **A late mitotic regulatory network controlling cyclin destruction in *saccharomyces cerevisiae*.** *Mol Biol Cell* 1998, **9**: 2803-17.
17. Tinker KR, Morgan DO: **Pds1 and Esp1 control both anaphase and mitotic exit in normal cells and after DNA damage.** *Genes Dev* 1999, **13**: 1936-49.

18. Visintin R, Craig K, Hwang ES, Prinz S, Tyers M, Amon A: **The phosphatase Cdc14 triggers mitotic exit by reversal of Cdk-dependent phosphorylation.** *Mol Cell* 1998, 2: 709-18.
19. Cohen-Fix O, Koshland D: **Pds1p of budding yeast has dual roles: inhibition of anaphase initiation and regulation of mitotic exit.** *Genes Dev* 1999, 13: 1950-9.
20. Visintin R, Hwang ES, Amon A: **Cfi1 prevents premature exit from mitosis by anchoring Cdc14 phosphatase in the nucleolus.** *Nature* 1999, 398: 818-23.
21. Shirayama M, Toth A, Galova M, Nasmyth K: **APC(Cdc20) promotes exit from mitosis by destroying the anaphase inhibitor Pds1 and cyclin Clb5.** *Nature* 1999, 402: 203-7.
22. Blat Y, Kleckner N: **Cohesins bind to preferential sites along yeast chromosome III, with differential regulation along arms versus the centric region.** *Cell* 1999, 98: 249-59.
23. Uhlmann F, Nasmyth K: **Cohesion between sister chromatids must be established during DNA replication.** *Curr Biol* 1998, 8: 1095-101.
24. Goshima G, Yanagida M: **Establishing biorientation occurs with precocious separation of the sister kinetochores, but not the arms, in the early spindle of budding yeast.** *Cell* 2000, 100: 619-33.
25. Richardson HE, Wittenberg C, Cross FR, Reed SI: **An essential G1 function for cyclin-like proteins in yeast.** *Cell* 1989, 59: 1127-1133.
26. Wach A, Brachat A, Pohlmann R, Philippsen P: **New heterologous modules for classical or PCR-based gene disruptions in *Saccharomyces cerevisiae*.** *Yeast* 1994, 10: 1793-808.

27. Tang Y, Reed SI: **The Cdk-associated protein Cks1 functions both in G1 and G2 in *Saccharomyces cerevisiae*.** *Genes & Dev.* 1993, **7**: 822-832.
28. Straight AF, Marshall WF, Sedat JW, Murray AW: **Mitosis in living budding yeast: anaphase A but no metaphase plate.** *Science* 1997, **277**: 574-8.
29. Segal M, Clarke DJ, Reed SI: **Clb5-associated kinase activity is required early in the spindle pathway for correct preanaphase nuclear positioning in *Saccharomyces cerevisiae*.** *J Cell Biol* 1998, **143**: 135-45.
30. Mondesert G, Clarke DJ, Reed SI: **Identification of genes controlling growth polarity in the budding yeast *Saccharomyces cerevisiae*: a possible role of N-glycosylation and involvement of the exocyst complex.** *Genetics* 1997, **147**: 421-34.
31. Haase SB, Lew DJ: **Flow cytometric analysis of DNA content in budding yeast.** *Methods Enzymol* 1997, **283**: 322-32.
32. Kaiser P, *et al*: **Cyclin-dependent kinase and Cks/Suc1 interact with the proteasome in yeast to control proteolysis of M-phase targets.** *Genes Dev* 1999, **13**: 1190-202.
33. Kaiser P, Sia RA, Bardes EG, Lew DJ, Reed SI: **Cdc34 and the F-box protein Met30 are required for degradation of the Cdk-inhibitory kinase Swe1.** *Genes Dev* 1998, **12**: 2587-97.
34. Skibbens RV, Corson LB, Koshland D, Hieter P: **Ctf7p is essential for sister chromatid cohesion and links mitotic chromosome structure to the DNA replication machinery.** *Genes Dev* 1999, **13**: 307-19.
35. Michaelis C, Ciosk R, Nasmyth K: **Cohesins: chromosomal proteins that prevent premature separation of sister chromatids.** *Cell* 1997, **91**: 35-45.

Figure Legends

Fig. 1 Maintenance of cohesion upon S-phase checkpoint activation depends on delayed Pds1p degradation

(A-B) Kinetics of spindle elongation and Pds1p degradation under conditions of slow DNA replication. Wild type and *pds1-128* cells, expressing endogenous epitope-tagged Pds1p or Pds1-128 respectively, were arrested in G1 with α -factor, then released into rich medium containing 100 mM HU. Cell aliquots were taken at intervals for analysing cellular protein and to monitor cell cycle progression. (A) Kinetics of spindle elongation. Budding index (grey fill), spindle formation (white fill), spindle elongation (black fill). Spindles were visualized by expressing a GFP-TUB1. Cycle progression estimated by FACScan analysis was comparable for both strains (not shown). (B) Detection of Pds1[HA]p, *pds1-128*[HA]p and Cdc28p (as a loading control) after SDS PAGE and Western blotting. Approximate time of initiation of anaphase is indicated for each strain with an arrow (numbers above blots show time in hours after release from G1).

(C) Loss of sister chromatid cohesion is linked to the extent of ongoing DNA replication in *pds1* cells. *pds1-128* cells [7] were arrested in G1 with α -factor, then released into rich medium containing 50 mM (squares), 100 mM (diamonds), or 150 mM HU (circles). Cell aliquots were taken at intervals for scoring budding index (grey fill) and sister centromere separation (SCS; white fill) [7], and for FACScan analysis. (C) FACScan data show DNA content profiles at approximately 60% SCS for each HU concentration.

Fig. 2 Maintenance of Pds1p levels by S-phase checkpoint controls requires Mec1p but not Rad53p kinase.

(A-B) Kinetics of Pds1p degradation and spindle elongation, under conditions of slow DNA replication in *mec1* or *rad53* mutants. *mec1* or *rad53* cells expressing epitope tagged Pds1p were arrested in G1 with α -factor, then released into rich medium containing 100 mM HU.

Detection of Pds1[HA] and monitoring of cell cycle progression were performed as described in Fig. 1. (A) Kinetics of Pds1p degradation. For reference, onset of spindle elongation is marked by an arrow. (B) Kinetics of spindle elongation. Budding index (grey fill), spindle formation (white fill), spindle elongation (black fill). Progression estimated by FACScan analysis was comparable for both strains (not shown).

(C) Representative spindle morphologies of wild type, *mec1*, *rad53* and *pds1* mutants during cell cycle progression in the presence of 100 mM HU. For wild type: G2 spindle (cell on right) and anaphase spindle (cell on left). For *pds1*: G2 spindle (top left panel), anaphase spindles (top right and bottom left panels), and a cell in which the spindle has disassembled following elongation (bottom right). For *rad53*: anaphase spindles. For *mec1*: G2 spindles (top left panel), anaphase spindles (top right and bottom left panels), disassembled spindles (bottom right panels).

Fig. 3 *mec1* and *pds1* mutants initiate a second cell cycle in the presence of 100 mM HU
mec1 and *pds1* mutants, but not *rad53* mutants, rebud in the presence of HU. Wild type, *pds1*-128, *rad53* and *mec1* cells were arrested in G1 with α -factor, released by washing, then plated onto solid rich medium (upper panel), or rich medium containing 100 mM HU (lower panel) at

30°C. Bud emergence (grey fill , 1st bud) and appearance of new buds (black fill , re-budding) were scored at intervals.

Fig. 4 Spindle elongation in early S-phase is independent of Esp1p/Pds1p complex function

(A) Kinetics of spindle elongation in *rad53* vs. *rad53 pds1-128* cells. Cell cycle progression in the presence of 100 mM HU was monitored as described in Fig. 1. Budding index (gray fill), spindle formation (white fill) and spindle elongation (black fill) are shown. (B) Immunoprecipitation of Esp1p-Pds1p complexes from wild type or *rad53* cells grown in the presence of HU. Samples taken from kinetic experiments as shown in Figure 2 were used for immunoprecipitating either Esp1[myc18]p (upper panel) or Pds1[HA]p (not shown). Lanes marked (1) - samples taken 1 h 20 min after release from G1; lanes marked (2) - samples taken after 2h 20 min. For wild type, (1) and (2) contain cells arrested with short G2 spindles and partially replicated DNA. For *rad53*, the samples either contain cells arrested with short G2 spindles and partially replicated DNA (1), or anaphase cells with partially replicated DNA (2). The amounts of Esp1p and Pds1p in the protein extracts used are shown in the lower panel. A strain with an untagged Esp1p was used as a control (lane marked, C).

(C) Kinetic analysis of the initiation of spindle elongation in *esp1-B3 rad53* mutants. *rad53*, *esp1-B3* and *rad53 esp1-B3* mutants were arrested in G1 with α -factor, then released into rich medium (upper panel) or rich medium containing 100 mM HU (lower panel) at 31°C. Cell aliquots were taken at intervals for scoring spindle morphology (white fill, spindle formation; black fill, spindle elongation).

Fig. 5 The S-phase checkpoint consists of two distinct branches regulated by Mec1p kinase that act sequentially during DNA replication

Two pathways coordinate replication with mitosis. In early S, the Mec1p/Rad53p pathway prevents spindle elongation by an unknown mechanism (X) that does not involve inhibition of Esp1p. A mechanistically distinct checkpoint system (the Mec1p/Pds1p pathway) becomes essential part-way through S, once cohesion is established (dashed line). Mec1p is required to maintain Pds1p levels in late S-phase. The late S-phase, Mec1p/Pds1p-dependent pathway inhibits Esp1p, thereby preventing loss of sister cohesion, and blocking spindle elongation. Pds1p might prevent spindle elongation independently of loss of cohesion [34, 35], either via inhibition of Esp1p, or independently of Esp1p (dotted lines). We propose that sequential checkpoint systems are required because, once cohesion has been established, spindle elongation and loss of cohesion must be regulated coordinately, whereas before cohesion has been established, spindle elongation must be inhibited independently of loss of cohesion.

Figure 1

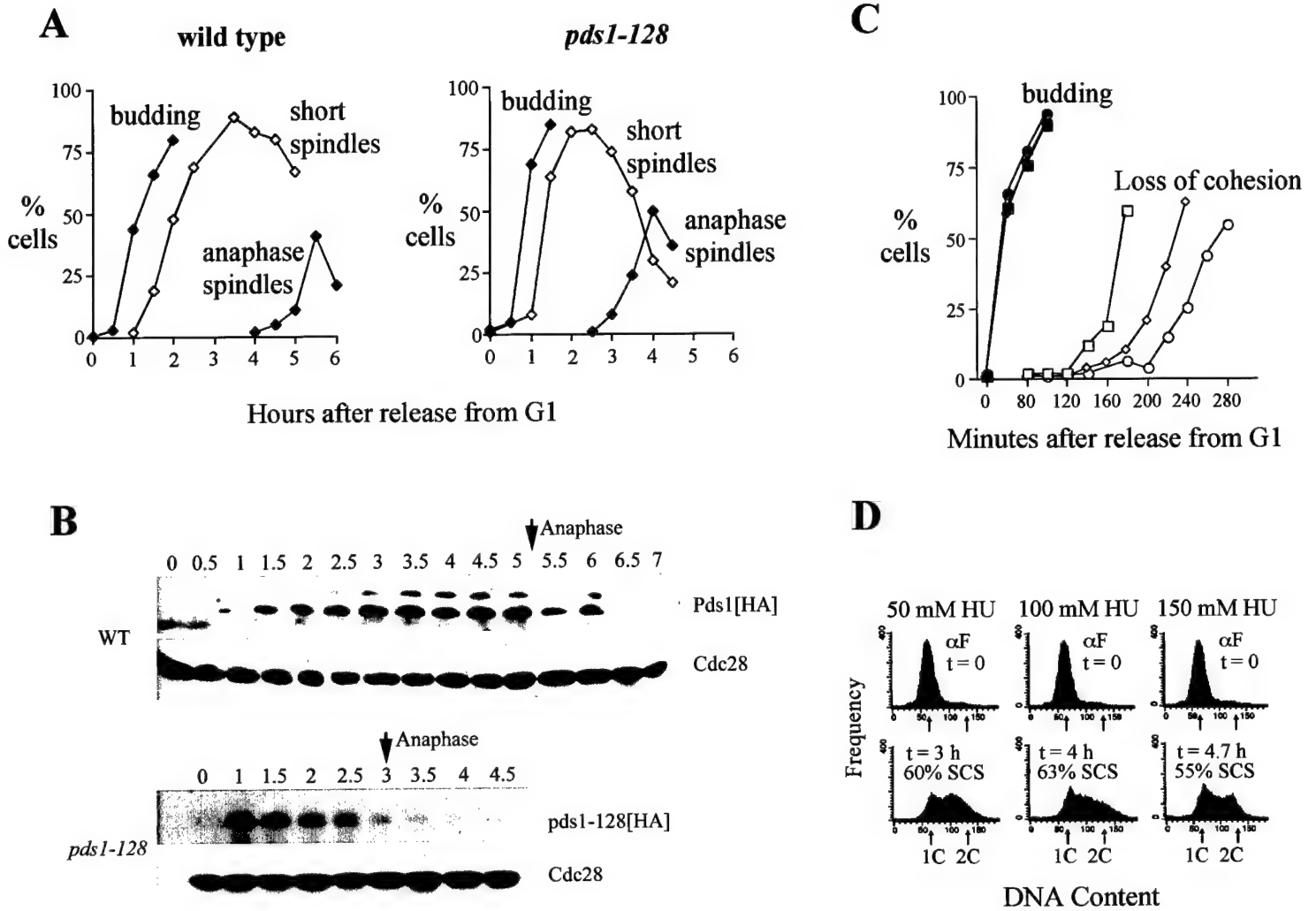


Figure 2

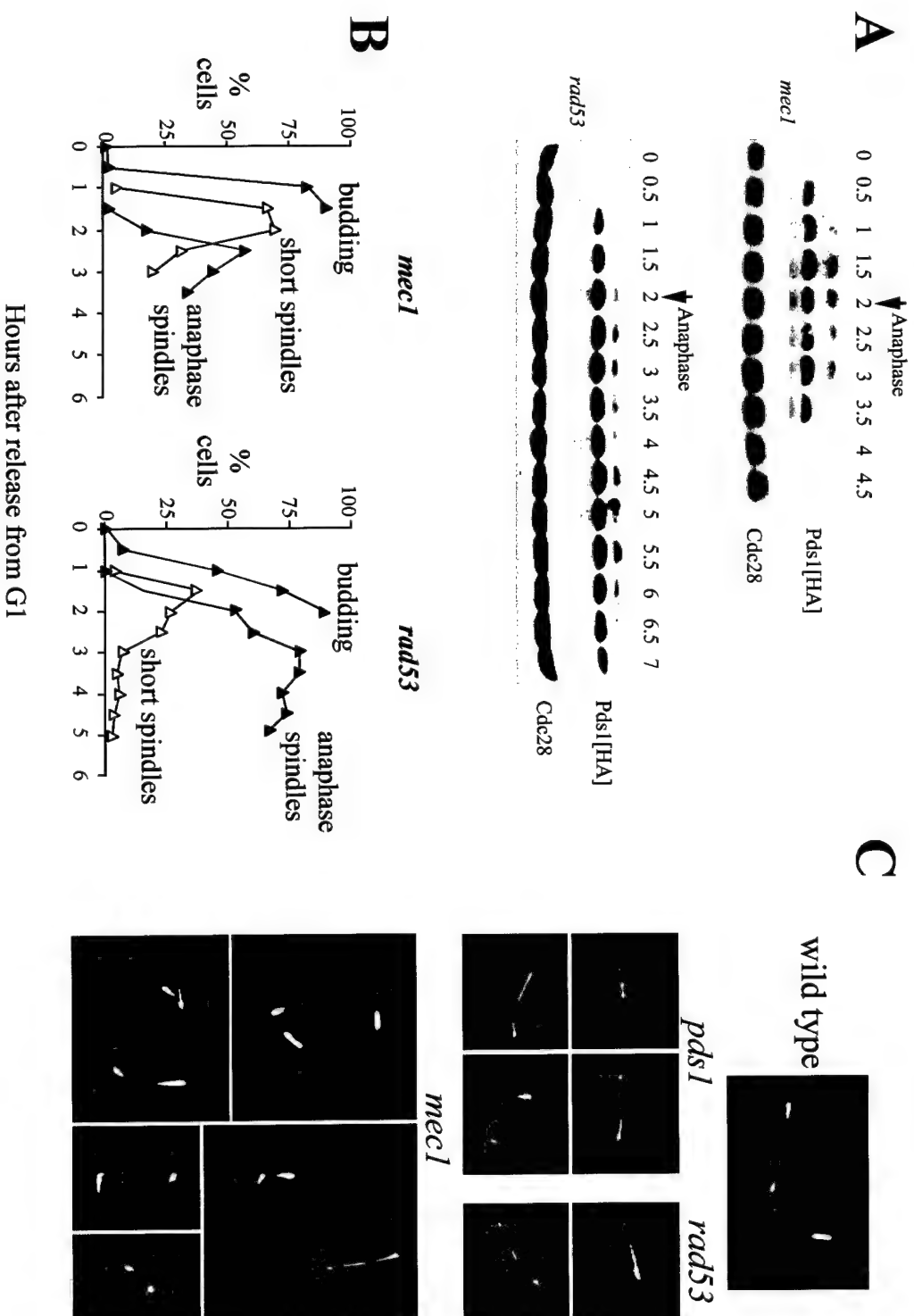


Figure 3

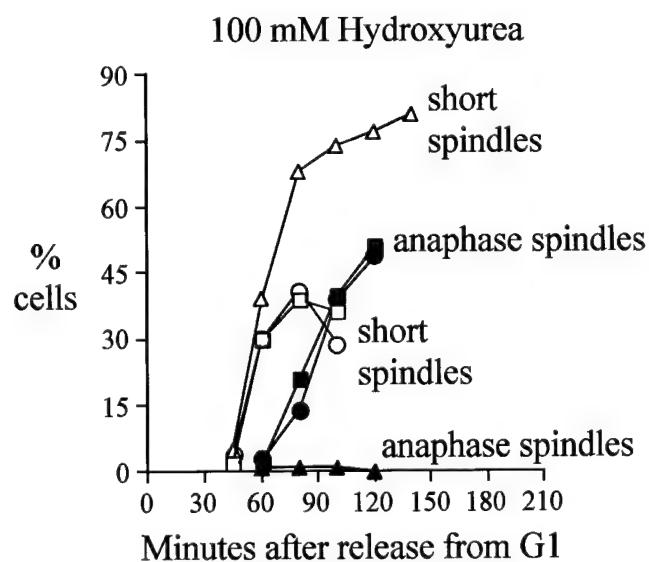
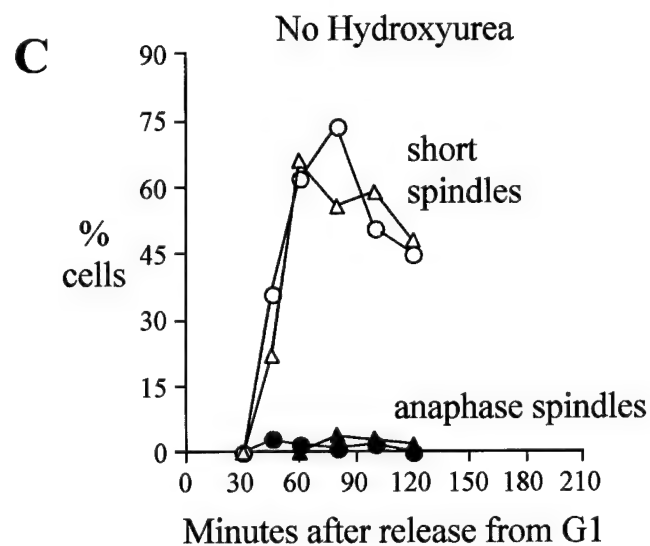
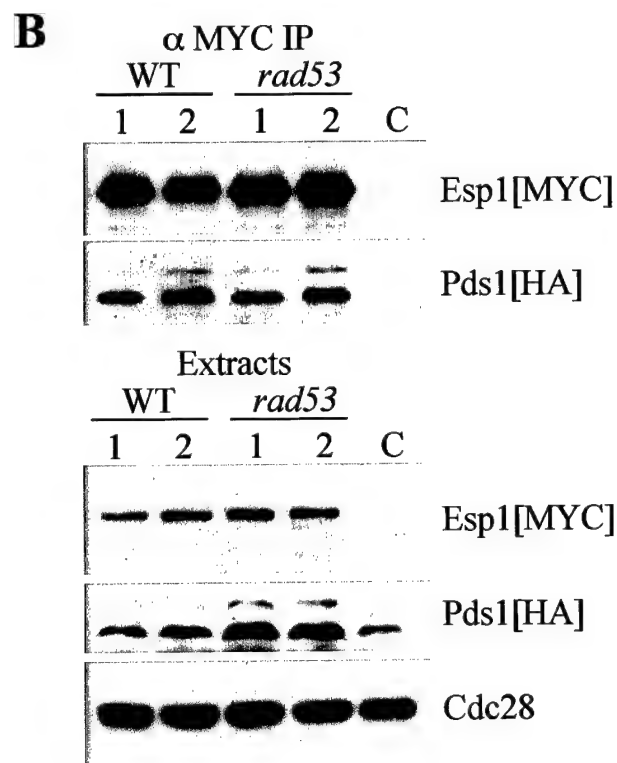
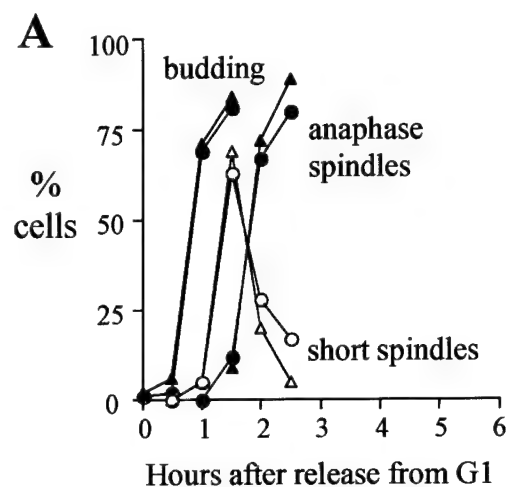


Figure 4

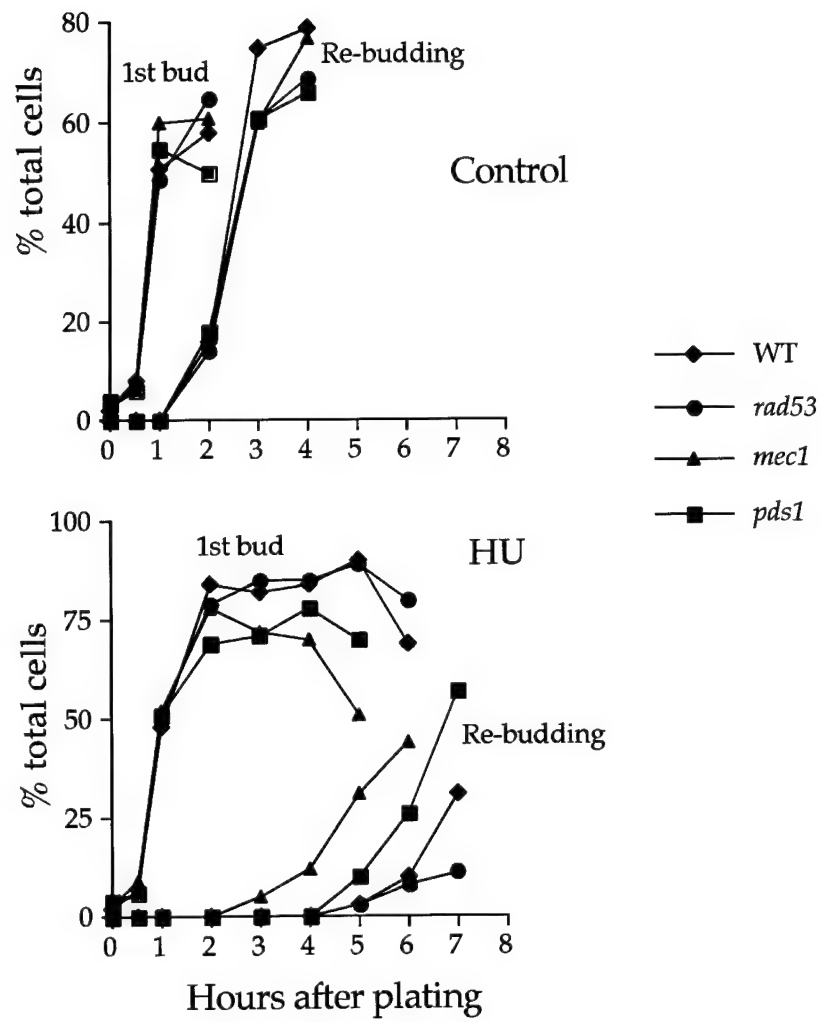
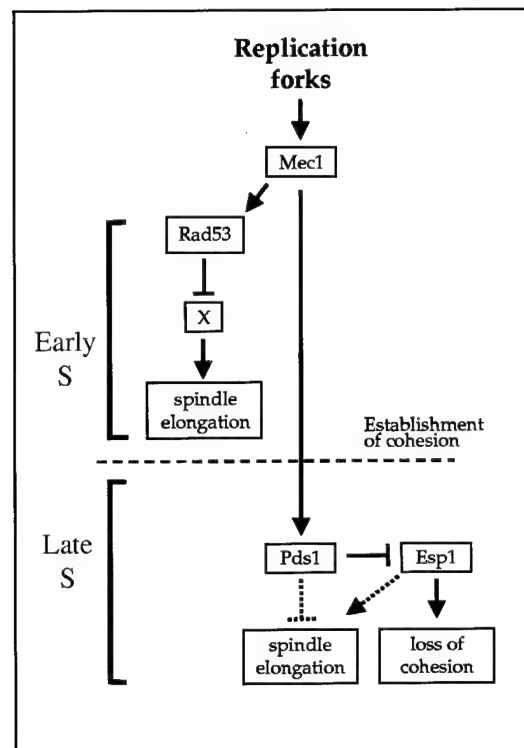


Figure 5



**Live cell imaging of the mitotic regulators Esp1 and Pds1 in budding yeast:
evidence that localization of Esp1 to the nucleus and mitotic spindle is regulated by Pds1**

Sanne Jensen, Marisa Segal, Duncan J. Clarke, and Steven I. Reed

Department of Molecular Biology, MB7,
The Scripps Research Institute,
10550 North Torrey Pines Road,
La Jolla, California 92037, USA

The present address of Sanne Jensen is Division of Yeast Genetics, National Institute for Medical Research, The Ridgeway, Mill Hill, NW7 1AA, London, UK

Corresponding author: Steven I. Reed
The Scripps Research Institute,
10550 North Torrey Pines Road,
La Jolla, CA 92037
Tel: (858) 784-9836. Fax: (858) 784-2781
E-mail: sreed@scripps.edu

Running title: Regulation of Esp1 localization in budding yeast

Key words: cell cycle; Esp1/Pds1 complex; metaphase-anaphase transition; spindle elongation; budding yeast

59,997 characters

Abstract. In *S. cerevisiae*, the metaphase-anaphase transition is initiated by the APC-dependent degradation of Pds1, whereby Esp1 is activated to promote sister chromatid separation. Although this is a fundamental step in the cell cycle, little is known about the regulation of Esp1. To address this issue, we performed a detailed analysis of the localization of Esp1 and Pds1 in live cells. Esp1 accumulates in the nucleus in G2 and is mobilized onto the spindle at anaphase onset, where it persists into mid-anaphase. Association with Pds1 occurs during S-phase and is required for efficient nuclear localization of Esp1, as *pds1* mutants exhibit no detectable nuclear or spindle labeling of Esp1. Spindle association is not fully restored in *pds1* mutants expressing an Esp1-nuclear localization sequence (NLS) fusion protein, suggesting that Pds1 is also required to promote Esp1 spindle binding. In agreement, Pds1 interacts with the spindle at the metaphase-anaphase transition and a fraction remains at the spindle pole bodies (SPBs) and the spindle midzone in anaphase cells. Finally, the conserved C-terminal region of Esp1 is important for spindle interaction. Mutants in a putative calcium-binding domain cannot complement an *esp1^{ts}* mutation and exhibit a reduced spindle binding ability. Also, *esp1^{ts}* mutants are suppressed by calcium suggesting that calcium may regulate Esp1 activity by promoting spindle interaction.

Introduction. Faithful chromosome segregation during cell division is of fundamental importance to the continued viability of a cell. A key event is the separation of sister chromatids at the transition from metaphase to anaphase, which in budding yeast is triggered by the ubiquitin-dependent proteolysis of the anaphase inhibitor Pds1 (Cohen-Fix *et al.*, 1996). This event is mediated by the 20S anaphase-promoting complex (APC), which is also responsible for the destruction of other target proteins including the spindle component Ase1 and mitotic cyclins (King *et al.*, 1995; Zachariae *et al.*, 1996; Juang *et al.*, 1997). Degradation of Pds1 is necessary for the separation of sister chromatids, as mutant variants of Pds1 that cannot be degraded due to the absence of a destruction box block this process (Cohen-Fix *et al.*, 1996).

Recently, Pds1 was revealed to form a complex with Esp1, a protein essential for viability and crucial for sister chromatid separation (Ciosk *et al.*, 1998). *esp1^{ts}* mutants exhibit a failure in proper spindle behavior at the time of elongation at anaphase, and although sister chromatid separation is blocked at the restrictive temperature, cell cycle progression is not arrested in these mutants, leading to a catastrophic mitosis (McGrew *et al.*, 1992; Ciosk *et al.*, 1998). Esp1 is thought to be inhibited by its association with Pds1, and only when the latter is degraded is Esp1 activated to trigger destruction and dissociation of cohesin proteins such as Scc1 from chromosomes. This event presumably allows sister chromatids to separate when pulled by microtubules connecting their kinetochores to opposite poles of the mitotic spindle. A failure to separate sisters in the presence of a non-cleavable version of Scc1 in cells with functional Esp1 protein is accompanied by a block in spindle elongation, consistent with the idea that loss of cohesion triggers anaphase (Uhlmann *et al.*, 1999). It is not yet clear how the separation of duplicated sister chromatids (anaphase A) is coordinated with spindle elongation (anaphase B).

Recent work by Uhlmann *et al.* (1999) implies that Esp1 may function as a novel protease cleaving cohesin proteins, but the exact mechanism of action and the regulation of this essential protein has not been elucidated. Functional homologues of the Esp1/Pds1 complex have been identified in *S. pombe* (Cut1/Cut2) (Uzawa *et al.*, 1990; Funabiki *et al.*, 1996) and Esp1 related proteins exist in *A. nidulans* (BimB) (May *et al.*, 1992), *Xenopus* and human (Zou *et al.*, 1999), suggesting that control of sister chromatid separation and anaphase onset is conserved in evolutionarily diverse organisms.

In this study, we report the localization of Esp1 and Pds1 during the cell cycle in live cells. We show that Pds1 interaction is required to obtain efficient transport of Esp1 to the nucleus and for subsequent binding of the protein to the mitotic spindle, which appears to be crucial for proper anaphase progression. Consistent with this, both Esp1 and a fraction of Pds1 are associated with the spindle and SPBs during anaphase, and the kinetics of Esp1 spindle localization suggest a direct role in spindle elongation (anaphase B). Furthermore, evidence is provided that an intact putative calcium-binding site in the conserved C-terminal region of Esp1 is important to form and maintain spindle association during anaphase. A possible role of calcium in Esp1 spindle function is discussed.

Materials and Methods

Yeast Strains and Methods

The relevant genotypes of the yeast strains used in this study are listed in Table I. All strains are isogenic derivatives of BF264-15 15DU: *a ura3Δns ade1 his2 leu2-3,112 trp1-1^a* (Richardson *et al.*, 1989). Yeast media and genetic procedures were according to Guthrie and Fink (1991). Gene disruptions were performed by PCR-targeting technique (Wach *et al.*, 1994).

Induction of integrated *ESP1GFP* from the *GAL1* promoter was performed as follows. A 2 ml aliquot (approx. 5×10^6 cells/ml) of a YEP Raffinose culture was filtered onto 47-mm 0.45 μ m GN-6 Metrical membrane (Gelman Sciences, Ann Arbor, MI). Filters were then placed on YEP Galactose plates for 15-30 min at room temperature. Cells were eluted from the filter into 1 M sorbitol and Esp1GFP fluorescence visualized by microscopy. As *ESP1* is an essential gene the induction is performed in strains that in addition express the endogenous protein. For induction of Esp1GFP in timecourse experiments, cells were diluted in YEP Raffinose at 30°C to an $OD_{600}=0.15$. α -factor (200 ng/ml) was added and cells incubated at 30°C for 1 hr, 2% galactose was added and incubation continued for 1 hr. Cells were released in YEP Dextrose at 30°C and samples collected for analysis of cell cycle progression by DAPI and protein fluorescence by microscopy.

Plasmids

ESP1-pRSG is an integrative plasmid carrying the *ESP1* open reading frame in addition to 200 bases of the 5' flanking sequence under the control of the *GAL1* promoter. ESP1GFP-pRSG is derived from this plasmid by inserting a PCR generated sequence encoding the GFP epitope (F64L, S65T,

Q80R mutant) into a *Sma*I site introduced just before the stop codon. All pRSG derived plasmids are linearized at the unique *Stu*I site in the *URA3* marker and integrants isolated by selecting for growth on dex-ura media. The parental pRSG plasmid is a derivative of pRS406 (Sikorski & Hieter, 1989), where the *Nae*I-*Pvu*I fragment spanning the multiple cloning site (MCS) linker has been substituted by the *Nae*I-*Pvu*I fragment from pYES2 (Invitrogen) containing a MCS and the *GAL1* promoter.

The ESP1myc18-pTRP1 plasmid was used to generate strains, where the endogenous Esp1 protein is tagged with 18 myc epitopes at the C-terminus. The integrative pTRP1 plasmid carries the sequence encoding 6 myc epitopes, which can be fused to a protein of interest at the *Not*I site (Mondesert *et al.*, 1997). A *Sal*I-*Not*I fragment spanning the last 480 bases of the *ESP1* gene was cloned into this plasmid. The oligos used were: 5' GTCGACATAATCGATGCAAAACCTTC 3' and 5' GCGGCCGCCTGATACGAACTTGATCGGTAACCCA 3', where the *Sal*I and *Not*I sites are underlined, respectively. An additional fragment encoding 12 myc epitopes was subsequently introduced into the *Not*I site generating the final ESP1myc18-pTRP1 construct. The plasmid was linearized with *Xba*I and integrants isolated by selecting for growth on dex-trp.

The vector pOC78 (Cohen-Fix *et al.*, 1996) was employed for tagging endogenous Pds1 internally with 3 HA epitopes. To tag the Pds1-128 protein in a similar fashion, the *Xba*I-*Avr*II fragment of *pds1-128* Yep24 constituting the 3' end of the gene with the mutation was cloned into the *Xba*I/*Avr*II sites of a pBSII derived plasmid containing the *Sac*I-*Apa*I Pds1(HA)₃ fragment from pOC78. The *Avr*II-*Apa*I *pds1-128*(HA)₃ fragment was used for transformation, *Leu*⁺ colonies isolated and the presence of HA epitopes verified by PCR.

The integrative pGAL1-Pds1Δdb plasmid described previously (Kaiser *et al.*, 1999) was used to construct the strain expressing the non-degradable version of Pds1.

A panel of *esp1^{ts}* alleles was generated by error-prone PCR followed by *in vivo* gap repair as described previously (Tang and Reed, 1993). PCR mutagenesis was performed on separate *ESP1* fragments to isolate temperature sensitive alleles mapping to the N-terminal-, central- and C-terminal region of Esp1. All *esp1^{ts}* alleles exhibited similar phenotypes. To generate a stable integrant of the *esp1*-N5 allele, the XhoI-SpeI fragment containing the promoter region and the first 1800 bp of the *ESP1* coding region including the mutation was cloned into pBSII. A *TRP1* marker was introduced into the HindIII site located approx. 300 bp upstream of the starting codon, and the *ESP1* XhoI-SpeI fragment used for transformation. Trp⁺ colonies were screened for temperature sensitivity and *esp1^{ts}* phenotype by DAPI.

The integrative pKGFP plasmid, which carries the *KAN^R* marker for G418 resistance was used to generate a strain with the endogenous Esp1 protein fused to GFP. pKGFP was designed with the GFP encoding sequence inserted after NotI allowing in frame fusion to any protein of interest. In this case, the *ESP1* SalI-NotI fragment used to construct ESP1myc18-pTRP1 was inserted in pKGFP cut with SalI and NotI. The plasmid was linearized with XbaI and integrants isolated by selecting for G418 resistance.

pKGFP2, a modified version of pKGFP, was used to tag endogenous Pds1 protein at the C-terminus. This plasmid carries a GFP sequence with additional mutations: V163A and S175G, which produces a brighter GFP fluorescent signal (Straight *et al.*, 1998). To tag Pds1, a PCR derived SalI-NotI fragment covering the last 500 bases of the *PDS1* gene was introduced in the pKGFP2 vector at SalI/NotI. The oligoes used were: 5' CTAGGTCGACAAAGGTGGTCTGCAACAA 3' and 5' CTAGGCGGCCGCCAGTAACTAAGTCCTCTAGTT 3' (SalI and NotI sites underlined,

respectively). The Pds1-pKGFP2 plasmid was linearized with *Stu*I and integrants selected by growth on G418 plates.

Plasmids ESP1(1-1568)-pRSG, ESP1(D1568A)-pRSG and ESP1(D1568A/D1570A)-pRSG were used to produce strains expressing the C-terminal truncation mutant and mutants in the putative calcium binding site of Esp1 from the *GALI* promoter, respectively. To generate ESP1(1-1568)-pRSG, a *Sal*I-*Sma*I PCR fragment spanning the region from the internal *Sal*I site in *ESP1* to the sequence encoding residue 1568 followed by a stop codon was introduced into the ESP1-pRSG plasmid digested with *Sal*I and *Sma*I thereby replacing the 3' region of the *ESP1* gene. The oligos used were: 5' CCGAACGGAGATTTGTCC 3' and 5' CGACCCCGGGAGTTACATCC-CACAGATTA 3', where the *Sma*I site is underlined. Site-directed PCR according to Landt *et al.* (1990) was employed to make ESP1(D1568A)-pRSG. Primers 5' CCGAACGGAGATTTGTCC 3' and 5' GCTAAATTTATCG*ATATCTTTGGCAGTTACATCCC 3' were used to generate a mutated fragment resulting in a single amino acid substitution shown in bold and a silent mutation resulting in the generation of an *Eco*RV restriction site shown underlined. This PCR product was used in a second reaction together with primer 5' GACGAGATCTTTACCCCGGGT-GATACGAACTTGATCGG 3', where the *Sma*I site has been underlined. The cut fragment was introduced into the ESP1-pRSG vector digested with *Sal*I and *Sma*I to remove the corresponding wildtype fragment. The double mutant ESP1(D1568A/D1570A)-pRSG was created by a similar PCR scheme using the following primers: 5' CCGAACGGAGATTTGTCC 3', 5' GCTAAATTTATCG*ATAG*CTTTGGCAGTTACATCCC 3' (the modified *Eco*RV site is underlined and the mutation resulting in the second amino acid substitution shown in bold), and 5' GACGAGATCTTTACCCCGGGTGATACGAACTTGATCGG 3' (*Sma*I site is underlined). The cut fragment was introduced into the ESP1(D1568A)-pRSG vector cut with *Sal*I and

SmaI to restore the *ESPI* gene to its full length. Clones carrying the double mutation were selected by screening for loss of the EcoRV site and subsequently sequenced. GFP tagged versions of the three *ESPI* mutant constructs described above were generated by inserting a SmaI fragment encoding the GFP epitope into the respective ESP1-pRSG plasmids opened by SmaI.

The integrative plasmid ESP1GFPNLS-pRSG was used to make strains expressing Esp1GFP fused at the C-terminus to the SV40 NLS from the *GAL1* promoter. A PCR fragment produced with following primers: 5' CTAGCCCCGGGAAGAAAAAGCGAAAGGTCG-GCCGCATGAGTAAAG 3' and 5' GCTACCCGGGGACCTTTCGCTTCTTCTTGGGT-TTGTATAGTTCATCCATGC 3', where SmaI sites are underlined and the SV40 NLS sequence shown in bold, was inserted into the ESP1-pRSG plasmid digested with SmaI.

Plasmid ESP1-pRS415 was made by inserting the *ESPI* promoter sequence and open reading frame amplified by PCR into the ARS/CEN plasmid pRS415 digested with SalI and SacI (Sikorski and Hieter, 1989). To generate ESP1(1-1568)-pRS415, the SpeI fragment from ESP1(1-1568)-pRSG containing the 3' end of the *ESPI* gene was introduced into the ESP1-pRS415 plasmid cut with SpeI. The *ESPI* calcium binding site mutants were cloned into pRS415 by substituting the NdeI fragment derived from ESP1(D1568A)- and ESP1(D1568A/D1570A)-pRSG with the corresponding fragment in ESP1-pRS415. All plasmids were subjected to sequencing to verify their integrity.

Cell Biology Protocols

Fluorescence and differential interference contrast (DIC) microscopy of live or fixed cells was performed using an Eclipse E800 microscope (Nikon Inc., Melville, NY) with a 100X objective. Cell images were captured with a Quantix CCD (Photometrics, Tuscon, AZ) camera using IPlab Spectrum

software (Signal Analytics Co., Vienna, VA). Spindle measurements were performed on captured images using the NIH Image measuring tool calibrated with a stage micrometer. For microscopy of live cells expressing either wildtype/mutant Esp1GFP or Pds1GFP, cells were grown in YEP Raffinose or YEP Dextrose, respectively, containing extra supplement of adenine (0.2 mg/ml) and in most experiments induced on solid YEP Galactose media as described above. Images were acquired using 500-ms exposures. Nuclei were visualized with DAPI as described previously (Mondesert *et al.*, 1997). For double staining, cells expressing either Esp1GFP or Pds1GFP were fixed for 30 min at room temperature in 3.75 % formaldehyde followed by DAPI staining.

Cells were prepared for indirect immunofluorescence according to Mondesert and Reed (1996). Myc tagged Esp1 was detected with the 9E10 monoclonal antibody and a CY3-conjugated secondary antibody.

Cell cultures were analyzed for DNA content using flow-cytometry as described previously (Mondesert *et al.*, 1997).

Immunoprecipitation and Immunostaining

Protein isolation was essentially as previously described (Kaiser *et al.*, 1998). Cells were broken by glass beads (40 sec, 3 times) using an FP120 machine (Savant) in NP-40 buffer (50mM Tris-HCl pH 7.5, 150 mM NaCl, 0.1% NP40, 10 mM sodium pyrophosphate, 5 mM EDTA, 5 mM EGTA, 0.1 mM orthovanadate, 1 mM PMSF, 2 mg/ml aprotinin, leupeptin and pepstatin A). Following centrifugation at 14,000 rpm for 10 min the supernatant was used for immunoprecipitation. A total of 750 µg protein extract was incubated with myc9E10 antibody pre-bound to protein A sepharose or with 12CA5 antibody cross-linked to protein A-sepharose for 2 hrs, and immunocomplexes were washed four times

with 1 ml of extraction buffer. Bound proteins were eluted by boiling in 2xSDS sample buffer, separated by SDS-PAGE (7.5% protein gels) and analyzed by immunostaining with anti-HA antibody (12CA5, BabCO), anti-myc antibody (9E10) and anti-GFP antibody (Clontech). Extracts prepared solely for immunostaining were separated on 8.5% SDS-polyacrylamide gels and analyzed by immunoblotting. Cdc28 protein serving as a loading control was recognized by the anti-PSTAIR antibody.

Results

Cell Cycle-dependent Distribution of Esp1 in Live Yeast Cells

To gain insight into the regulation and function of Esp1 in *S. cerevisiae*, we initiated a study of the localization of this protein in live cells. Unlike Pds1, the level of Esp1 is not highly regulated in the cell cycle. The abundance of Esp1 protein was examined in synchronized cells expressing endogenous Esp1 fused to 18 myc epitopes at its C-terminus following release from an α -factor induced G1 block (Fig. 1A). The level of this fully functional fusion protein is approximately three fold lower in G1 than in the rest of the cell cycle, where it appears to be constant. The synchrony of the cells was verified by flow cytometry (data not shown).

In order to monitor if the localization profile of Esp1 in living cells changes through the cell cycle, a gene encoding Esp1 tagged with the green fluorescent protein (GFP) was integrated into a wild-type strain. This fusion protein complements an *esp1^{ts}* mutation, and cells overexpressing Esp1GFP under the control of the *GAL1* promoter grow normally (not shown). The strain was arrested in G1 using α -factor and Esp1GFP protein induced transiently by addition of galactose 30 min prior to release from the arrest into glucose-containing medium, which terminated synthesis. At given intervals, the localization of Esp1GFP was monitored in live cells by microscopy and the cell cycle distribution followed by DAPI staining (Fig. 1B). Fluorescent signal of Esp1GFP was delocalized throughout the entire cell in unbudded cells (G1). In G2, the protein was concentrated in the nucleus, and shortly thereafter was mobilized to the SPBs and the metaphase spindle (but see below). Since SPBs and kinetochores are in close proximity through most of the cell cycle in yeast (Straight *et al.*, 1997), colocalization experiments with Esp1 and the SPB component CNM67 were performed to confirm that Esp1 indeed labeled the SPBs (data not shown). As cells progressed into anaphase, Esp1 was observed

almost exclusively along the spindle, with most intense staining at the 2 μ m region of the spindle midzone in addition to the SPBs. The localization of Esp1GFP at different stages of the cell cycle is illustrated in Fig. 1C, where the protein was induced for 15 min on solid galactose-containing medium, resulting in approximately 10-fold higher levels of Esp1 compared to endogenous level (not shown). The distribution of Esp1 observed under these circumstances is not a result of overexpression, as the same localization pattern is observed in a strain expressing Esp1GFP from the endogenous promoter (Fig. 1C, i). The length of the spindles labeled by Esp1GFP exhibited a broad distribution (Fig. 1D). Relatively few Esp1-decorated spindles were measured as 2 μ m and shorter, and in all cases the spindles were already oriented along the mother-bud axis. This is in contrast with tubulin staining of an analogous population, where 2 μ m metaphase spindles are the most frequently observed class and anaphase spindles of intermediate length (frequently containing Esp1) are quite rare (data not shown). These data indicate that Esp1 labels the spindle at the metaphase-anaphase transition and not in G2 or during the bulk of metaphase. The majority of Esp1GFP anaphase spindles fell into the 3-6 μ m intermediate range but even spindles up to 9 μ m were observed, although fully extended anaphase spindles of 10-12 μ m did not contain Esp1. The appearance of Esp1 on spindles at the metaphase-anaphase transition, its persistence on anaphase spindles, and the specific enrichment of Esp1 at the spindle midzone, a structure important for anaphase spindle elongation in yeast (Pellman *et al.*, 1995) is suggestive of a role of Esp1 in spindle elongation at anaphase.

Association with Pds1 is Essential for Proper Esp1 Localization

Given the localization of Esp1 at the midzone, we examined the possible connection between this association and a known component of the spindle midzone in yeast, Ase1. Although this protein is

important for efficient anaphase spindle elongation, it is not essential, and *ase1* mutants are able to faithfully segregate chromosomes despite their unstable spindles (Pellman *et al.*, 1995; Juang *et al.*, 1997). The *ESP1GFP* gene was integrated into an *ase1Δ* mutant and the protein visualized following transient induction as described above. The localization of Esp1 to the nucleus and the SPBs was not affected in this mutant, however, signal at the spindle midzone was not observed in over 500 cells analyzed (Fig. 2A). There are two possible explanations for this result. Either Ase1 interaction is required to mediate midzone binding of Esp1 or the structure of the midzone in *ase1* mutants is perturbed hampering Esp1 association. Co-immunoprecipitation experiments using a strain with epitope-tagged versions of Esp1 and Ase1 expressed from their chromosomal loci revealed no interaction between the two components under a variety of test conditions (data not shown). It is therefore more likely that the absence of Esp1 at the midzone in *ase1* mutants is due to structural alterations of the midzone. Deletion of *ASE1* in an *esp1^{ts}* mutant exacerbates the temperature sensitivity of the strain, consistent with the idea that the spindle midzone is important for Esp1 function (data not shown).

The only protein identified to date that interacts with Esp1 is the anaphase inhibitor Pds1. To examine what effect Esp1/Pds1 complex formation has on the subcellular distribution of Esp1, the Esp1GFP protein was expressed and followed in a *pds1Δ* mutant at the permissive temperature. Surprisingly, the fluorescent signal was delocalized within the whole cell throughout the entire cell cycle. There was no detectable accumulation of Esp1GFP in the nucleus or spindle association (Fig. 2B). Although the *pds1Δ* strain is viable, the mutant grows poorly and the cells die at 28°C in the genetic background used for these studies. We therefore examined the localization of Esp1 in the less severe *pds1-128^{ts}* mutant, which has a restrictive temperature of 37°C. Esp1GFP exhibited a similar localization profile in this mutant at the permissive temperature to that observed in the *pds1Δ* strain (Fig. 2C).

Indirect immunofluorescence on cells expressing endogenous myc18 tagged Esp1 further confirmed the requirement of a functional Pds1 for correct localization of Esp1, as *pds1-128* cells failed to show nuclear or spindle staining of Esp1 (data not shown).

By two-hybrid analysis we found that the N-terminal domain of Esp1 spanning residues 1-535 interacts with the C-terminal region (residues 300-373) of Pds1 (data not shown). Since the *pds1-128^{ts}* mutation affects the extreme C-terminus of Pds1 (D. J. C. and S.I.R., unpublished data), it is possible that the mutant Pds1 protein is incapable of interacting with Esp1. To test this directly, a strain was constructed encoding endogenous Esp1 fused to 18 myc epitopes and wildtype Pds1 or Pds1-128 protein tagged with 3 copies of the HA epitope. Following growth at the permissive temperature (25°C), extracts from the strains were subjected to immunoprecipitation using anti-myc antibody. As is evident from the immunoblot in Fig. 2D, the level of co-precipitated Pds1-128 protein is significantly lower than the amount of Pds1 present in the immunoprecipitated wildtype sample. The reduction in Esp1/Pds1 complex formation in the *pds1-128* strain, however, is not due to an inability of the mutant Pds1 protein to interact with Esp1, as is evident by two-hybrid analysis (data not shown), but rather reflects the high instability and low steady-state level of the Pds1-128 protein. The level of Esp1 is not affected by the reduction in Pds1 protein level in the *pds1-128* mutant. Thus, we conclude that complex formation between Esp1 and Pds1 is required to ensure proper movement of Esp1 to the nucleus and spindle, where it can exert its anaphase functions.

Pds1 Transports Esp1 into the Nucleus and Promotes Spindle Association

To address the question of whether the lack of Esp1 spindle association in strains compromised for Pds1 function could simply reflect the absence of nuclear accumulation of Esp1, we investigated the

effect of fusing a nuclear localization sequence (NLS) to Esp1 on its localization. For this purpose, a peptide encoding the potent SV40 NLS (KKKRKV) was fused to the C-terminus of the Esp1GFP protein. This chimeric protein retains the ability to complement an *esp1^{ts}* mutation when overexpressed from the *GALI* promoter (not shown). In wildtype cells the Esp1GFPNLS protein exhibited a localization profile similar to that of Esp1 fused to GFP alone (Fig. 3A upper panel). In contrast, expression of Esp1GFPNLS in the *pds1-128* mutant now resulted in accumulation of the protein in the nucleus and subsequent labeling of the SPBs and weak spindle association. However, increasing the nuclear import of Esp1 in *pds1-128* cells was not sufficient to achieve a strong spindle fluorescence, as seen in wildtype cells (Fig. 3A middle panel), suggesting that Pds1 association may also be required to obtain efficient Esp1 spindle interaction. This is consistent with the observation that there is no detectable spindle fluorescence in *pds1Δ* cells expressing Esp1GFPNLS (Fig. 3A lower panel). Esp1 did label the SPBs in this mutant demonstrating that Esp1 has the ability to bind the SPBs in the absence of Pds1. This is perhaps not surprising as mutants deleted for *PDS1* are viable at low temperatures and unless the essential function of Esp1 is independent of its spindle localization, which must be considered unlikely, Esp1 must have intrinsic spindle binding activity sufficient for viability. This association, however, is clearly more efficient when Pds1 is present. Shifting the distribution of Esp1 in favor of the nucleus by expressing the Esp1GFPNLS version in a *pds1Δ* mutant leads to partial suppression of the temperature sensitive phenotype at 30°C, whereas the *pds1Δ* mutant expressing Esp1GFP is dead at this temperature (data not shown). This further supports the notion that an important function of Pds1 is to target Esp1 to the nucleus and subsequently to the spindle.

Surprisingly, the timing of nuclear concentration of Esp1GFPNLS in wildtype cells is unaltered compared to that of Esp1 fused to GFP alone. Both proteins accumulate in the nucleus in G2. This suggests that additional mechanisms regulate nuclear translocation of Esp1 (see Discussion).

To further confirm that association with Pds1 directs Esp1 localization, we constructed a strain expressing Esp1GFP and a non-degradable version of Pds1 (Pds1 Δ db) from the *GALI* promoter. After a 1-hr induction by addition of galactose cells were fixed briefly, stained with DAPI to visualize the nucleus, and examined by microscopy. Cells expressing only Esp1GFP served as a control. The presence of Pds1 Δ db protein led to a strong nuclear accumulation of Esp1GFP in unbudded cells, which was never observed in unbudded control cells, where the level of endogenous Pds1 is low due to the active proteolysis machinery (Fig. 3B). Of more than 300 unbudded cells counted, approx. 65% showed a strong Esp1 signal always colocalizing with the DAPI signal. This number is probably a low estimate as fixation often reduced the intensity of the Esp1GFP signal. Thus, expressing Pds1 prematurely in the cell cycle, promotes early translocation of Esp1 to the nucleus.

Pds1 Localizes to the Spindle Apparatus in Budding Yeast

Given the observation that Esp1 localization is controlled by Pds1, one would expect the two components to display similarities in their distribution at times of the cell cycle when Esp1 localization is changing. To investigate the localization of Pds1 in live cells, a strain was constructed expressing endogenous Pds1 fused at its C-terminus to GFP, which is fully functional (not shown). Cells were synchronized with α -factor and following release from G1, the localization of Pds1GFP was monitored by fluorescence microscopy. Nuclear morphology scored by DAPI and bud development were used as markers for cell cycle progression (Fig. 4A). Cells in G1 contained no Pds1GFP fluorescence, as

expected, since Pds1 protein first appears after bud emergence. As cells progressed through S-phase, Pds1GFP protein accumulated almost exclusively in the nucleus. The nuclear localization of Pds1 has been shown in an earlier study by indirect immunofluorescence (Alexandru *et al.*, 1999), where Pds1myc18 protein was shown to localize in the nucleus concomitant with bud emergence. In our study, there is a temporal lag between bud emergence and nuclear signal of Pds1 (approx. 10-15 min), which may reflect the relatively weaker signal obtained with a single GFP tag. Alternatively, the differential kinetics could be a consequence of strain differences. At the metaphase to anaphase transition the majority of Pds1GFP disappeared, but surprisingly a fraction remained nuclear and often associated with the spindle apparatus. As in the case of Esp1, there was a strong fluorescent signal of Pds1 at the SPBs and a 2 μ m bar at the spindle midzone in anaphase cells (Fig. 4B). The length distribution of spindles labeled by Pds1 was less broad than that observed with Esp1 (Fig. 4C and Fig. 1D). Most spindles were within the 2-4 μ m range but anaphase spindles stained by Pds1 were seen up to 7 μ m long. According to live cell measurements in haploid cells, a yeast spindle is between 2.5-3 μ m long when chromosome separation begins (Straight *et al.*, 1997). The association of Pds1 with mitotic spindles is consistent with the idea that Pds1 promotes Esp1 spindle binding by actually loading Esp1 onto the spindle apparatus at the metaphase-anaphase transition. Furthermore, the bias toward shorter spindles stained with Pds1, as compared to Esp1, suggests that Esp1 can be retained on the spindle once Pds1 is removed or degraded. Finally, the localization of Pds1 to the spindle is not altered in an *esp1^{ts}* mutant suggesting that Esp1 is not required for this process (data not shown).

Complex Formation between Esp1 and Pds1 is Established Early in the Cell Cycle

To establish when in the cell cycle the complex between Esp1 and Pds1 is formed, cells expressing endogenous myc18 tagged Esp1 and HA3 tagged Pds1 were arrested in G1 by treatment with α -factor. The cells were released at 22°C in order to slow down the cell cycle, providing a broader temporal window in which to monitor the timing of Esp1/Pds1 complex formation. Following release, samples were collected at intervals for immunoprecipitation, immunoblotting, and FACS analysis to confirm the synchrony. Extracts were subjected to immunoprecipitation using anti-HA antibody directed against Pds1. After SDS-PAGE the presence of Esp1 in the precipitate was revealed by immunostaining with anti-myc antibody. As is evident, the Esp1/Pds1 complex is formed at the time Pds1 first appears in the cell cycle and persists until anaphase, where Pds1 degradation is initiated (Fig. 5A and 5B). Therefore, Esp1 activity is likely to be controlled by Pds1 through most of the cell cycle. A reconstitution experiment, where extract containing Esp1myc18 protein was mixed with extract containing Pds1HA3 protein followed by immunoprecipitation showed that a complex between the two components could not be formed under these *in vitro* conditions (Fig. 5C). This confirms that the Esp1/Pds1 association shown in Fig. 5B reflects the true *in vivo* situation and is not an artifact of extraction. The co-precipitation result also correlates with the similar localization profile of the Esp1 and Pds1 proteins.

A Putative Calcium Binding Site in the C-terminal Domain of Esp1 is Important for Spindle Binding

Esp1 is a large protein composed of a total of 1630 amino acid residues (McGrew *et al.*, 1992). Little information can be derived from the primary amino acid sequence of Esp1. The N-terminal third of the protein retains the ability to interact with Pds1 (data not shown). The equivalent region in Cut1, the *S. pombe* homolog, has been shown to interact with Cut2, the functional homolog of Pds1, despite lack

of conservation at the primary amino acid level (Kumada *et al.*, 1998). The C-terminal region of Esp1 exhibits considerable homology to that of Cut1, *Aspergillus* BimB and human Esp1 (30-40% identity), and it contains a putative calcium binding site (Fig. 6A).

To address the importance of the potential calcium binding motif for Esp1 function, we constructed mutants of Esp1, where aspartic acid residues in the site were altered to alanine residues. The basis for this approach is that oxygen containing residues such as aspartic acids are known to coordinate the interaction with calcium ions in calcium binding proteins (Kreutsinger, 1980). Deletion of the extreme C-terminal region of Esp1 including the putative calcium binding site rendered the mutant protein incapable of complementing an *esp1^{ts}* mutation, even when the protein was overexpressed from the *GALI* promoter (Fig. 6B). In fact, overexpression at the permissive temperature is lethal in an *esp1^{ts}* background (data not shown). A mutant protein with a single aspartic acid to alanine substitution at position 1568 could rescue an *esp1^{ts}* mutation when overexpressed from the *GALI* promoter, whereas a lower dose derived from a low copy plasmid and the endogenous promoter only provided weak suppression of the *esp1^{ts}* phenotype (Fig. 6B). A second point mutation introducing the D1570A substitution yielded a mutant Esp1 protein unable to complement growth of an *esp1^{ts}* mutant even when expressed from the *GALI* promoter. In fact, overexpression of the D1568A/D1570A protein in the *esp1^{ts}* background, as in the case of 1-1568 protein, was lethal at the permissive temperature. That the mutant Esp1 proteins exacerbated the *esp1^{ts}* phenotype but did not alter the growth of wildtype cells (not shown) suggests a weak dominant interfering effect, possibly due to competition for Pds1. These data taken together indicate that the putative calcium binding site in the C-terminal region plays a crucial role for Esp1 function.

We set out to characterize the essential function of the calcium binding site in Esp1 by analyzing the nature of the defects of the Esp1 mutant proteins. Immunoprecipitation experiments on extracts derived from strains expressing endogenous levels of HA3 tagged Pds1 in combination with the different Esp1GFP mutants induced from the *GALI* promoter demonstrated that the Esp1 mutants are not defective in Pds1 interaction (Fig. 6C). The localization of the Esp1 mutant proteins in live cells was subsequently examined following a brief induction resulting in a comparable 10-fold overexpression in all strains (not shown). The C-terminal truncation mutant 1-1568 was delocalized throughout the cell at all stages of the cell cycle, suggesting that the C-terminal region of Esp1 is required for nuclear translocation and interaction with the spindle (Fig. 6D, a). The Esp1 D1568A mutant protein exhibited a distribution similar to wildtype Esp1 protein (Fig. 6D, b; Table II), consistent with the fact that overexpression of the mutant from the *GALI* promoter rescues an *esp1^{ts}* mutation. However, the Esp1 protein carrying two aspartic acid to alanine substitutions in the calcium binding site (D1568A/D1570A) had a severely reduced ability to bind the spindle (Fig. 6D, c; Table II). Of more than 400 large-budded cells examined, only 1.5% displayed spindle labeling compared to 28.8% in wildtype cells. In addition, no spindles were observed exceeding 4 μ m in length. This reduction in spindle association may account for the loss of complementation ability of this double mutant protein. Thus, the putative calcium binding site in the conserved C-terminal domain of Esp1 is essential for initiating and/or maintaining spindle association, which is crucial for Esp1 function at anaphase.

To elucidate whether calcium may play a role in Esp1 function, we tested for a possible effect of calcium on the growth of *esp1^{ts}* mutants. Addition of extra CaCl_2 to the growth medium rescued the temperature sensitivity of the strain (Fig. 6E). This suppression could not be achieved by other divalent cations, but was specific to Ca^{2+} and reversible by the addition of the calcium chelator EGTA to the

medium (Fig. 6E). Interestingly, two genes with roles in maintaining intracellular calcium levels were identified in a synthetic lethality screen with an *esp1^{ts}* mutant (unpublished data). Taken together, these observations suggest that calcium may regulate the activity of Esp1 by promoting spindle association at anaphase.

Discussion

A Role of Esp1 in Anaphase Spindle Elongation

Esp1 is a key player in sister chromatid separation. Its liberation from Pds1 mediated by APC-dependent proteolysis is essential to remove cohesion between duplicated sister chromatids, allowing them to separate when microtubule-dependent forces are exerted by the spindle. To date it is unclear whether the Esp1/Pds1 complex, in addition, regulates aspects of anaphase spindle elongation. Here we have shown that both Esp1 and Pds1 exhibit cell cycle-dependent spindle association in live cells. Esp1 has previously been shown to bind the spindle apparatus by indirect immunofluorescence but in this study only a fraction of the protein was reported to bind the spindle (Ciosk *et al.*, 1998). By monitoring the localization of Esp1 fused to GFP in real time studies, we found that the majority of Esp1 protein associates with the SPBs and the spindle as cells progress from metaphase to anaphase (Fig. 1). In G1- and S- phase the protein is uniformly dispersed in the cell until G2, where Esp1 transiently accumulates in the nucleus prior to spindle binding. Esp1 does not associate significantly with the G2/M spindles, which are characteristically 2 μ m in length (Fig. 1, d). It is therefore tempting to speculate that Esp1 first associates transiently with chromatin to mediate sister chromatid separation, after which it serves as an anaphase signal transducer, translocating to the spindle. Interestingly, Esp1 remains bound to the spindle well into anaphase, labeling spindles up to 9 μ m in length, suggesting more than a transient role in spindle function. A significant pool of Esp1 is located at the spindle midzone during anaphase. This central region of the spindle, where polar microtubules overlap, plays an important role in elongation of the anaphase spindle (Winey *et al.*, 1995; Pellman *et al.*, 1995). Although there is still controversy as to whether anaphase elongation occurs by a pushing- or pulling mechanism, studies suggest that in *S. cerevisiae* the nuclear microtubules generate the forces for anaphase spindle elongation (Sullivan and

Huffaker, 1992). A recent study of spindle dynamics reveals that elongation of the anaphase spindle in yeast is coupled to microtubule growth at the overlapping plus ends of the spindle midzone (Maddox *et al.*, 2000). The midzone usually becomes highly organized during anaphase with microtubules from one pole lying adjacent to those from the opposite pole. Electron microscopic studies have revealed that the midzone in *esp1^{ts}* mutants lacks organization of the antiparallel microtubules (McGrew *et al.*, 1992). Although, this could be an indirect result of the inability of *esp1^{ts}* mutants to separate sister chromatids, it more likely reflects a direct role for Esp1 in maintaining proper interdigitation of pole-to-pole microtubules that drive spindle elongation. The timing of Esp1 spindle localization, and the persistence of the protein on anaphase spindles with particular concentration at the midzone strongly suggests that it is not only required for sister chromatid separation at the metaphase to anaphase transition but also plays an important role in aspects of spindle elongation at anaphase. Whether this involves regulation of an unidentified anaphase motor protein, microtubule polymerization or a structural role in the organization of microtubules from opposite poles remains unknown. The Esp1 protein itself does not show significant homology to any known motor protein, and it does not interact directly with the known midzone protein Ase1. Identification of potential components of the midzone that interact with Esp1 will provide valuable clues to the exact mechanism of action of Esp1 and how the midzone functions during anaphase spindle elongation in general.

Pds1 Localization Reflects a Regulatory Role of the Esp1/Pds1 Complex during Anaphase

Pds1 has previously been shown to be a nuclear protein from the time it is produced after bud emergence until it is turned over at the onset of anaphase (Yamamoto *et al.*, 1996). We report the novel finding that Pds1 associates with the spindle apparatus at the metaphase-anaphase transition and that a

fraction of Pds1 protein persists concentrated at the SPBs and the spindle midzone into mid-anaphase. Pds1 may therefore, like Esp1, be involved in regulating aspects of early anaphase spindle function. The surprising observation that a pool of Pds1 escapes destruction at anaphase onset raises the intriguing question whether distinct subpopulations of Pds1, with specialized tasks, exist in the cell. This would be consistent with the recent report that Pds1 besides its regulatory role at anaphase also regulates exit of mitosis by preventing release of Cdc14 from the nucleolus and thus inhibiting cyclin degradation (Cohen-Fix and Koshland, 1999; Tinker-Kulberg and Morgan, 1999; Shirayama *et al.*, 1999). To this end, it is possible that the remaining pool of Pds1 molecules located on the SPB and anaphase spindle may be involved in coupling exit of mitosis with the prior completion of anaphase, either in conjunction with or independently of Esp1. In fact, several components of the mitotic exit network that govern exit of mitosis exhibit SPB localization (Jaspersen *et al.*, 1998; Kormarnitsky *et al.*, 1998; Luca *et al.*, 1998; Song *et al.*, 2000). The reason why a subset of Pds1 resists early degradation is not clear but may reflect modification or interaction with specific components that delay recognition by the proteolysis machinery.

Pds1 Targets Esp1 to the Nucleus and Mitotic Spindle

The general view of Pds1 is that it functions as an inhibitor of Esp1 activity. However, the current model does not explain the observations that Esp1 in high dosage can suppress a *pds1^{ts}* mutation or that *esp1^{ts}* and *pds1^{ts}* mutations exhibit synthetic lethality (D.J.C. and S.I.R. , unpublished data), which argue that the two components have overlapping functions in addition to their antagonistic ones. In this study we present evidence that Pds1 also promotes Esp1 function by ensuring efficient localization of the latter to the nucleus and the spindle, providing an explanation for this apparent

paradox. Esp1 only accumulated in the nucleus and associated with the spindle in the presence of functional Pds1 (Fig. 2, b-c). The absence of Esp1 spindle binding in a *pds1Δ* strain was also noted in an earlier study but the reason for this was not understood (Ciosk *et al.*, 1998). We observed that the lack of Esp1 spindle fluorescence in strains with impaired Esp1/Pds1 complex formation could not be accounted for by the absence of nuclear accumulation of Esp1. An increase in the nuclear import of Esp1 by NLS fusion only partially bypassed the requirement for Pds1 in that spindle association was not restored to wildtype levels (Fig. 3). It is possible that prior association with Pds1 is needed merely to induce a conformational change in the structure of Esp1 to render it more competent to interact with the spindle. An alternative, and perhaps more plausible, ~~explanation~~ in the light of our data is that Pds1 is directly involved in mediating Esp1 spindle interaction. Thus, there exists a dual-step requirement for Pds1: first, to transport Esp1 into the nucleus and second, to presumably load it onto the early mitotic spindle. A loading function of Pds1 is consistent with the observation that Pds1 itself interacts with the spindle with similar timing as Esp1, and the relatively brief kinetics of interaction manifest in the shorter spindle length distribution of Pds1 labeled spindles, as compared to Esp1 decorated spindles. Esp1 has the ability to bind the SPBs in the absence of Pds1, when introduced into the nucleus, as Esp1GFPNLS stains the SPBs brightly in a *pds1Δ* mutant. However, the SPB signal is only observed in cells at the metaphase stage, where the nucleus is positioned at the neck and is lost as cells progress into anaphase, suggesting that Pds1 is needed to initiate and/or maintain efficient early anaphase spindle binding of Esp1.

Although Pds1 is required to accumulate Esp1 in the nucleus, Esp1 is not ostensibly excluded from this compartment when Pds1 is absent, either in wildtype G1 cells or *pds1Δ* cells. This, albeit

reduced, activity of Esp1 in the nucleus may indeed explain why deletion of *PDS1* is not lethal at low temperatures.

Pds1 may not be the sole factor that regulates Esp1 localization. In cells expressing Esp1GFPNLS, we saw no significant difference in the timing of nuclear and spindle association of Esp1 as compared with cells expressing Esp1GFP alone. There are several possibilities which could account for this unexpected result. First, the NLS may only become exposed following a structural change in Esp1 as a result of modification induced by an unknown event in late G2. Alternatively, and perhaps more likely, a cytoplasmic component may retain most Esp1 protein in the cytoplasm in the early stages of the cell cycle. Studies on the Esp1 homolog in *S. pombe*, Cut1 have hinted at the existence of such a cytoplasmic retention factor, although its identity remains unknown (Kumada *et al.*, 1998). The presence of such a regulatory factor could also explain the temporal lag between Esp1 and Pds1 nuclear localization. Early work has shown that Pds1 is mostly nuclear at S-phase (Yamamoto *et al.*, 1996), whereas we have demonstrated both in live cells and by indirect immunofluorescence that Esp1 first concentrates in the nucleus in late G2. Yet we know that Esp1 and Pds1 form a complex as soon as Pds1 protein appears in the cell cycle. Therefore, the complex must be retained in the cytoplasm until late G2 unless the amount of complex formed early in the cell cycle is below the detection limit of our readout, which cannot be entirely excluded. If a cytoplasmic retention factor exists, it must be limiting as overexpression of Pds1 Δ db protein from the *GALI* promoter allows nuclear accumulation of Esp1 in unbudded cells (Fig. 3B).

Our data favor a model in which Pds1 through physical interaction carries Esp1 into the nucleus and positions it efficiently on the spindle at the onset of anaphase. Pds1 must have a docking site on the spindle independent of Esp1, as Pds1 spindle localization is unperturbed in *esp1^{ts}* mutants. The

Esp1/Pds1 complex binds both SPBs and the early anaphase spindle. What event actually triggers the spindle association is not clear at present but it may require APC activity and initial degradation of Pds1 (Ciosk *et al.*, 1998; unpublished observations). Upon Pds1 proteolysis, Esp1 is activated to promote sister chromatid separation and then presumably in conjunction with remaining Pds1 is translocated to the spindle to mediate anaphase elongation perhaps through interaction with components of the spindle midzone. This model is consistent with the observation that Esp1 can promote loss of cohesion in the absence of functional kinetochores or mitotic spindles (Ciosk *et al.*, 1998). If Pds1 is indeed directly mediating Esp1 spindle interaction, Esp1 must be loaded on the spindle when a stoichiometric amount of Pds1 still remains, as a sizeable fraction of soluble Pds1 is estimated to be complexed with Esp1 (Ciosk *et al.*, 1998). Esp1 persists on the spindle through an independent docking site after spindle-bound Pds1 is degraded, an interaction which requires an intact C-terminal domain of Esp1 (see below).

Function of the Conserved C-terminal Domain in Esp1-related Proteins

The ability to associate with the spindle apparatus depends on the C-terminal region of Esp1 as well as the N-terminal third of the protein, which mediates interaction with Pds1. We found, more specifically, that a putative calcium binding site in the C-terminus of Esp1 is important for proper anaphase spindle function, as an Esp1 mutant with the two amino acid substitutions D1568A/D1579A in this motif had a strongly reduced (approx. 20-fold) spindle binding ability and only labeled spindles shorter than 4 μm (Table II). Indeed, a single mutation at position 1568 was sufficient to yield a mutant Esp1 protein unable to complement an *esp1^{ts}* mutation. A similar behavior was recently described for Cut1 alleles mutated in the C-terminal region (Kumada *et al.*, 1998). In this study, a Cut1 mutant with a single amino acid change at position 1767, which lies within the potential calcium binding motif, was

shown to localize to metaphase spindles but was excluded from anaphase spindles. Thus, the C-terminal calcium-binding motif is likely to have equivalent essential roles in Esp1 and Cut1, ensuring proper association of the protein with the spindle during anaphase.

Whether the conserved calcium binding motif in Esp1 and Cut1 actually mediates calcium binding remains to be shown. Interestingly, *esp1^{ts}* mutations were suppressed by the addition of calcium to the growth medium, which could be reversed by simultaneous addition of the chelating agent EGTA. This, together with our finding that mutations in two genes important for calcium homeostasis are lethal in combination with an *esp1^{ts}* mutation, raises the intriguing possibility that calcium may regulate Esp1 activity. *pds1* mutants are not rescued by calcium consistent with the idea that calcium may be a specific regulator of Esp1 spindle association during anaphase (not shown). It has previously been reported that calcium oscillations occur at the metaphase to anaphase transition and play an important role in anaphase onset (Groigno *et al.*, 1998), although this has yet to be established in yeast.

It is not surprising that Esp1 is regulated by several mechanisms given the importance of sister chromatid separation for the survival of the cell. Once cohesion has been established during DNA replication it becomes pivotal that Esp1 activity is controlled to coordinate loss of cohesion with anaphase spindle elongation. The fact that *pds1*Δ cells do not separate sisters prematurely (Ciosk *et al.*, 1998; D. J. Clarke, unpublished data) clearly indicates that alternative mechanisms exist to regulate Esp1 activity.

The Esp1 and Pds1 complex appears to be conserved in organisms of different origin. Their best characterized homologs in *S. pombe*, Cut1 and Cut2 apparently perform equivalent vital roles in mitosis. Recently, both Cut1 and Cut2 were found to interact with the spindle and this association (but not the nuclear localization of Cut1) was dependent on Cut2 and important for anaphase spindle movement.

Thus, given the overall similarities in the regulation and function of the Esp1/Pds1- and Cut1/Cut2 complexes, it seems reasonable to assume that similar functional relationships exist between homologues of Esp1 and Pds1 in higher eukaryotic cells.

Acknowledgments

We are grateful to D. Koshland and O. Cohen-Fix for kindly providing the Pds1 tagging vector, T. Davis for providing the CNM67 tagging construct, and N. Rhind and P. Russell for help with microscopy. We thank members of the McGowan-, Reed-, Russell- and Wittenberg laboratories for stimulating discussions.

S. Jensen was supported by a fellowship from the Danish Medical Research Council. M. Segal acknowledges support from EMBO and HFSP fellowships and D. J. Clarke was funded by EMBO and US Army Breast Cancer Research fellowships. This research was supported by US Public Health Service Grant GM38328 to SIR.

Footnotes

1. *Abbreviations used in this paper:* DAPI, 4', 6'-diamidino-2-phenylindole; DIC, differential interference contrast; SPB, spindle pole body

References

Alexandru, G., W. Zachariae, A. Schleiffer, and K. Nasmyth. 1999. Sister chromatid separation and chromosome re-duplication are regulated by different mechanisms in response to spindle damage. *EMBO J.* 18:2707-2721.

Ciosk, R., W. Zachariae, C. Michaelis, A. Shevchenko, M. Mann, and K. Nasmyth. 1998. An ESP1/PDS1 complex regulates loss of sister chromatid cohesion at the metaphase to anaphase transition in yeast. *Cell* 93:1067-1076.

Cohen-Fix, O., J.-M. Peters, M. W. Kirschner, and D. Koshland. 1996. Anaphase initiation in *Saccharomyces cerevisiae* is controlled by the APC-dependent degradation of the anaphase inhibitor Pds1p. *Genes Dev.* 10:3081-3093.

Cohen-Fix, O., and D. Koshland. 1999. Pds1p of budding yeast has dual roles: inhibition of anaphase initiation and regulation of mitotic exit. *Genes Dev.* 13:1950-1959.

Funabiki, H., K. Kumada, and M. Yanagida. 1996. Fission yeast Cut1 and Cut2 are essential for sister chromatid separation, concentrate along the metaphase spindle and form large complexes. *EMBO J.* 15:6617-6628.

Groigno, L., and M. Whitaker. 1998. An anaphase calcium signal controls chromosome disjunction in early sea urchin embryos. *Cell* 92:193-204.

Guthrie, C. and G. R. Fink. 1991. Guide to yeast genetics and molecular biology, Vol. 194, Academic Press, Inc., San Diego, CA.

Jaspersen, S. L., J. F. Charles, R. L. Tinker-Kulberg, D. O. Morgan. 1998. A late mitotic regulatory network controlling cyclin destruction in *Saccharomyces cerevisiae*. *Mol. Biol. Cell.* 9:2803-17.

Juang, Y-L, J. Huang, J-C. Peters, M. E. McLaughlin, C-Y. Tai, and D. Pellman. 1997. APC-mediated proteolysis of Ase1 and the morphogenesis of the mitotic spindle. *Science* 275:1311-1314.

Kaiser, P., R. A. Sia, E. G. Bardes, D. J. Lew, and S. I. Reed. 1998. Cdc34 and the F-box protein Met30 are required for degradation of the Cdk-inhibitory kinase Swe1. *Genes Dev.* 12:2587-2597.

Kaiser, P., V. Moncollin, D. J. Clarke, M. H. Watson, B. L. Bertolaet, S. I. Reed and E. Bailly. 1999. Cyclin-dependent kinase and Cks/Suc1 interact with the proteasome in yeast to control proteolysis of M-phase targets. *Genes Dev.* 13:1190-1202.

King, R. W., J. Peters, S. Tugendreich, M. Rolfe, P. Hieter, and M. W. Kirschner. 1995. A 20S complex containing CDC27 and CDC16 catalyzes the mitosis-specific conjugation of ubiquitin to cyclin B. *Cell* 81:279-288.

Kormarnitsky, S. I., Y. C. Chiang, F. C. Luca, J. Chen, J. H. Toyn, M. Winey, L. H. Johnston, and C. L. Denis. 1998. DBF2 protein kinase binds to and acts through the cell cycle-regulated MOB1 protein. *Mol. Cell. Biol.* 18:2100-2107.

Kretsinger, R. H. 1980. Crystallographic studies of calmodulin and homologs. *Ann. NY Acad. Sci. USA* 356:14-19.

Kumada, K., T. Nakamura, K. Nagao, H. Funabiki, T. Nakagawa and M. Yanagida. 1998. Cut1 is loaded onto the spindle by binding to Cut2 and promotes anaphase spindle movement upon Cut2 proteolysis. *Current Biol.* 8:633-641.

Landt, O., H. P. Grunert, and U. Hahn. 1990. A general method for rapid site-directed mutagenesis using the polymerase chain reaction. *Gene* 96: 125-128.

Luca, F. C. and M. Winey. 1998. MOB1, an essential yeast gene required for completion of mitosis and maintenance of ploidy. *Mol Biol. Cell.* 9:29-46.

Maddox, P. S., K. S. Bloom, and E. D. Salmon. 2000. The polarity and dynamics of microtubule assembly in the budding yeast *Saccharomyces cerevisiae*. *Nat. Cell Biol.* 2:36-41.

May, G. S., C. A. McGoldrick, C. L. Holt, and S. H. Denison. 1992. The *bimB3* mutation of *Aspergillus nidulans* uncouples DNA replication from the completion of mitosis. *J. Biol. Chem.* 267:15737-15743.

McGrew, J. T., L. Goetsch, B. Byers, and P. Baum. 1992. Requirement for ESP1 in the nuclear division of *Saccharomyces cerevisiae*. *Mol. Biol. Cell.* 3:1443-1454.

Mondesert, G., and S. I. Reed. 1996. BED1, a gene encoding a galactosyltransferase homologue, is required for polarized growth and efficient bud emergence in *Saccharomyces cerevisiae*. *J. Cell Biol.* 132:137-151.

Mondesert, G., D. J. Clarke, and S. I. Reed. 1997. Identification of genes controlling growth polarity of the budding yeast *Saccharomyces cerevisiae*: a possible role of N-glycosylation and involvement of the exocyst complex. *Genetics* 147:421-434.

Pellman, D., M. Bagget, H. Tu, and G. R. Fink. 1995. Two microtubule-associated proteins required for anaphase spindle movement in *Saccharomyces cerevisiae*. *J. Cell Biol.* 130:1373-1385.

Richardson, H. E., C. Wittenberg, F. R. Cross, and S. I. Reed. 1989. An essential G1 function for cyclin-like proteins in yeast. *Cell* 59:1127-1133.

- Shiramaya, M., A. Toth, M. Galova, and K. Nasmyth. 1999. APC^{Cdc20} promotes exit from mitosis by destroying the anaphase inhibitor Pds1 and cyclin Clb5. *Nature* 11:203-207.
- Sikorski, R. S. and P. Hieter. 1989. A system of shuttle vectors and yeast host strains designed for efficient manipulation of DNA in *Saccharomyces cerevisiae*. *Genetics* 122:19-27.
- Song, S., T. Z. Grenfell, S. Garfield, R. L. Erikson, and K. S. Lee. 2000. Essential function of the polo box of Cdc5 in subcellular localization and induction of cytokinetic structures. *Mol. Cell. Biol.* 20:286-298.
- Straight, A. F., W. F. Marshall, J. W. Sedat, and A. W. Murray. 1997. Mitosis in living budding yeast: anaphase A but no metaphase plate. *Science* 277:574-578.
- Straight, A. F., J. W. Sedat, and A. W. Murray. 1998. Time-lapse microscopy reveals unique roles for kinesins during anaphase in budding yeast. *J. Cell Biol.* 143:687-694.
- Sullivan, D. S., and T. C. Huffaker. 1992. Astral microtubules are not required for anaphase B in *Saccharomyces cerevisiae*. *J. Cell Biol.* 119:379-388.
- Tang, Y., and S. I. Reed. 1993. The Cdk-associated protein Cks1 functions both in G1 and G2 in *Saccharomyces cerevisiae*. *Genes Dev.* 7:822-832.

Tinker-Kulberg, R. L., and D. O. Morgan. 1999. Pds1 and Esp1 control both anaphase and mitotic exit in normal cells and after DNA damage. *Genes Dev.* 13:1936-1949.

Uhlmann, F., F. Lottspeich and K. Nasmyth. 1999. Sister-chromatid separation at anaphase onset is promoted by cleavage of the cohesin subunit Scc1. *Nature* 400:37-42.

Uzawa, S., I. Sameijima, T. Hirano, K. Tanaka, and M. Yanagida. 1990. The fission yeast *cut1⁺* gene regulates spindle pole body duplication and has homology to the budding yeast ESP1 gene. *Cell* 62:913-925.

Wach, A., A. Brachat, R. Pohlmann, and P. Philippsen. 1994. New heterologous modules for classical or PCR-based gene disruptions in *Saccharomyces cerevisiae*. *Yeast* 10:1793-1808.

Winey, M., C. L. Mamay, E. T. O'Toole, D. N. Mastronarde, T. H. Giddings, K. L. McDonald, and J. R. McIntosh. 1995. Three-dimensional ultrastructural analysis of the *Saccharomyces cerevisiae* mitotic spindle. *J. Cell Biol.* 129:1601-1615.

Yamamoto, A., V. Guacci, and D. Koshland. 1996. Pds1p is required for faithful execution of anaphase in the yeast, *Saccharomyces cerevisiae*. *J. Cell Biol.* 133:85-97.

Zachariae, W., and K. Nasmyth. 1996. TPR proteins are required for anaphase progression mediate ubiquitination of mitotic B-type cyclins in yeast. *Mol. Biol. Cell* 7: 791-801.

Zou, H., T. J. McGarry, T. Bernal, M. W. Kirschner. 1999. Identification of a vertebrate sister-chromatid separation inhibitor involved in transformation and tumorigenesis. *Science* 285:418-422.

Figure legends

Figure 1. Cell cycle dependent regulation of Esp1. A. Esp1 protein level during the cell cycle. A strain carrying epitope-tagged Esp1 integrated at the chromosomal locus was arrested in G1 with α -factor. Cells were released from the block into YEPDextrose at 25°C and aliquots removed at the indicated times for analysis of cell morphology, Esp1 and Cdc28 protein levels and FACS analysis. B. Cell cycle changes in the localization of Esp1 in live cells. A strain carrying *GAL1* inducible *ESP1GFP* integrated at the *URA3* locus was grown in synthetic medium and arrested in G1 with α -factor. 30 min prior to release, 2% galactose was added to induce Esp1GFP. Cells were released into YEPDextrose at 30°C and aliquots removed at given time-points for analysis by real time microscopy, determination of budding index and cell cycle progression by DAPI stain on fixed samples. Open squares: cells with pre-anaphase nuclear morphology; filled squares: cells with anaphase- and telophase nuclear morphology; triangles: budding index; diamonds: nuclear localization of Esp1; circles: spindle localization of Esp1. C. Localization of Esp1GFP at different stages of the cell cycle. Diploid cells carrying an integrated *ESP1GFP* allele grown in YEP Raffinose were collected on a nitrocellulose filter and transferred onto a YEP Galactose plate. After 15 min of induction, cells were examined by microscopy and images acquired of GFP signal and DIC. a-b: nuclear Esp1GFP signal in late G2 cells; c: metaphase spindle and SPB stain of Esp1; d-h: anaphase spindles stained by Esp1; i: anaphase spindle stain in cell expressing Esp1GFP from the native promoter. Bar is 10 μ m. D. The length distribution of spindles labeled by Esp1GFP. Spindles measured on cells treated as described in C.

Figure 2. Proper Esp1 localization depends on Pds1. A (a-b). Esp1 signal at the spindle midzone is absent in *ase1Δ* mutant. Image of a diploid *ase1Δ* strain carrying *GALI*-inducible *ESP1GFP* integrated at the *URA3* locus is examined by microscopy following induction on solid YEPGalactose media, as described in Fig. 1., B (a-b). Localization of Esp1 in *pds1Δ* mutant. Haploid *pds1Δ* cells expressing Esp1GFP from the *GALI* promoter is treated as in A. C (a-b). Movement of Esp1 to nucleus and spindle is reduced in a *pds1-128^{ts}* mutant. Haploid *pds1-128* cells with *ESP1GFP* integrated are analyzed as above. D. Comparison of Esp1/Pds1 complex formation in exponentially growing wildtype cells and *pds1-128* cells. Strains carrying endogenous myc18 tagged Esp1 and HA3 tagged Pds1 (wt) or Pds1-128 (ts) are grown at 25°C. Extract from the strains is immunoprecipitated with anti-myc antibody. Samples were analyzed by SDS-PAGE followed by immunostaining with anti-myc antibody and anti-HA antibody. An isogenic control strain expressing endogenous Pds1HA3 protein is included to show specificity of the anti-myc antibody. Note that the additional amino acids at the C-terminus of the Pds1-128 protein causes it to migrate at a slightly lower mobility. Also, due to the instability of the Pds1-128 protein, the slower migrating form is only observed with high amounts of protein.

Figure 3. Pds1 is required to load Esp1 onto the spindle. A. A version of Esp1GFP fused at its C-terminus to the SV40 NLS is integrated into a wildtype strain (upper panel), a *pds1-128* mutant (middle panel), and a *pds1Δ* mutant (lower panel). The Esp1GFPNLS protein is induced for 20 min from the *GALI* promoter on solid YEPGalactose medium and cells examined by microscopy. Images on the left are GFP fluorescence and on the right DIC. Bar is 10 μm. B. Expression of a non-destructable Pds1 (Pds1Δdb) leads to premature nuclear localization of Esp1. A strain carrying *GALI*-inducible integrated *ESP1GFP* and *PDS1Δdb* alleles (b) is grown overnight in YEP Raffinose. Following 1 hr induction with

2% galactose at 30°C, cells are fixed briefly in 3.75 % formaldehyde and stained with DAPI to visualize nuclei. Image on the left is Esp1GFP fluorescence and the right image is a DAPI/DIC overlay. A control strain carrying only a *GALI*-inducible *ESP1*GFP allele is analyzed in a similar fashion (a).

Figure 4. Pds1 associates with the mitotic spindle apparatus. A. A strain carrying *PDS1* fused at the C-terminal end to GFP integrated at the chromosomal locus is arrested in G1 with α -factor. Following release into YEPDextrose at 30°C, aliquots are taken for scoring budding index, cell cycle progression by DAPI and real time localization of Pds1GFP. Open squares: cells with pre-anaphase nuclear morphology; filled squares: cells with anaphase- and telophase nuclear morphology; triangles: budding index; diamonds: nuclear localization of Pds1; circles: spindle localization of Pds1. B (a-b). Live cell localization of Pds1GFP. A diploid strain with one endogenous copy of Pds1 fused to GFP is grown in YEPDextrose and cells examined by microscopy. Bar is 10 μ m. C. The length distribution of spindles visualized by Pds1GFP. Spindles measured on cells treated as described in B.

Figure 5. Complex formation between Esp1 and Pds1. A. A strain expressing endogenous Esp1 tagged with 18 myc epitopes and Pds1 fused to 3 HA tags was arrested in G1 by addition of α -factor. Following release into YEPDextrose at 22°C, samples were removed at the indicated time-points. Extract was prepared and analyzed by SDS-PAGE and immunostaining with anti-myc antibody (top panel), anti-HA antibody (middle panel), and anti-PSTAIRE antibody, the latter to visualize Cdc28 protein, which serves as a loading control. B. Extracts prepared from samples in A were subjected to immunoprecipitation using anti-HA antibody to pull down Pds1 protein. SDS-PAGE and immunostaining was carried out with anti-myc antibody to reveal the presence of Esp1 in the precipitate

(upper panel) and anti-HA antibody to show amount of precipitated Pds1 (lower panel). C. Esp1/Pds1 complex is not formed *in vitro*. Extract from a strain expressing Esp1myc18 protein was mixed with extract containing Pds1HA3 protein. Following immunoprecipitation with anti-HA antibody and SDS-PAGE, samples were analyzed by immunostaining using anti-myc antibody (upper panel) and anti-HA antibody (lower panel).

Figure 6. The role of the putative calcium binding site in the conserved C-terminal domain of Esp1. A. A schematic representation of the domain structure of Esp1. The N-terminal domain constituting 1/3 of the protein is sufficient to interact with Pds1 by two-hybrid analysis. The conserved C-terminal region contains a putative calcium binding site, which is conserved in the *S. pombe* homolog Cut1. B. Complementation ability of various Esp1 mutant proteins in an *esp1^{ts}* mutant strain. Proteins were either expressed from an integrated allele driven by the *GALI* promoter (*GALI*) or expressed from their own promoter on a low copy plasmid (*ARS/CEN*). The Esp1 mutants were tested for complementation with or without the GFP tag with similar results. C. Mutation in the C-terminal region of Esp1 does not affect the ability to interact with Pds1. A strain expressing Pds1 tagged at the C-terminus with 3 HA epitopes was transformed with integrating plasmids encoding the different Esp1GFP mutant proteins inducible from the *GALI* promoter. The resulting strains were grown in YEPRaffinose, induced for 80 min with 2% galactose, and extract prepared for immunoprecipitation with anti-HA antibody to bring down Pds1. After SDS-PAGE immunostaining was performed with anti-GFP antibody to visualize possible Esp1GFP in the precipitate (upper panel) and anti-HA antibody to confirm Pds1 precipitation. The presence of Esp1GFP, Pds1HA3 and Cdc28 protein in the extract from the different strains is shown in the panel to the right. An isogenic strain expressing only Pds1HA3 protein is included as a

control. D. Localization of mutant Esp1GFP protein in live cells. Strains expressing either *GALI*-inducible Esp1(1-1568)GFP, Esp1(D1568A)GFP, or Esp1(D1568A/D1570A)GFP were examined by microscopy following 20 min induction on solid YEPGalactose media. The expression level of the three different Esp1 mutant proteins was similar (not shown). a: Esp1(1-1568)GFP, b: Esp1(D1568A)GFP, c: Esp1(D1568A/D1570A)GFP. Pictures in upper panel are GFP signals, and lower panel shows DIC. Bar is 10 μ m. E. Calcium added to the growth medium can suppress the temperature sensitive phenotype of *esp1^{ts}* mutant. An *esp1^{ts}* mutant and an isogenic wildtype strain grown at room temperature is replica plated onto following plates: a: YEPDextrose + 50 mM CaCl₂, b: YEPDextrose, c: YEPDextrose + 50 mM EGTA/CaCl₂, d: YEPDextrose + 50 mM MgCl₂. All plates were incubated for 1 day 2°C above the restrictive temperature of the *esp1^{ts}* mutation (37°C). The ability of calcium to suppress the lethality of an *esp1^{ts}* mutation was confirmed in several different *esp1^{ts}* alleles.

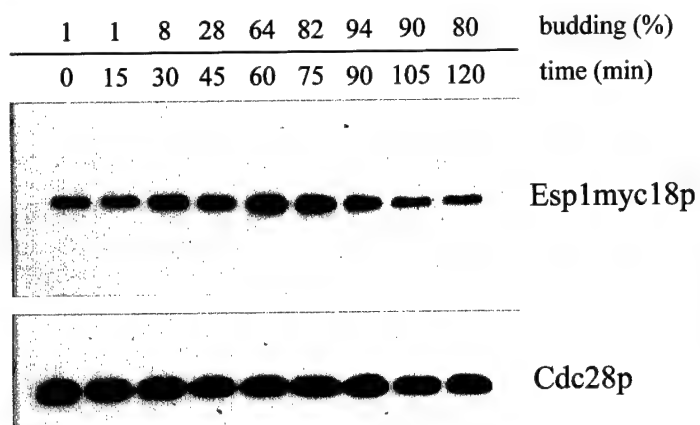
Tables

Table I. Yeast strains used in this study

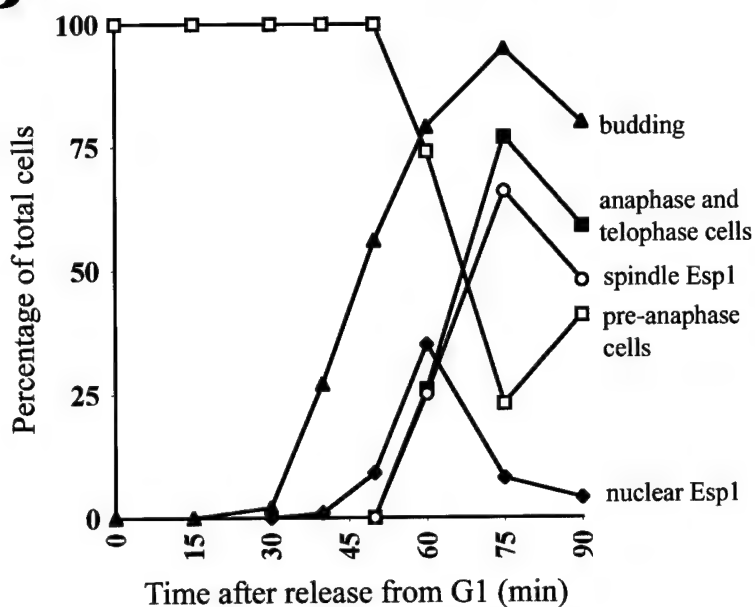
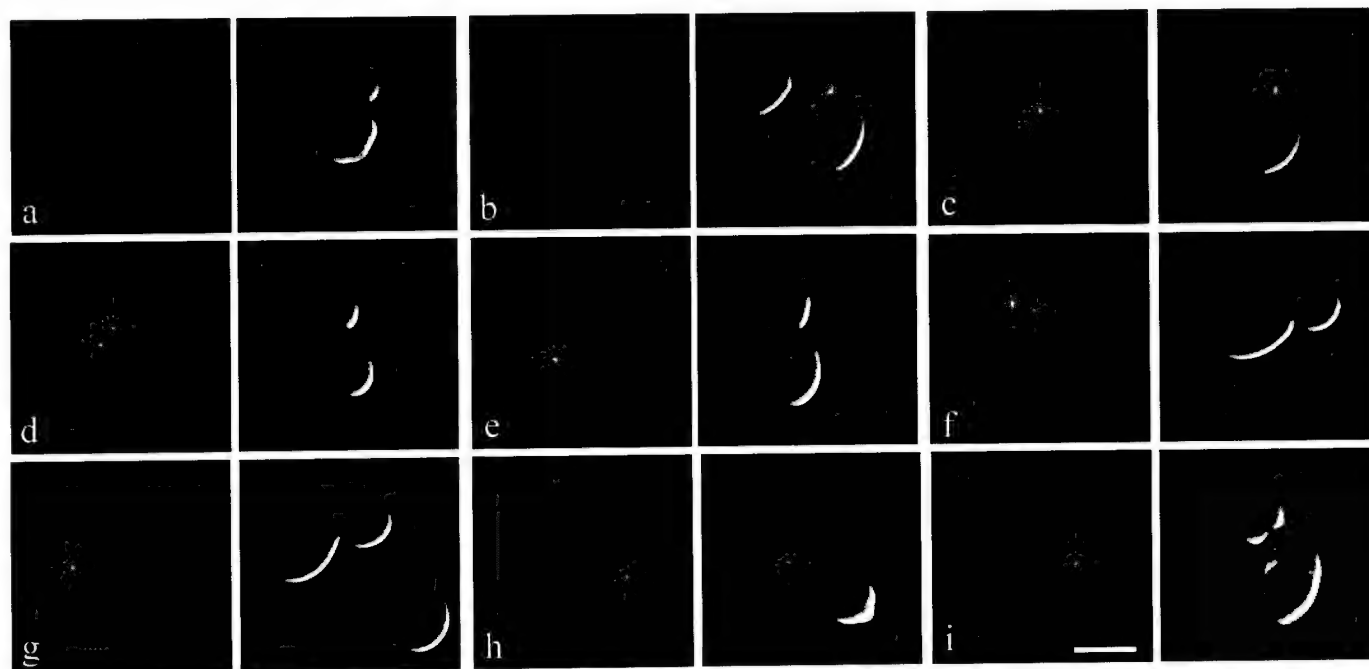
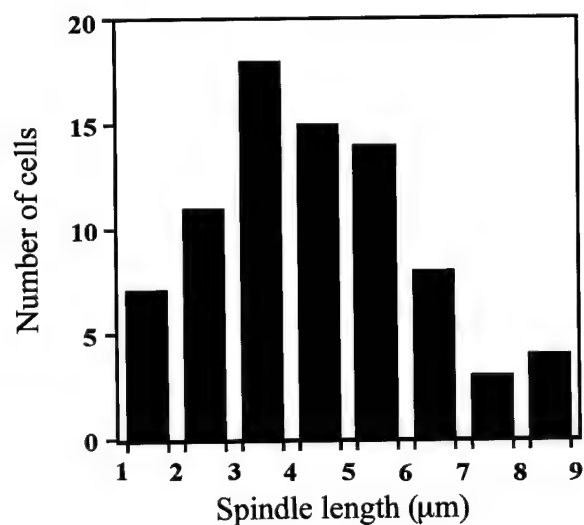
Strain	Relevant genotype
SY101	<i>MATa bar1Δ GAL1:ESP1:GFP (URA3)</i>
SY102	<i>MATa pds1::KAN^R GAL1:ESP1:GFP (URA3)</i>
SY103	<i>MATa pds1-128 GAL1:ESP1:GFP (URA3)</i>
SY104	<i>MATa GAL1:ESP1:GFP (URA3)</i>
SY105	<i>MATa GAL1:ESP1:GFP:NLS (URA3)</i>
SY106	<i>MATa pds1::KAN^R GAL1:ESP1:GFP:NLS (URA3)</i>
SY107	<i>MATa pds1-128 GAL1:ESP1:GFP:NLS (URA3)</i>
SY108	<i>MATa bar1Δ pep4::URA3 ESP1::ESP1(MYC)18(TRP1)</i>
SY109	<i>MATa bar1Δ pep4::URA3 ESP1::ESP1(MYC)18(TRP1)</i> <i>PDS1::PDS1(HA)3(LEU2)</i>
SY110	<i>MATa bar1Δ pep4::URA3 ESP1::ESP1(MYC)18(TRP1)</i> <i>pds1-128::pds1-128(HA)3(LEU2)</i>
SY111	<i>MATa PDS1::PDS1(HA)3(LEU2) GAL1:ESP1:GFP(URA3)</i>
SY112	<i>MATa PDS1::PDS1(HA)3(LEU2) GAL1:ESP1(1-1568):GFP(URA3)</i>
SY113	<i>MATa PDS1::PDS1(HA)3(LEU2) GAL1:ESP1(D1568A):GFP(URA3)</i>
SY114	<i>MATa PDS1::PDS1(HA)3(LEU2) GAL1:ESP1(D1568A/D1570A):GFP(URA3)</i>
SY115	<i>MATa bar1Δ PDS1::PDS1:GFP (KAN^R)</i>

SY116	<i>MATa GAL1:ESP1(1-1568):GFP(URA3)</i>
SY117	<i>MATa esp1::KAN^R trp1::esp1-N5:TRP1</i>
SY201	<i>MATa/α ESP1::ESP1:GFP(KAN^R)/ESP1::ESP1:GFP(KAN^R)</i>
SY202	<i>MATa/α PDS1::PDS1:GFP(KAN^R)</i>
SY203	<i>MATa/α GAL1:ESP1(D1568A):GFP(URA3)/ura3</i>
SY204	<i>MATa/α GAL1:ESP1(D1568A/D1570A):GFP(URA3)/ura3</i>
SY205	<i>MATa/α ase1::KAN^R/ase1::KAN^R GAL1:ESP1:GFP (URA3)/ura3</i>

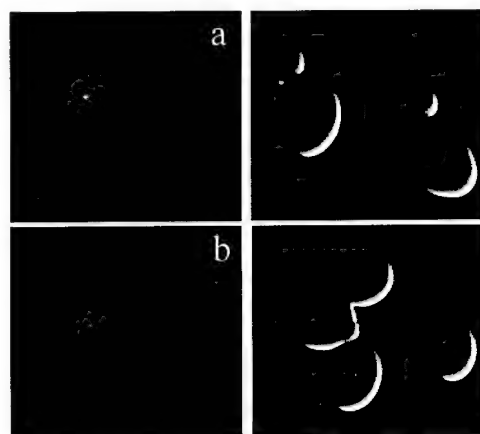
Table II. The distribution of mutant Esp1GFP proteins in live cells compared to wildtype Esp1GFP. Cells derived from the strains described in Fig. 6D were analyzed for Esp1GFP localization. For each strain more than 400 cells were counted and placed in the following categories: nuclear localization, spindle localization or no/dispersed fluorescent signal. The experiment was repeated at least three times with similar results.

A**B**

Reed Figure 1

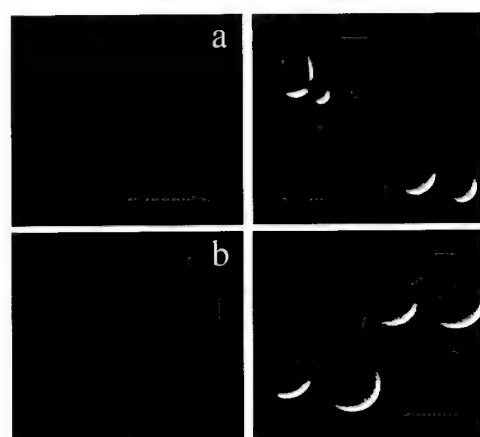
**C****D**

A



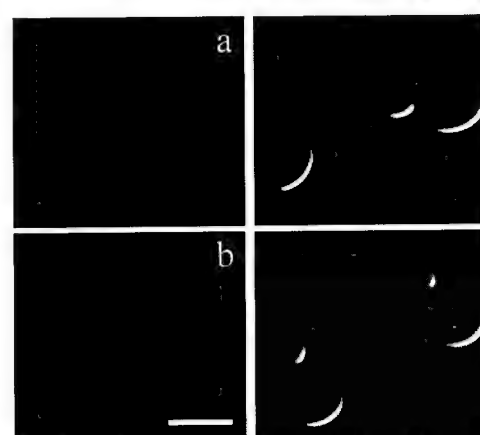
ase1Δ

B



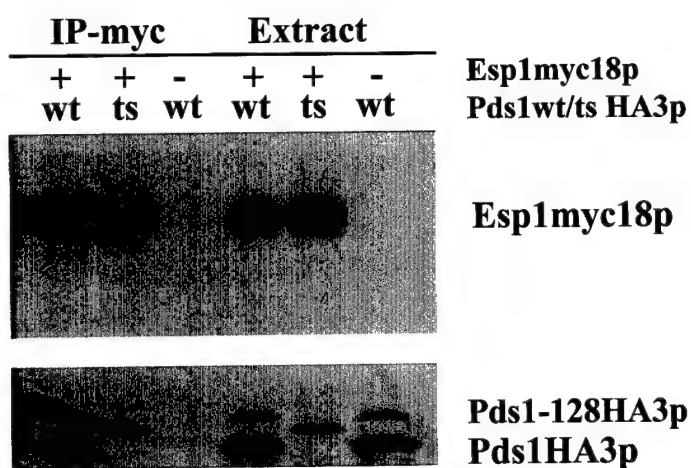
pds1Δ

C



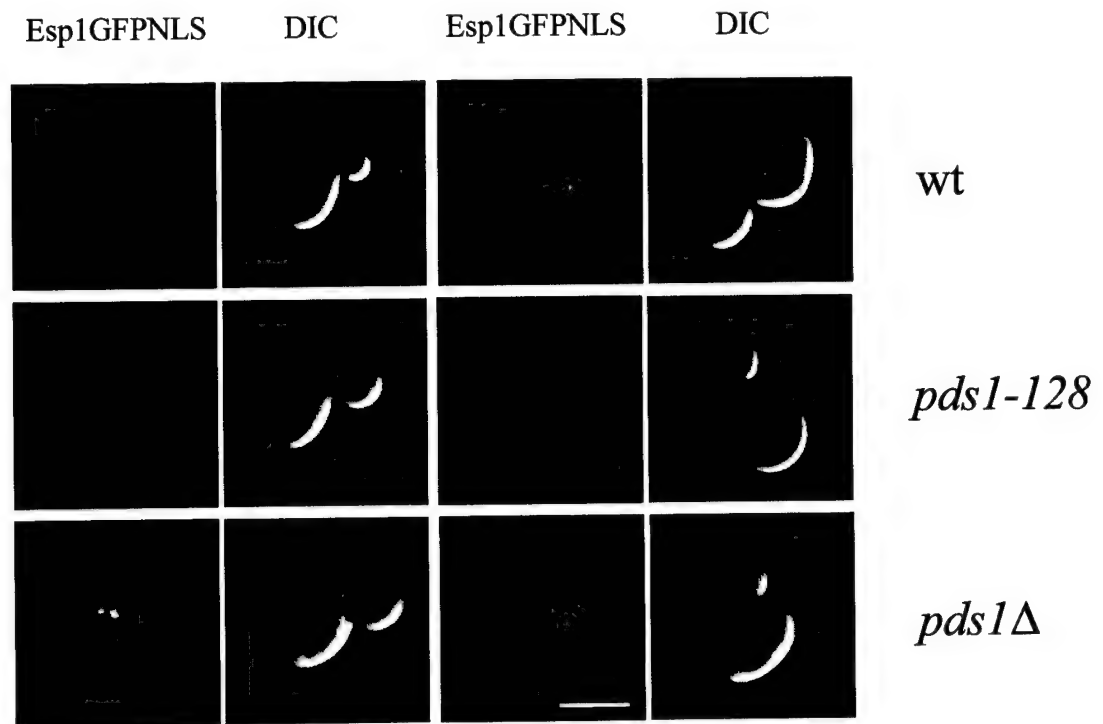
pds1-128

D

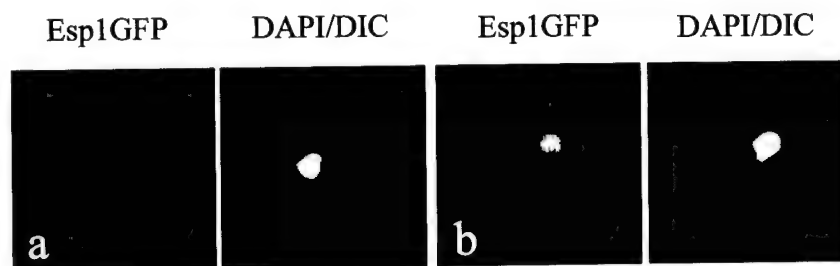


Reed Figure 3

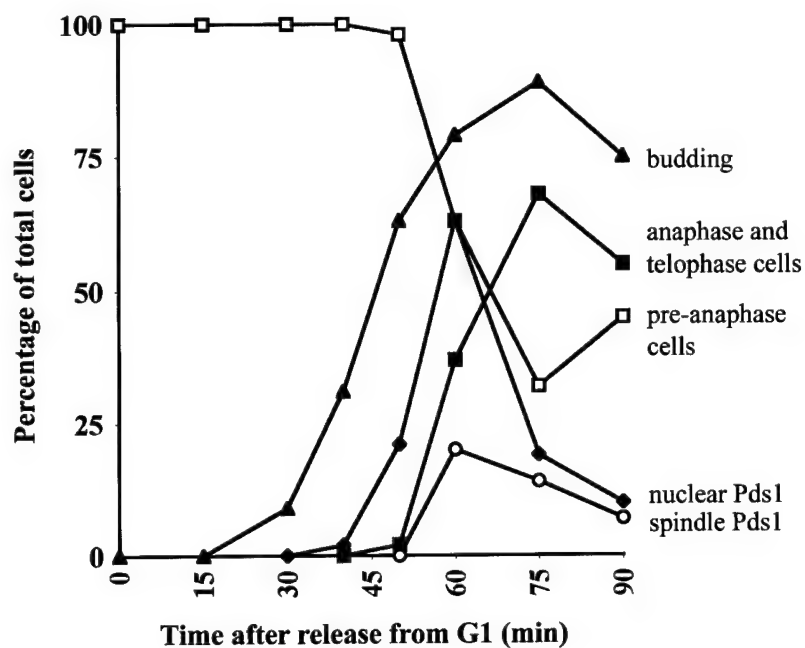
A



B



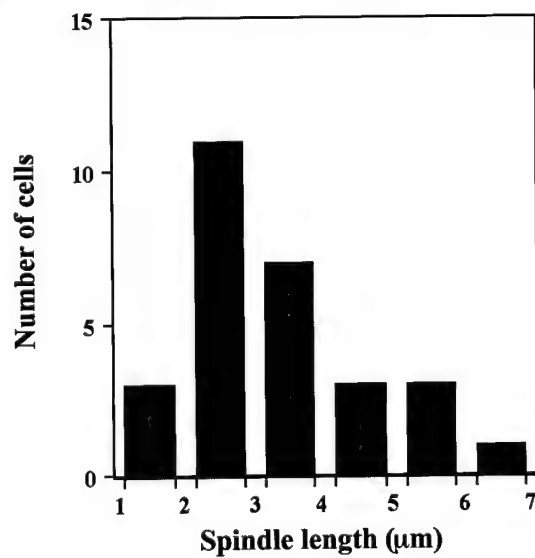
A



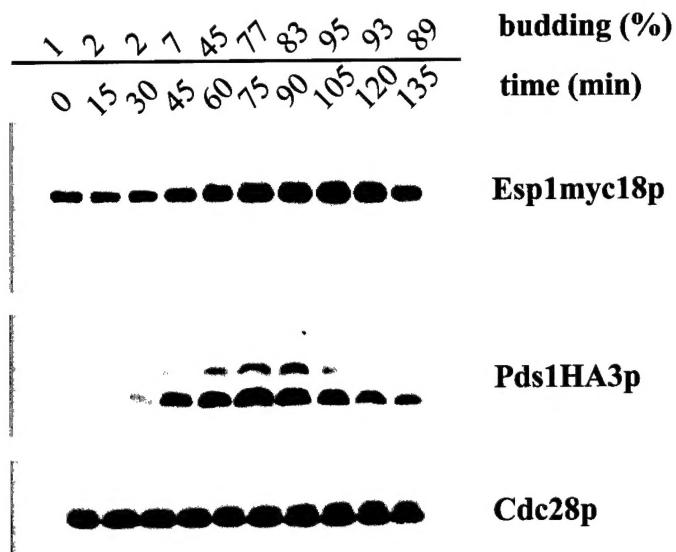
B



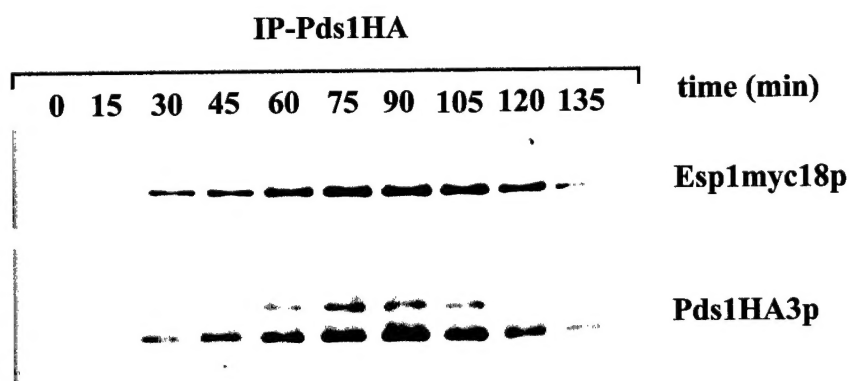
C



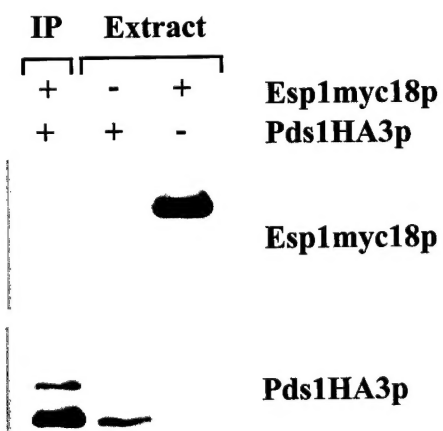
A

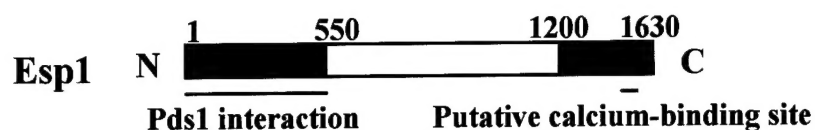


B



C



A


Cut1 (1766-1778) DKDIDRFSLKMLE
 ***** ** *
 Esp1 (1568-1580) DKDIDKFSEELFE
 _ _

B

Complementation of *esp1^{ts}*

		<u>GAL1</u>	<u>ARS/CEN</u>
Wildtype		+	+
1-1568		-	-
D1568A		+	+/-
D1568A D1570A		-	-

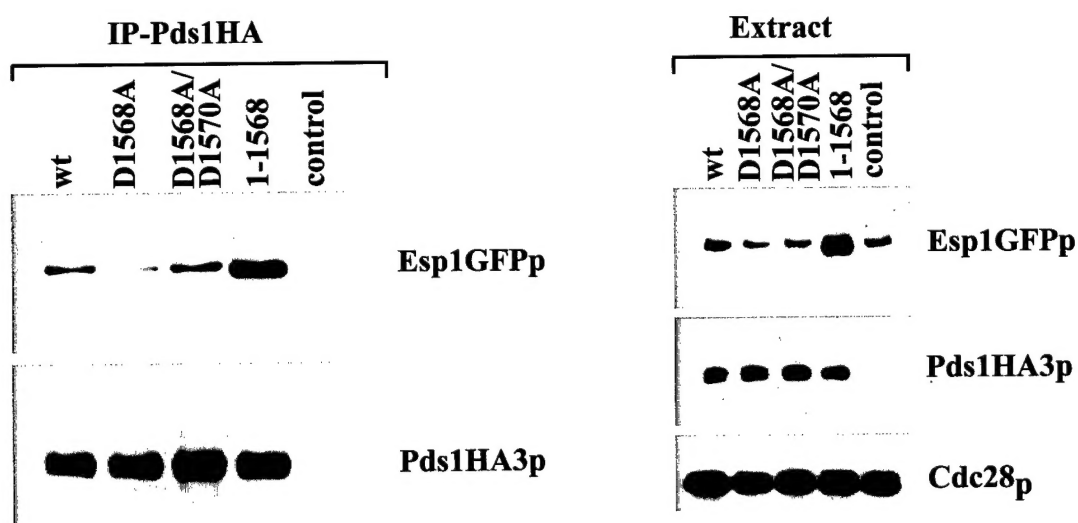
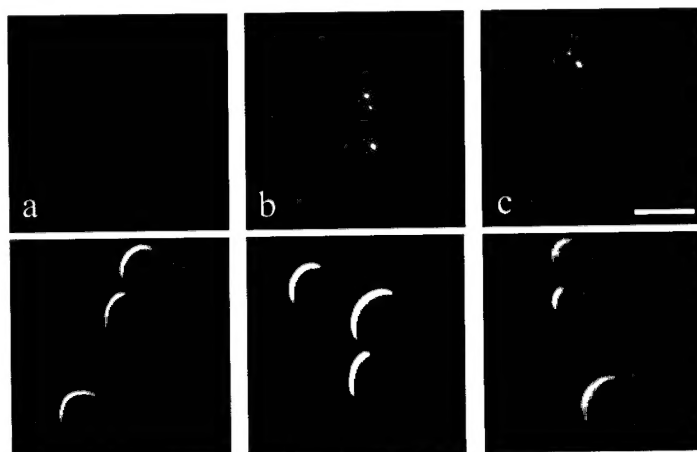
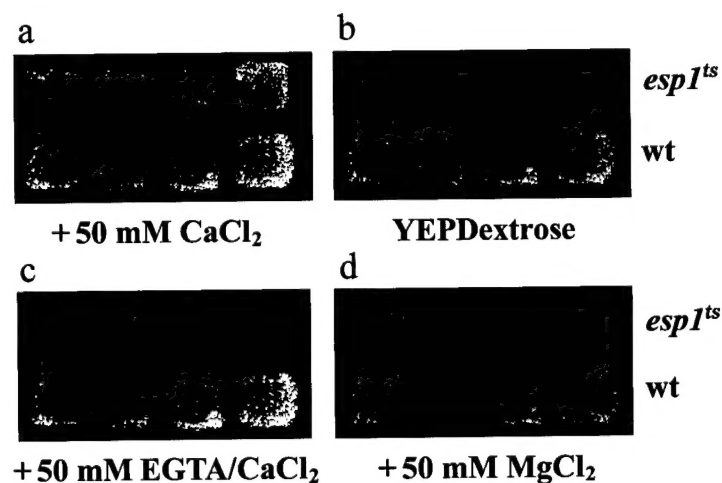



C

D

E


Table II. Localization of wildtype and mutant Esp1GFP

			
	%	%	%
wt Esp1GFP	11.6	28.8	59.6
Esp1(D1568A)GFP	10.0	21.0	69.0
Esp1(D1568A/D1570A)GFP	5.3	1.5	93.2

HOSPITAL # _____

Brief Pain Inventory (Short Form)

Time: _____

Last

First

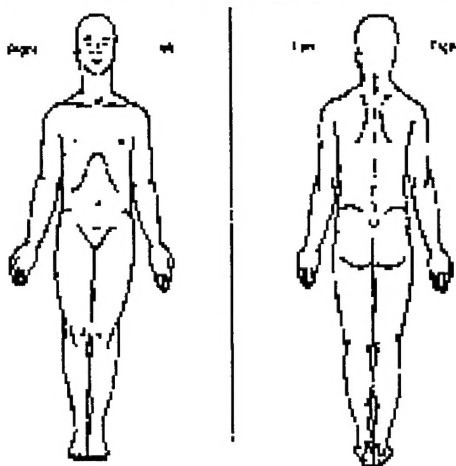
Middle Initial

1. Throughout our lives, most of us have had pain from time to time (such as minor headaches, sprains, and toothaches). Have you had pain other than these everyday kinds of pain today?

1. Yes

2. No

2. On the diagram, shade in the areas where you feel pain. Put an X on the area that hurts the most.



3. Please rate your pain by circling the one number that best describes your pain at its **worst** in the last 24 hours.

0 1 2 3 4 5 6 7 8 9 10
No Pain as bad as you can imagine

4. Please rate your pain by circling the one number that best describes your pain at its least in the last 24 hours.

0 1 2 3 4 5 6 7 8 9 10
No Pain as bad as
Pain you can imagine

5. Please rate your pain by circling the one number that best describes your pain on the average.

[illegible]

6. Please rate your pain by circling the one number that tells how much pain you have right now.

[illegible]